Molecular Biological Studies on the Post-Transcriptional Regulation of *Pou5f1/Oct4* mRNA during Mouse Oogenesis and Embryogenesis

(マウス卵形成と胚発生における *Pou5f1/Oct4* mRNA の転写後制御の分子生物学的研究)

A DISSERTATION
Submitted to the Graduate School of Life Science,
Hokkaido University
in partial fulfillment of the requirements for the degree
DOCTOR OF LIFE SCIENCE

By
Yuki Takada

2022.3

CONTENTS

ACKNOWLEDGMENTS

I express my sincere appreciation to Associate Prof. Tomoya Kotani for his invaluable advice and encouragement throughout the course of this study. I am also grateful to Drs. Yoshinao Katsu, Asato Kuroiwa, and Atsushi Kimura for helpful suggestion, discussion and practical guidance. Thanks are also due to the members of the Kotani laboratory and all members of the laboratories of Reproductive and Developmental Biology for their cooperation and encouragement.

GENERAL INTRODUCTION

Translational control of mRNAs after transcription is an important regulatory system for achieving temporally and spatially restricted expression of genetic information. In particular, transcription is inactivated during oocyte maturation and early development in most animals. Thus, the supply of proteins during these periods is dependent on translation of maternal mRNAs which are stored in oocytes during oogenesis. In other words, development of animals is promoted by the translation of maternal mRNAs. In mouse, growing oocytes are transcriptionally highly active, and the transcription continues until oocytes reach its maximum size (Moore and Lintern-Moore., 1978). A number of genes encoding maternal factors, which play important roles in oogenesis, oocyte maturation, and early development, are transcribed and stored in the oocytes. The transcription ceases in fully grown oocytes arrested at the prophase of meiosis I, which is called the germinal vesicle (GV) stage (Moore and Lintern-Moore., 1978). In response to hormonal stimuli, oocytes resume meiosis and are arrested again at the metaphase of meiosis II (MII). After ovulation, MII-stage oocytes are fertilized with sperms, and resulting zygotes begin mitotic cleavage and embryogenesis.

Many dormant mRNAs required for progression of meiosis such as transcripts encoding c-Mos, Cyclin B, and Wee1 are stored in immature oocytes. These mRNAs are translated at appropriate timings after initiation of oocyte maturation to properly regulate the progression of meiosis (Sagata et al., 1989; Furuno et al., 1994; Hochegger et al., 2001; Gaffré et al., 2011; Nakajo et al., 2000). Moreover, thousands of dormant mRNAs are translated after fertilization at appropriate timings (Winata et al., 2018).

Pou5f1/Oct4 (also known as Oct3 and Oct5) is a transcriptional factor which plays a key role in the maintenance of undifferentiated state of pluripotent cells including embryonic stem (ES) cells and in the inner cell mass (ICM) of blastocysts (Nichols et al., 1998; Jaenisch and Young., 2008). Moreover, changes in the level of Pou5f1/Oct4 can direct lineage-specific differentiation in ES cells (Niwa et al., 2000). In vertebrate development, Pou5f1/Oct4 is essential for embryogenesis. Deletion of *Pou5f1/Oct4* transcripts impairs the continuous growth of preimplantation embryos in mouse and human (Fogarty et al., 2017; Frum et al., 2013; Nichols et al., 1998). Also, overexpression of Pou5f1/Oct4 in zygotes impairs developmental competency in mouse (Fukuda et al., 2016). Thus, it is considered that the control of Pou5f1/Oct4 expression at the appropriate levels is important for development in vertebrates. However, although many knowledges on the functions of Pou5f1/Oct4 have been reported, the mechanism of translational regulation of Pou5f1/Oct4 remains unknown.

Translation has been shown to be regulated through interactions between *cis*-elements of mRNAs and *trans*-acting factors such as RNA-binding proteins (RBPs). In mammalian cells, 860 proteins were identified as RBPs (Castello et al., 2012). Extensive studies have been conducted to reveal the mechanisms of translational control of maternal mRNAs during oocyte maturation. For example, cytoplasmic polyadenylation element (CPE)-binding protein (CPEB) has been shown to regulate the translation of target mRNAs through regulating a polyadenylation during oocyte maturation (Hake and Richter., 1994; Mendez et al., 2000). Accumulating evidences have unveiled the mechanisms of translational control of maternal mRNAs during oocyte maturation, whereas the regulatory mechanisms of maternal mRNAs in fertilized eggs are still elusive.

To elucidate the regulatory mechanisms of maternal transcripts after fertilization, I studied the precise expression pattern and the mechanisms of translational regulation of *Pou5f1/Oct4* during mouse development. In chapter I, I demonstrate that *Pou5f1/Oct4* mRNA is accumulated in oocytes, whereas the expression of Pou5f1/Oct4 protein begins in early 2-cell stage embryos. These results showed that the expression of Pou5f1/Oct4 is regulated by post-transcriptional mechanisms. In chapter II, I show that *Pou5f1/Oct4* mRNA is regulated by a novel mechanism of translational control that is a shortening of the 3' end of mRNA. This RNA processing may be accompanied by changes in RNA-protein interactions.

Chapter I

Analysis of the maternal *Pou5f1/Oct4* expression during mouse oogenesis and embryogenesis

ABSTRACT

Protein syntheses at appropriate timings are important for promoting diverse biological processes and are controlled at the levels of transcription and translation. Pou5f1/Oct4 is a transcription factor that is essential for vertebrate embryonic development. However, the precise timings when the mRNA and protein of Pou5f1/Oct4 are expressed during oogenesis and early stages of embryogenesis remain unclear. I analyzed the expression patterns of mRNA and protein of Pou5f1/Oct4 in mouse oocytes and embryos by using a highly sensitive *in situ* hybridization method and a monoclonal antibody specific to Pou5f1/Oct4, respectively. *Pou5f1/Oct4* mRNA was detected in growing oocytes from the primary follicle stage to the fully grown GV stage during oogenesis. In contrast, Pou5f1/Oct4 protein was undetectable during oogenesis, oocyte maturation and the first cleavage stage but subsequently became detectable in the nuclei of early 2-cell-stage embryos. Pou5f1/Oct4 protein at this stage was synthesized from maternal mRNAs stored in oocytes. Inhibition of Pou5f1/Oct4 protein synthesis resulted in the developmental arrest by the 4-cell sage, indicating the importance of Pou5f1/Oct4 for development. These results indicate that the synthesis of Pou5f1/Oct4 protein during oogenesis and early stages of embryogenesis is controlled at the level of translation and suggest that precise control of the amount of this protein by translational regulation is important for oocyte development and early embryonic development.

INTRODUCTION

Synthesis of proteins at the right time and right place is fundamentally important for promoting various cellular and developmental processes. This temporal and spatial protein expression is controlled by transcriptional machineries in the nucleus and translational machineries in the cytoplasm. Recent studies have demonstrated that the localization and translational control of mRNAs after transcription are critical for the spatial and temporal control of protein syntheses in many types of cells in diverse organisms (Besse and Ephrussi., 2008; Buxbaum et al., 2015; Kloc and Etkin., 2005; Susor and Kubelka., 2017).

Pou5f1/Oct4 (also known as Oct3 and Oct5) was identified as one of the POU family transcriptional factors expressed specifically in germ cells and early embryonic cells in mouse (Scholer et al., 1989, 1990a; Okamoto et al., 1990). High levels of Pou5f1/Oct4 expression were found in pluripotent inner cell mass (ICM) cells of blastocyst-stage embryos and in embryonic stem (ES) cells derived from the ICM (Scholer et al., 1989; Palmieri et al., 1994). Knockout of the zygotic *Pou5f1/Oct4* transcript was shown to impair the differentiation of ICM cells and the growth of preimplantation embryos in mouse and human (Fogarty et al., 2017; Frum et al., 2013; Nichols et al., 1998). A deficiency of *Pou5f1/Oct4* transcripts resulted in the loss of pluripotency in ES cells (Nichols et al., 1998; Jaenisch and Young., 2008). Similar to the effects of knockout, overexpression of Pou5f1/Oct4 in zygotes was shown to impair developmental competency and to cause arrest at early cleavage stages in mouse (Foygel et al., 2008; Fukuda et al., 2016). Therefore, it is thought that the expression levels of Pou5f1/Oct4

should be appropriately controlled for promoting the normal progression of embryonic development.

Pou5f1/Oct4 mRNA has been shown to be maternally expressed in fully grown and ovulated mouse oocytes (Rosner et al., 1990; Scholer et al., 1990b; Yeom et al., 1991). However, little is known about the expression pattern of *Pou5f1/Oct4* mRNA during mammalian oogenesis due to limitations in the isolation of sufficient amounts of growing oocytes in distinct stages and the low level of expression of *Pou5f1/Oct4* mRNA. Conversely, previous studies showed high levels of expression of Pou5f1/Oct4 protein during mouse oogenesis (Pesce et al., 1998; Zuccotti et al., 2009), although other studies showed very low levels of expression of Pou5f1/Oct4 protein in fully grown oocytes, zygotes and early cleavage-stage embryos (Palmieri et al., 1994; Fukuda et al., 2016). Since these fragmentary results are unable to show the precise expression patterns of Pou5f1/ Oct4 throughout the course of oogenesis and early stages of embryogenesis, the mRNA and protein expression should be analyzed comprehensively in the entire period.

After differentiation from oogonia, oocytes begin meiosis until the diplotene stage of meiotic prophase I. The meiosis is arrested at this stage, and oocytes grow through the period called primordial-, primary- and secondary-follicle stages. The growing oocytes are transcriptionally highly active until they reach their maximum size, and then the transcription becomes quiescent in fully grown mouse oocytes (Abe et al., 2010; Moore and Lintern-Moore., 1978). Many germ cell specific factors, which play important roles in oogenesis and embryogenesis, are transcribed during oogenesis (Jagarlamudi and Rajkovic., 2012; Zhang and Smith., 2015). In response to hormonal stimuli, fully grown oocytes resume meiosis and are arrested again at the metaphase of meiosis II (MII).

This process, in which oocytes gain fertility, is called oocyte maturation. After ovulation, MII-stage oocytes are fertilized with sperms, and the resulting zygotes begin mitotic cleavages and embryogenesis. Temporally controlled translation of the maternal mRNAs stored in oocytes is crucial for promoting oocyte maturation and development after fertilization (Kotani et al., 2017; Winata and Korzh., 2018). Although hundreds of mRNAs have been shown to be translationally activated during mouse oocyte maturation (Chen et al., 2011), little is known about mRNAs translated after fertilization in mammals.

In various types of cells including germ cells, neurons and cultured somatic cells, many translationally repressed mRNAs have been shown to be assembled into cytoplasmic granules (Kedersha et al., 2013; Martin and Ephrussi., 2009; Schisa 2012). In zebrafish and mouse oocytes, dormant cyclin B1, *mos*, *Mad2* and *Emi2* mRNAs were shown to form granules in the cytoplasm (Horie and Kotani., 2016; Kotani et al., 2013; Takei et al., 2020; Takei et al., 2021). These RNA granules disassembled at the timing of translational activation during oocyte maturation. Experimental manipulations to disassemble and stabilize cyclin B1 RNA granules resulted in facilitation and inhibition of the translational activation of mRNA, respectively (Kotani et al., 2013; Takei et al., 2020). These results suggest translational regulation of dormant mRNAs through assembly and disassembly of RNA granules.

In this study, I analyzed the precise expression patterns of maternal Pou5f1/Oct4 throughout the course of mouse oogenesis and early embryogenesis. I found that accumulation of *Pou5f1/Oct4* mRNA began at the primary-follicle stage, and then the mRNA was stored in the cytoplasm of oocytes during oogenesis. The *Pou5f1/Oct4* mRNA formed RNA granules in growing and fully grown oocytes, whereas the mRNA

was disassembled in oocytes arrested at MII. Pou5f1/Oct4 protein was undetectable in oocytes during oogenesis and oocyte maturation, whereas it was synthesized from mRNAs stored in oocytes and accumulated in the nuclei of early 2-cell stage embryos. Inhibition of Pou5f1/Oct4 protein synthesis resulted in the developmental arrest by the 4-cell stage. These results show that the expression of Pou5f1/Oct4 is regulated by translational machineries and suggest that temporal control of Pou5f1/Oct4 expression is important for oogenesis and early embryogenesis.

MATERIALS AND METHODS

Animals

All animal experiments in this study were approved by the Committee on Animal Experimentation, Hokkaido University. ICR mice (CLEA-Japan Inc.) were maintained on a 14 h light/10 h dark cycle at 25˚C with free access to food and water.

Collection of oocytes and embryos

Growing and fully grown oocytes were isolated by puncturing ovaries with a needle in M2 medium (94.7 mM NaCl, 4.8 mM KCl, 1.7 mM $CaCl_2$, 1.2 mM KH_2PO_4, 1.2 mM $MgSO_4$, 4.2 mM $NaHCO_3$, 20.9 mM Hepes, 23.3 mM sodium lactate, 0.3 mM sodium pyruvate, 5.6 mM Glucose, 0.1 mM gentamicen, 0.01 mg/ml phenol red, 4 mg/ml BSA; pH 7.2~7.4) containing 10 μM milrinone as an inhibitor of resumption of meiosis (M2+). Oocyte maturation was induced by incubation of fully grown oocytes, that were obtained by puncturing of the largest follicles, with M16 medium (94.7 mM NaCl, 4.8 mM KCl, 1.7 mM $CaCl_2$, 1.2 mM KH_2PO_4, 1.2 mM $MgSO_4$, 25.0 mM $NaHCO_3$, 20.9 mM Hepes, 23.3 mM sodium lactate, 0.3 mM sodium pyruvate, 5.6 mM Glucose, 0.1 mM gentamicen, 0.01 mg/ml phenol red, 4 mg/ml BSA; pH 7.2~7.4) in an atmosphere of 5% CO_2 in air at 37˚C. After being incubated for 18 h, oocytes extruding polar body were collected and analyzed by immunoblotting and immunofluorescence. Alternatively, oocyte maturation was induced in vivo by injection of 5 U of human chorionic gonadotropin (hCG) 48 h after injection of 5 U of pregnant mare serum gonadotropin (PMSG) into female mice. Ovulated mature oocytes were collected from oviducts and incubated with M2 medium containing 300 μg/ml hyaluronidase (Sigma)

to remove cumulus cells. After being washed three times with M2 medium, mature oocytes were collected and subjected for RT-PCR.

Embryos were collected after mating by flushing oviducts and/or uteri with phosphate buffered saline (PBS; 137 mM NaCl, 2.7 mM KCl, 10 mM Na_2HPO_4, and 2 mM KH_2PO_4; pH 7.2). One-cell-stage embryos were recovered from oviducts on day 1 of pregnancy, referred as embryonic day (E) 0.5. Two-cell-stage embryos were recovered from oviducts on day 2 of pregnancy (E1.5). Blastocysts were recovered from uteri on day 4 of pregnancy (E3.5).

Section *in situ* hybridization

In situ hybridization with the tyramide signal amplification (TSA) Plus DNP system (PerkinElmer) was performed according to the procedure reported previously (Takei et al., 2018). Briefly, mouse ovaries (for growing and fully grown oocytes) or oviducts (for mature oocytes and 2-cell-stage embryos) were fixed with 4% paraformaldehyde (PFA) in PBS overnight at 4˚C. Fixed ovaries or oviducts were dehydrated, embedded in paraffin, and cut into 10-μm-thick section. The RNA probes for detection of *Pou5f1/Oct4* transcripts were prepared as follows. The full length of *Pou5f1/Oct4* was obtained by RT-PCR with mouse ovary cDNA and a primer set specific to *Pou5f1/Oct4* mRNA, mPou5f1/Oct4-f1 (5'-GAG GTG AAA CCG TCC CTA GGT G-3') and mPou5f1/Oct4-r1 (5'-AGC TAT CTA CTG TGT GTC CCA-3'), and then subcloned into pCRII-TOPO vector (Invitrogen) by TA-cloning. The resulting plasmid was linearized with XhoI or SpeI for making sense and antisense RNA probes, respectively. Digoxigenin (DIG)-labeled RNA probes were synthesized using a DIG RNA labeling kit (Roche) with SP6 RNA polymerase for a sense probe and T7 RNA polymerase for

an antisense probe, and then used for detection of *Pou5f1/Oct4* transcripts. No signal was detected with the sense RNA probe. After hybridization and washing, samples were incubated with anti-DIG-horseradish peroxidase (HRP) antibody (1:500; Roche) for 30 min at room temperature. After washing, samples were treated with tyramide-dinitrophenyl (DNP) (PerkinElmer, Inc.) (1:50, followed by dilution with an equal volume of double distilled water (DDW)) for 20 min at room temperature.

For detection of signals by alkaline phosphatase (AP) staining, samples were treated with anti-DNP-AP antibody (1:500; PerkinElmer, Inc.) for 30 min at room temperature. After washing with a staining buffer (100 mM Tris, 100 mM NaCl, 50 mM $MgCl_2$; pH 9.5), samples were reacted with mixture of 225 μg/ml of nitro blue tetrazolium (NBT) and 175 μg/ml of 5-bromo-4-chloro-3-indolyl phosphate (BCIP) in staining buffer. The reaction was stopped with a stop solution (10 mM Tris, 1 mM EDTA; pH 8.0). The samples were mounted with glycerol and observed under an Axioskop microscope (Carl Zeiss) with a Plan NEOFLUAR 5x/0.15 and 10x/0.30 lens.

For detection of signals with fluorescence, samples were treated with anti-DNP-Alexa 488 antibody (1:500; Molecular Probes) for overnight at room temperature. After washing, samples were treated with 10 μg/ml Hoechst 33258 for 10 min to detect nuclei. The samples were mounted with Fluoro-KEEPER Antifade Reagent (Nacalai Tesque) and observed under an LSM 5 LIVE confocal microscope (Carl Zeiss) with a Plan Apochromat 63x/1.4 NA oil differential interference contrast lens and LSM 5 DUO 4.2 software (Carl Zeiss).

Quantitative RT-PCR

The expression of *Pou5f1/Oct4* mRNA in GV-, MII-stage oocytes and early 2-cell-

stage embryos was quantified by using a real-time PCR system with SYBR green PCR Master Mix (Applied Biosystems) according to the manufacturer's instructions. Total RNA from 150 oocytes and embryos was extracted by using NucleoSpin RNA XS (Takara). Four μl of the total RNA was used for reverse transcription with SuperScript III First Strand Synthesis System (Invitrogen) using random hexamers. The *Pou5f1/Oct4* transcript was amplified with the cDNA and a primer set specific to *Pou5f1/Oct4* mRNA, mPou5f1/Oct4-qPCR-f (5'-ACA TGA AAG CCC TGC AGA AG-3') and mPou5f1/Oct4-qPCR-r (5'-GCT GAA CAC CTT TCC AAA GAG- 3').

Immunoblotting

The crude extracts from 50 oocytes and embryos were separated by SDS-PAGE with Bolt 4-12% Bis-Tris Plus gels (Novex) and blotted onto an Immobilon membrane using a Bolt Mini Blot Module (Novex). The membranes were blocked with 5% skim milk in Tris buffered saline (TBS; 20 mM Tris and 150 mM NaCl; pH 7.5) containing 0.1% Tween 20 (TTBS) for 15 min at room temperature. Then, the membranes were incubated with anti-Pou5f1/Oct4 antibody (1:100; Santa Cruz; C-10) overnight at room temperature. After being washed three times with TTBS, the membranes were incubated with an anti-mouse IgG secondary antibody fused with alkaline phosphatase (1:1000; American Qualex) for 2 h at 37˚C. After being washed three times with TTBS, the membranes were incubated with NBT and BCIP in diethanolamine buffer (100 mM diethanolamine, 5 mM $MgCl_2$; pH 9.5) to detect signals.

Immunofluorescence

Immunofluorescence of mouse oocytes and embryos was performed according to the

procedure described previously (Fukuda et al., 2016). Oocytes and embryos were fixed with 2% PFA for 20 min followed by permeabilization in 0.25% Triton X-100 for 10 min at room temperature. Samples were then incubated with a blocking/washing solution (PBS containing 0.3% BSA and 0.01% Tween-20) for 1 h at room temperature and incubated with the anti-Pou5f1/Oct4 antibody (1:100) for overnight at 4˚C. The samples were washed with blocking/washing solution and then incubated for 1 h at room temperature with Alexa Flour 488-conjugated anti-mouse IgG secondary antibody (1:200; Molecular Probes). After being washed with washing solution, the samples were mounted with VECTASHIELD Mounting Medium with DAPI (Funakoshi) and observed under the LSM 5 LIVE confocal microscope with the Plan Apochromat 63x/1.4 NA oil differential interference contrast lens and LSM 5 DUO 4.2 software. For quantification of immunofluorescence analysis, the same laser intensity was applied to all samples. The signal intensities of at least three samples were measured by using ImageJ software and calculated as the mean of one experiment, and the final mean intensity was calculated from three independent experiments.

Morpholino oligonucleotide injection

The sequences of antisense morpholino oligonucleotides (MOs) (Gene Tools, LLC) are as follows: *Pou5f1/Oct4* ATG-MO, 5'-GTCTGAAGCCAGGTGTCCAGCCATG-3', that specifically targets the translational start site of the *Pou5f1/Oct4* mRNA and *Pou5f1/Oct4* 5mm-MO, 5'-CTCTCAAGCCACGTGTGCAGCGATG-3', that contains 5-nts mismatches (underlines) and was used as control. One-cell-stage embryos were injected with 10 pl of a solution containing 0.6 mM and 0.2 mM *Pou5f1/Oct4* ATG-MO or 0.6 mM *Pou5f1/Oct4* 5mm-MO using an IM-9B microinjector (Narishige) under a

Dmi8 microscope (Leica) in M2 medium. After being injected, the embryos were cultured in M16 medium containing 0.01 mM EDTA (M16+EDTA) in an atmosphere of 5% CO_2 in air at 37℃ for 4 days. For immunofluorescence analysis, embryos were fixed with 2% PFA at the early 2-cell and 4-cell stages.

Parthenogenetic activation

Parthenogenetic activation was performed according to the procedure described previously (Piotrowska and Zernicka-Goetz., 2002) with brief modifications. Mature oocytes were collected from oviducts 16-17 h after injection of hCG. Oocytes were artificially activated by treatment with 7% ethanol in M2 medium for 5.5 min. After being washed three times with M16, oocytes were incubated with M16 medium containing 0.01 mM EDTA (M16 + EDTA) and 1 μg/ml cytochalasin D for 3 h in an atmosphere of 5% CO_2 in air at 37˚C to inhibit the extrusion of the second polar body. After being washed three times with M16, oocytes were cultured in M16 + EDTA in an atmosphere of 5% CO_2 in air at 37˚C.

α-Amanitin treatment

Treatment of embryos with α-Amanitin was performed according to the procedure described previously (Carol and Larry., 1974). To inhibit the zygotic transcription, one-cell-stage embryos were cultured with M16 + EDTA containing 1 μg/mL α-Amanitin (Tocris Bioscience) in an atmosphere of 5% CO_2 in air at 37˚C. α-Amanitin was dissolved in DDW as a stock and diluted in M16 + EDTA before use. As a control, embryos were cultured in M16 + EDTA adding 0.1% DDW.

Polysomal fractionation

Polysomal fractionation was performed according to the procedure described previously (Masek et al., 2020). Briefly, 200 oocytes or embryos were treated with 100 µg/ml of cycloheximide (CHX) for 10 min and collected in 350 µl of lysis buffer (10 mM Hepes, pH 7.5; 62.5 mM KCl, 5 mM $MgCl_2$, 2 mM DTT, 1% TritonX-100) containing 100 µg/ml of CHX and 20U/ml of Ribolock (Thermo Fisher Scientific). After disruption of the zona pellucida with 250 µl of zirconia-silica beads (BioSpec), lysates were centrifuged at 8,000 g for 5 min at 4˚C. Supernatants were loaded onto 10-50% linear sucrose gradients containing 10 mM Hepes, pH 7.5; 100 mM KCl, 5 mM $MgCl_2$, 2 mM DTT, 100 µg/ml of CHX, Complete-EDTA-free Protease Inhibitor (1 tablet/100 ml: Roche) and 5U/ml of Ribolock. Centrifugation was performed using Optima L-90 ultracentrifuge (Beckman) at 35,000 g for 65 min at 4˚C. Polysome profiles were recorded using ISCO UA-5 UV absorbance reader. Ten equal fractions were collected from each sample and subjected to RNA isolation by Trizol reagent (Sigma-Aldrich). Fractions 6 to 10 were taken as for polysome bound RNA. Further, the library was prepared using SMART-seq v4 ultra low-input RNA kit (Takara Bio). Sequencing was performed by HiSeq 2500 (Illumina) as 150-bp paired-end. Reads were trimmed using Trim Galore v0.4.1 and mapped to the mouse GRCm38 genome assembly using Hisat2 v2.0.5. Gene expression was quantified as fragments per kilobase per million (FPKM) values in Seqmonk v1.40.0.

RESULTS

Accumulation of *Pou5f1/Oct4* mRNA during oogenesis as cytoplasmic granules

The expression pattern of *Pou5f1/Oct4* mRNA in mammalian oocytes during oogenesis remains elusive due to low levels of expression. Indeed, I could not detect this transcript in mouse oocytes by a conventional *in situ* hybridization method (Takei et al., 2018). To overcome this, I used the highly sensitive *in situ* hybridization method combined with paraffin sections of ovaries (Takei et al., 2018), in which the signal of RNA probe hybridized with the target mRNA is amplified by a tyramide signal amplification (TSA) system. Using this method, I could detect the expression of *Pou5f1/Oct4* mRNA in fully grown oocytes in adult mouse ovaries (Fig. 1A) (Takei et al., 2018).

To precisely analyze the expression pattern of *Pou5f1/Oct4* mRNA during oogenesis, ovaries from female mice in postnatal day (PD) 8 were isolated and examined. *Pou5f1/Oct4* mRNA was not detected in oocytes at the primordial-follicle stage, while the mRNA was clearly detected in the cytoplasm of oocytes at the primary- and secondary-follicle stages (Fig. 1B). No signal was detected in follicle cells at any stages (Fig. 1A and B), showing the restricted expression of *Pou5f1/Oct4* mRNA in germ cells. I then investigated the subcellular distribution of *Pou5f1/Oct4* mRNA by fluorescence *in situ* hybridization (FISH) with the TSA system (Kotani et al., 2013; Takei et al., 2018). The FISH analysis confirmed that no *Pou5f1/Oct4* mRNA was detected in oocytes at the primordial-follicle stage. In contrast, signals of *Pou5f1/Oct4* mRNA was detected as granular structures in the oocyte cytoplasm from the primary-follicle stage to the fully grown GV-stage (Fig. 1C). Therefore, these results demonstrate the

accumulation of *Pou5f1/Oct4* mRNA in the oocyte cytoplasm from the primordial-follicle stage by assembling into RNA granules.

Disassembly of *Pou5f1/Oct4* RNA granules in ovulated oocytes and 2 cell-stage embryos

To examine the fate of *Pou5f1/Oct4* RNA granules, I then performed FISH analysis in oocytes at the MII stage and embryos at the 2-cell stage. *Pou5f1/Oct4* RNA granules, which were observed in GV-stage oocytes, disappeared in MII-stage oocytes and in 2-cell-stage embryos (Fig 2A). The amount of *Pou5f1/Oct4* mRNA was not significantly changed in oocytes at the MII stage and embryos at the 2-cell stage (Fig 2B), consistent with the results reported previously (Fukuda et al., 2016). These results indicated that the disappearance of *Pou5f1/Oct4* RNA granules in MII-stage oocytes was caused by disassembly of them but not degradation of the mRNA. Previous studies showed that dormant cyclin B1 and *Mos* mRNAs form granules in the cytoplasm of oocytes, and the granules disappear at the timing of translation during oocyte maturation (Kotani et al., 2013; Horie and Kotani, 2016). Thus, these data raised the possibility that the *Pou5f1/Oct4* mRNA is stored in a dormant state in growing and fully grown GV oocytes and is translationally activated in MII-stage oocytes and 2-cell-stage embryos.

Accumulation of Pou5f1/Oct4 protein in an early period of 2-cell-stage embryos

To examine the expression pattern of Pou5f1/Oct4 protein during oogenesis and early embryogenesis, I first confirmed the specificity of anti-Pou5f1/Oct4 antibody (C10) by immunoblot and immunofluorescence analyses of blastocyst-stage embryos. Immunoblot analysis showed that the anti-Pou5f1/Oct4 antibody recognized a strong

band of Pou5f1/Oct4 in crude extracts of blastocysts (Fig.3A, left). Immunofluorescence analysis showed the expression of Pou5f1/Oct4 in the nuclei of ICM cells of blastocysts (Fig. 3A, middle), consistent with the expression patterns in previous studies (Fukuda et al., 2016; Nichols et al., 1998; Wu et al., 2013). I then analyzed the expression of Pou5f1/Oct4 during oogenesis and early stages of embryogenesis. Immunofluorescence analysis showed a low level of Pou5f1/Oct4 expression in the nucleus of oocytes at the primary- and secondary-follicle stages (Fig. 3B), although the intensity of signals was not statistically different in oocytes incubated with and without the primary antibody (Fig. 3C). Furthermore, Pou5f1/Oct4 was undetectable in oocytes at the GV- and MII-stages and embryos at the early period of 1-cell stage (Fig. 3B and C). Subsequently, certain levels of Pou5f1/Oct4 were detected in the nuclei of embryos at the 2-cell stage (Fig. 3B and C). No signal was detected in the cytoplasm of oocytes and embryos at all stages examined (Fig. 3B and C). Pou5f1/Oct4 was still undetectable in 2-cell stage embryos in immunoblot analysis, showing that the expression level is low compared with that in blastocyst-stage embryos (Fig. 3A, right).

Because I observed various levels of signals in 2-cell-stage embryos in some batches, I hypothesized that the expression level of Pou5f1/Oct4 protein is different between early and late periods of 2-cell-stage embryos. To address this, 2-cell-stage embryos in an early period were collected in the second day of pregnancy at embryonic day (E) 1.5. Half of the embryos were fixed and stored in PBS (Early 2-cell). The other half was cultured in M16 medium at least for 7.5 h and then was fixed (Late 2-cell). Immunofluorescence analysis revealed the high level of Pou5f1/Oct4 expression in the nuclei of Early 2-cell embryos, while the expression level was low in Late 2-cell

embryos (Fig. 3D and E). In contrast, the intensity of signals in the cytoplasm was unchanged (Fig. 3D and E).

I finally confirmed the specificity of signals detected in the nuclei of early 2-cell embryos by injecting the 0.6 mM antisense *Pou5f1/Oct4* MOs into one-cell-stage embryos. Injection of the *Pou5f1/Oct4* ATG-MO significantly reduced the signals (Fig. 3F). In contrast, the signals were not changed by injection of the control *Pou5f1/Oct4* 5mm-MO (Fig. 3F). Taken together, the results indicate that Pou5f1/Oct4 was present in the nuclei of early 2-cell-stage embryos.

Translational activation of maternal *Pou5f1/Oct4* mRNA in ovulated oocytes and early cleavage-stage embryos

Accumulation of Pou5f1/Oct4 protein in the early period of 2-cell-stage embryos would be resulted from a translational activation of maternal mRNAs or that of zygotically transcribed mRNAs. To assess these possibilities, I first analyzed parthenogenetically activated embryos by immunofluorescence. Pou5f1/Oct4 protein was detected in the nuclei of 2-cell-stage parthenogenetic embryos (Fig. 4A), suggesting the synthesis of Pou5f1/Oct4 protein from maternal mRNA stored in oocytes.

I then analyzed embryos treated with α-Amanitin, a transcriptional inhibitor, by immunofluorescence. To confirm the effect of α-Amanitin on zygotic transcription, I first analyzed embryos treated with α-Amanitin from the 1-cell stage (E0.5) to the 8-cell stage (E2.5). Pou5f1/Oct4 was clearly detected in the nuclei of 8-cell-stage embryos in control embryos, while no signal was detected in α-Amanitin-treated embryos (Fig. 4B), indicating that the zygotic Pou5f1/Oct4 expression was completely inhibited by the treatment with α-Amanitin. I then analyzed the expression of Pou5f1/Oct4 in the α-

Amanitin-treated embryos at the 2-cell-stage and found that Pou5f1/Oct4 was accumulated in the nuclei of embryos (Fig. 4C). Taken together, these results indicate that Pou5f1/Oct4 protein is synthesized from maternal mRNAs stored in oocytes and accumulated in the nuclei of embryos at an early period of the 2-cell stage.

I finally confirmed the state of *Pou5f1/Oct4* mRNA from GV-stage oocytes to 2-cell-stage embryos by polysomal fractionation (Masek et al., 2020). In this assay, mRNAs translated by ribosomes are fractionated in the polysomal fraction. The amount of mRNA in the polysomal fraction was small in GV-stage oocytes but was significantly increased in MII-stage oocytes and 1-cell-stage embryos (Fig. 5A). The amount of *Pou5f1/Oct4* mRNA in 1-cell-stage embryos was threefold larger than that in GV-stage oocytes. Since the total amounts of *Pou5f1/Oct4* mRNA were similar in GV- and MII-stage oocytes and 2-cell-stage embryos (Fig. 2B), the increase in the amount of mRNA in the polysomal fraction indicates translational activation of mRNA stored in oocytes. The amounts of *Pou5f1/Oct4* mRNA in the polysomal fraction were significantly reduced in the late 2-cell stages (Fig. 5B), consistent with the results of immunofluorescence showing the reduction of Pou5f1/Oct4 protein in the nuclei of late 2-cell-stage embryos (Fig. 3D and E). Therefore, the translational state of *Pou5f1/Oct4* mRNA was dramatically changed in the early and late periods of 2-cell stage.

Effect of knockdown of Pou5f1/Oct4 on developmental competence

To elucidate the significance of the expression of Pou5f1/Oct4 on mouse development, I analyzed the developmental competence of Pou5f1/Oct4-deficient embryos by injecting one-cell stage embryos with antisense morpholino oligonucleotide (MO) that targets the translational start site of *Pou5f1/Oct4* mRNA (ATG-MO).

Immunofluorescence analysis using anti-Pou5f1/Oct4 antibody showed that the low concentration of ATG-MO (0.2 mM) inhibited the expression of maternal Pou5f1/Oct4 protein in the early 2-cell stage embryos (Fig. 6A). On the other hand, at the 4-cell stage, embryos injected with ATG-MO (0.6 mM) showed no expression of Pou5f1/Oct4, whereas the embryos injected with ATG-MO (0.2 mM and 0.4 mM) showed weak expression of Pou5f1/Oct4 (Fig. 6B). These results suggest that the low concentration of ATG-MO (0.2 mM) was able to prevent Pou5f1/Oct4 synthesis from maternal mRNA but unable to prevent the synthesis from zygotic mRNA. In contrast, the high concentration of ATG-MO (0.6 mM) prevented Pou5f1/Oct4 synthesis from both maternal and zygotic mRNA.

To evaluate the effect of Pou5f1/Oct4 knockdown on developmental competence in detail, I injected high- and low-concentrations (0.6 mM and 0.2 mM) of ATG-MO and observed development. For an injection control, I used MO that contains 5-nts mismatches compared with ATG-MO (5mm-MO). At day 2 after fertilization (E 1.5), all of the ATG-MO (0.6 mM and 0.2 mM) and 5mm-MO (0.6 mM) injected embryos reached 2-cell stage. At day 3 after fertilization (E 2.5), only 54.5% (6/11) of ATG-MO (0.6 mM) injected embryos reached 4-cell stage, whereas 100% (17/17) of ATG-MO (0.2 mM) injected embryos and 92.3% (12/13) of 5mm-MO (0.6 mM) injected embryos reached 4-cell and morula-stages. At day 4 after fertilization (E 3.5), no embryos reached morula-stage in the ATG-MO (0.6 mM) injected group, whereas 94.1% (16/17) of ATG-MO (0.2 mM) injected embryos and 92.3% (12/13) of 5mm-MO injected embryos reached morula-stage. At day 5 after fertilization (E 4.5), no embryos reached blastocyst-stage and 54.5% (6/11) of embryos underwent fragmentation in the ATG-MO (0.6 mM) injected group, whereas 82.4% (14/17) of ATG-MO (0.2 mM) injected

embryos and 84.6% (11/13) of 5mm-MO (0.6 mM) injected embryos reached blastocyst-stage (Fig. 6C). These results indicate that the expression of Pou5f1/Oct4 protein from the 2-cell stage to 4-cell stage is essential for the progression of embryonic development beyond the 4-cell stage. The expression of Pou5f1/Oct4 from the maternal mRNA seems to be unnecessary in this experiment, although Pou5f1/Oct4 protein synthesized from maternal mRNA may have important roles in normal development (see Discussion).

DISCUSSION

During development of germline cells, *Pou5f1/Oct4* was shown to be transcribed in primordial germ cells (PGC) in later stages of embryogenesis in mouse (Rosner et al., 1990b; Scholer et al., 1990). However, transcription of *Pou5f1/Oct4* in female germ cells after differentiation into oocytes remained unknown. I showed for the first time that accumulation of *Pou5f1/Oct4* mRNA begins at the primary follicle-stage and persists during later stages of oogenesis in mouse (Fig. 1B and C). In the cytoplasm of oocytes in the all stages, the mRNA was found to be assembled into granules (Fig. 1C), suggesting the post-transcriptional regulation of this mRNA.

In contrast to the accumulation of mRNA in early stages of oogenesis, Pou5f1/Oct4 protein was only slightly detected in the nucleus of oocytes in the primary- and secondary-follicle stages, though quantitative analysis did not show statistical significance (Fig. 3B and C). In fully grown GV-stage oocytes, Pou5f1/Oct4 protein was in an undetectable level (Fig. 3B). These results suggest that the translation of cytoplasmic mRNA is repressed or in very low levels. Polysomal fractionation supports this notion since the amount of *Pou5f1/Oct4* mRNA in polysomal fraction was small in GV-stage oocytes compared with that in 1-cell-stage embryos (Fig. 5A). Formation of granular structures of *Pou5f1/Oct4* mRNA in the oocyte cytoplasm may function to stably repress the translation by sequestering mRNA from ribosomes as in the case of *oskar* mRNA in Drosophila oocytes (Chekulaeva et al., 2006) and cyclin B1 mRNA in zebrafish and mouse oocytes (Kotani et al., 2013).

In ovulated oocytes and early 1-cell-stage embryos, Pou5f1/Oct4 protein was still undetectable (Fig. 3B). However, in the subsequent early period of 2-cell-stage, the

certain amount of protein accumulation was observed in the nuclei (Fig. 3B-F, see also Fig. 7). FISH analysis showed the disassembly of *Pou5f1/Oct4* RNA granules in these stages (Fig. 2). Moreover, the amount of mRNA in polysomal fraction was gradually increased in MII-stage oocytes and 1-cell-stage embryos (Fig. 5A). These results resemble the translational activation of cyclin B1 mRNA during oocyte maturation, in which granular structures of the mRNA disassembles at the timing of translational activation (Kotani et al., 2013), although the function of granules of *Pou5f1/Oct4* mRNA remains to be addressed. Zygotic transcription is not required for the accumulation of protein, since the Pou5f1/Oct4 protein was detected even in parthenogenetically activated embryos and embryos treated with α-Amanitin (Fig. 4). Collectively, these results indicate that the amount of Pou5f1/Oct4 protein is controlled at the translation level during oogenesis and early cleavage stages and suggest that the precisely controlled expression of Pou5f1/Oct4 is important for progression of oogenesis and early embryogenesis.

The low levels of expression of Pou5f1/Oct4 in a period from fully grown GV-stage oocytes to early 1-cell-stage embryos are consistent with the results in previous studies (Palmieri et al., 1994; Fukuda et al., 2016). In contrast, other studies showed high levels of Pou5f1/Oct4 expression from the early stage of oogenesis to fully grown oocytes (Pesce et al., 1998; Zuccotti et al., 2009). The explanation for the differences in the expression patterns is that these studies were performed by different procedures for the detection of Pou5f1/Oct4 protein. In the study reported by Pesce (Pesce et al., 1998), Pou5f1/Oct4 was detected by purified rabbit polyclonal antibodies and the reaction was amplified with the avidin-biotinylated-peroxidase complex (ABC). The high levels of Pou5f1/Oct4 expression would be resulted from amplification of the reaction or

presence of other POU family members. The Pou5f1/Oct4 was also detected with purified rabbit polyclonal antibodies in the study reported by Zuccotti (Zucotti et al., 2009). I used the monoclonal antibody in this study and confirmed that it recognizes a strong band of Pou5f1/Oct4 in crude blastocyst extracts by immunoblot analysis (Fig. 3A, left). The signal of Pou5f1/Oct4 in immunofluorescence analysis disappeared by knockdown of Pou5f1/Oct4 by injecting ATG-MO, indicating that the antibody specifically recognized Pou5f1/Oct4 protein. Although the sensitivity of this method would not be high, the expression levels of Pou5f1/Oct4 protein were comparative in this analysis.

The amount of Pou5f1/Oct4 protein accumulated in the nuclei was significantly reduced in the late period of 2-cell stage (Fig. 3D and E). This rapid decrease in the expression level of Pou5f1/Oct4 suggest the existence of active degradation of the protein, in addition to the reduction in mRNA translation (Fig. 5B). Wwp2, an E3 ubiquitin ligase that specifically ubiquitinate Pou5f1/Oct4 in human and mouse ES cells, is one of the candidates for directing the rapid protein degradation (Xu et al., 2009; Xu et al., 2004). However, the expression of Wwp2 in oocytes and early stages of embryos remains unknown. Nevertheless, the transient expression of Pou5f1/Oct4 protein in the early period of 2-cell stage suggests the importance of nuclei accumulation of Pou5f1/Oct4 in this period for subsequent embryonic development.

I revealed that the depletion of Pou5f1/Oct4 at the both early 2- and 4-cell stages by injecting zygotes with high-concentration of ATG-MO resulted in the developmental arrest at the 4-cell stage (Fig. 6). However, the depletion of Pou5f1/Oct4 at the early 2-cell stage, but not at the 4-cell stage by injecting zygotes with low-concentration of ATG-MO resulted in the normal progression of development beyond 4-cell stage and

reaching blastocyst-stage (Fig. 6). These results indicate that the expression of Pou5f1/Oct4 protein in embryos during the 2-cell to 4-cell stages is required for development beyond 4-cell stage. During zebrafish embryogenesis, Pou5f3 (a paralogue of mouse *Pou5f1/Oct4*) was shown to be highly actively synthesized from mRNAs deposited in oocytes in cleavage stages and promote the zygotic gene activation (ZGA) that occur at the 1,000-cell stage in this species (Leichsenring et al., 2013; Lee et al., 2013). In mouse, the major ZGA occurs during the mid-period of 2-cell stage (Hamatani et al., 2004). The results that Pou5f1/Oct4 was synthesized from maternal mRNAs and was accumulated in the nuclei of early 2-cell-stage embryos suggest the function of Pou5f1/Oct4 in the mouse ZGA. Indeed, it has been reported that inhibition of Pou5f1/Oct4 protein synthesis by injecting zygotes with MO disturbed the expression of more than 600 genes in the 2-cell stage embryos including cell cycle-, mitosis-, transcription-, and translation-related genes, and resulted in developmental arrest by 4-cell stage (Foygel et al., 2008; Tan et al., 2013). These findings strongly suggest that maternal Pou5f1/Oct4 regulates global gene expression after 2-cell stage, including ZGA. Moreover, recent study showed that depletion of zygotic *Pou5f1/Oct4* transcripts, but not maternal *Pou5f1/Oct4* transcripts by introducing MII-stage oocytes with CRISPR components resulted in more than 90% of embryos reached morula-stage (Stamatiadis et al., 2021). This finding emphasizes the importance of Pou5f1/Oct4 protein synthesized from the maternal mRNA for development beyond 4-cell stage. In contrast, knock out of maternal transcript of *Pou5f1/Oct4* was shown not to affect embryonic development in mouse (Wu et al., 2013), suggesting that maternal Pou5f1/Oct4 is not essential for the mouse ZGA. However, the deficiency of maternal Pou5f1/Oct4 would be compensated by zygotically expressed Pou5f1/Oct4, which may

be transcribed by other transcriptional factors at ZGA, or the other POU family members that are functionally redundant via genetic compensation as observed in knock out model organisms (El-Brolosy et al., 2019; Ma et al., 2019). Future studies need to address mechanisms and biological significance of the translational control of Pou5f1/Oct4 during oogenesis and early embryogenesis.

In conclusion, I showed that the *Pou5f1/Oct4* mRNA was accumulated in the oocyte cytoplasm from the primary-follicle stage in a translationally repressed state and was translated mainly after fertilization. The synthesized protein was accumulated in the nuclei of 2-cell-stage embryos. These results show for the first time the existence of post-transcriptional regulation of *Pou5f1/Oct4* gene during oogenesis and early embryogenesis. Studies of the translational control of *Pou5f1/Oct4* mRNA will contribute to understanding the regulatory mechanisms of mRNAs translated after fertilization and those promoting embryonic development by temporal translation of dormant mRNAs.

Chapter II

Mechanisms of the post-transcriptional regulation of *Pou5f1/Oct4* mRNA

ABSTRACT

Translational regulation of maternal transcripts is crucial for promoting early development including oogenesis, oocyte maturation, and embryogenesis. However, the regulatory mechanisms of maternal mRNAs in fertilized eggs remain unclear. To elucidate the mechanisms of translational regulation of maternal transcripts after fertilization, I investigated the post-transcriptional regulation of maternal *Pou5f1/Oct4* mRNA. The poly(A) tail of *Pou5f1/Oct4* mRNA was shortened during oocyte maturation, followed by elongation after fertilization. Notably, the end of 3'UTR of *Pou5f1/Oct4* mRNAs were partially deleted during oocyte maturation and the early cleavage stage. This partial degradation of 3' end increased translational activity of *Pou5f1/Oct4* mRNA. In vitro RNA pull-down assay using extracts of zebrafish oocytes showed that the shortening of the 3' end altered interactions between RNA and RNA-binding proteins (RBPs). Knockdown of Gemin5 and Dhx9, candidate RBPs that specifically bind to a short-type *Pou5f1/Oct4* 3'UTR, downregulated the expression of Pou5f1/Oct4 in early 2-cell stage embryos. These results indicate that the translation of *Pou5f1/Oct4* mRNA is regulated through the novel mechanism, that is a shortening of the 3' end of mRNA, which is accompanied by alternations in the interaction between mRNA and RBPs.

INTRODUCTION

Since fully-grown and maturing oocytes and early embryos are transcriptionally quiescent, production of proteins that are necessary for oocyte maturation and embryogenesis depends on translational regulation of maternally stored mRNAs. The regulatory mechanisms of maternal transcripts that are translationally activated during oocyte maturation, such as cyclin B1 and *c-mos* mRNAs, have been well studied (Gebauer et al., 1994; Horie and Kotani., 2016; Kotani et al., 2013; Polanski et al., 1998; Sheets et al., 1994). Overexpression and downregulation of Cyclin B1 in mouse oocytes resulted in a failure in the progression of oocyte maturation and in the formation of normal spindle at the metaphase II (MII) stage, respectively (Ledan et al., 2001; Li et al., 2018). In addition, Mos-deficient oocytes underwent germinal vesicle breakdown (GVBD) but failed to form normal spindle, resulting in parthenogenetic activation (Choi et al., 1996; Gebauer et al., 1994). These findings demonstrate the importance of the translational control of maternal transcripts for normal progression of oocyte maturation.

Cytoplasmic polyadenylation is one of the pivotal mechanisms that regulates translation. Inhibition of global cytoplasmic polyadenylation has been shown to disrupt oocyte maturation and early embryonic development (Traverso et al., 2005; Winata et al., 2018; Zhang et al., 2009). In general, a lengthened poly(A) tail increases translational activity whereas a short poly(A) tail correlates with translational repression (Reyes and Ross., 2016). It has been demonstrated that the mRNAs encoding cyclin B1, c-mos, Mad2, and Emi2 are translationally activated at the timings of polyadenylation during oocyte maturation (Cao and Richter, 2002; Gebauer et al., 1994; Horie and

Kotani, 2016; Kotani et al., 2013; Sheets et al., 1994; Takei et al., 2020, 2021; Traverso et al., 2005). A long poly(A) tail serves as binding sites for the poly(A) binding protein (PABP), which together cooperates with the eukaryotic translation initiation factor 4G (eIF4G) and the cap-binding protein eIF4E, resulting in the promotion of translation (Cao and Richter., 2002). Cytoplasmic polyadenylation is controlled by interactions between *cis*-elements within the 3' untranslated regions (UTRs) of mRNAs and *trans*-acting factors such as RNA-binding proteins (RBPs). The polyadenylation-mediated translational control has been well studied by focusing on the translational regulation of cyclin B1 mRNA using *Xenopus* oocytes. In immature oocytes, both poly(A)-specific ribonuclease PARN and poly(A) polymerase GLD2 bind to cyclin B1 mRNA (Kim and Richter., 2006). Due to the high activity of PARN, the poly(A) tail of cyclin B1 mRNA is shortened. During oocyte maturation, cytoplasmic polyadenylation element (CPE)-binding protein (CPEB), which binds to CPE of cyclin B1 mRNA, is phosphorylated. The phosphorylated CPEB recruits cleavage and polyadenylation specificity factor (CPSF) on the polyadenylation signal (PAS) in the 3'UTR of mRNA, promoting the exclusion of PARN from the mRNA, and then enabling GLD2-mediated polyadenylation (Hake and Richter., 1994; Mendez et al., 2000). Pumilio (Pum) is another RNA-binding protein that regulates the translation of target mRNAs containing pumilio-binding elements (PBEs) in *Drosophila*, *Xenopus*, zebrafish, mouse, and human. Pum can act as a translational repressor by recruiting the deadenylase CCR4-NOT complex (Van Etten et al., 2012). Moreover, recent study showed Pumilio1 (Pum1) regulate the translation of target cyclin B1 and *Mad2* mRNAs through the changes in its structures and states during oocyte maturation (Takei et al., 2020). Results from these and other studies have unveiled the mechanisms of translational control of

maternal mRNAs during oocyte maturation, whereas the regulatory mechanisms of maternal mRNAs in fertilized eggs remain unclear. Considering that thousands of maternal mRNAs are translated after fertilization (Winata et al., 2018), elucidation of the regulatory mechanisms of maternal mRNAs after fertilization will lead to better understanding of the regulatory networks of gene expression during development. In chapter I, I revealed that *Pou5f1/Oct4* mRNA was stored in oocytes in a dormant state, and the translation was activated after fertilization. However, the regulatory mechanisms of the timely translation of *Pou5f1/Oct4* mRNA are unknown.

To elucidate the regulatory mechanisms of maternal transcripts after fertilization, I investigated how the translational activation of *Pou5f1/Oct4* mRNA occurs after fertilization. I showed that the poly(A) tail of *Pou5f1/Oct4* mRNA was shortened during oocyte maturation, and interestingly it was elongated again after fertilization. I found that the end of 3'UTR was partially degraded during oocyte maturation and early cleavage stage. This partial degradation of 3' end increased translational activity of *Pou5f1/Oct4* mRNA. Since zebrafish *Pou5f3* mRNA was also shortened at 3' end during oocyte maturation, similar to *Pou5f1/Oct4* in mouse, I performed RNA pull-down assay using zebrafish oocyte extracts with in vitro-synthesized *Pou5f3* 3'UTR to elucidate the mechanisms of the translational activation. By performing RNA pull-down assay, I found that the shortening of the 3' end increased the number of RBPs, which interact with the RNA, including Gemin5 and Dhx9. Knockdown of Gemin5 and Dhx9 downregulated the expression of Pou5f1/Oct4 in early 2-cell stage embryos. These results indicate that the translation of *Pou5f1/Oct4* mRNA is regulated through shortening of the 3' end of mRNA, which may be accompanied by alternation of interactions between mRNA and RBPs.

MATERIALS AND METHODS

Poly(A) test assay

Four hundreds ng of total RNA extracted from pools of 200-300 oocytes or embryos was ligated to 0.4 μg of P1 anchor DNA primer (5'-p-GGT CAC CTT GAT CTG AAG C-NH2-3') (Invitrogen) in a 10-μl reaction using T4 RNA ligase (New England Biolabs) for 30 min at 37℃. The ligase was inactivated for 5 min at 92℃. Eight μl of the reaction was used in a 10-μl reverse transcription reaction using SuperScript III First Strand Synthesis System with a P1' primer (5'-CCT TCA GAT CAA GGT CTT TTT TTT-3'). Two μl of the cDNA was used for 1st PCR in a total volume of 25 μl with a P1' primer and a *Pou5f1/Oct4*-3'RACE-forward-1st primer (5'-GCT GTG AGC CAA GGC AAG GGA-3') for 20 cycles. One μl of the 1st PCR reaction was used for 2nd PCR in a total volume of 25 μl with a P1' primer and a *Pou5f1/Oct4*-3'RACE-forward-2nd primer (5'-TAG ACA AGA GAA CCT GGA GCT-3') for 30 cycles. I confirmed that the change of PCR product length was due to the change of poly(A) tail length by cloning the 2nd PCR products and sequencing them.

Luciferase assay

Long-type and 9 nucleotide-deleted *Pou5f1/Oct4* 3'UTRs were amplified with mouse ovary cDNA using primer sets for long-type 3'UTR, mPou5f1/Oct4 3'UTR-f (5'-ACT AGT TGA GGC ACC AGC CCT CC-3') and mPou5f1/Oct4 3'UTR-r1 (5'-TCT AGA TCT ACT GTG TGT CCC A-3'), and for 9 nucleotide-deleted 3'UTR, mPou5f1/Oct4 3'UTR-f and mPou5f1/Oct4 3'UTR-r2 (5'-TCT AGA TCC CAG TCT TTA TTT AAG AAC AA-3'). These amplicons were ligated downstream of the *firefly* luciferase gene in

a pGL3-Basic vector (Promega) at the XbaI site, and I named the resulting constructs Luc-*Pou5f1/Oct4* 3'UTR (long) and Luc-*Pou5f1/Oct4* 3'UTR (-9 nt). These constructs were digested with XhoI and XbaI sites to obtain *firefly* Luciferase-*Pou5f1/Oct4* 3'UTR fragments. The *firefly* Luciferase-*Pou5f1/Oct4* 3'UTR fragments were ligated downstream of SP6 promoter sequence in a pCS2 vector, and I named the resulting constructs SP6-Luc-*Pou5f1/Oct4* 3'UTR (long) and SP6-Luc-*Pou5f1/Oct4* 3'UTR (-9 nt). SP6-Luc-*Pou5f1/Oct4* 3'UTR (14 nucleotide-deletion; -14 nt) was generated by using a KOD-Plus-Mutagenesis Kit (TOYOBO) with SP6-Luc-*Pou5f1/Oct4* 3'UTR (long) plasmid and primer set, -14 nt-f (5'-TCT AGA TCT ATA GTG AGT CGT ATT ACG T-3') and mutagenesis-r1 (5'-GTC TTT ATT TAA GAA CAA AAT GAT G-3'). Likewise, point mutations in the 3'end of *Pou5f1/Oct4* were generated by using a KOD-Plus-Mutagenesis Kit with SP6-Luc-*Pou5f1/Oct4* 3'UTR (long) plasmid. "5'-CAC ACA GUA-3'" sequence was replaced with "(2 nt mutations); 5'-CAC AAA UUA-3'", "(5 nt mutations); 5'-CAC CAC UGA-3'" and "(9 nt mutations); 5'-ACA CAC UGC-3'" by using primer sets, 2 nt-mut-f (5'-GGA CAC AAA TTA TCT AGA TCT ATA GTG AGT CGT ATT ACG T-3') and mutagenesis-r2 (5'-CAG TCT TTA TTT AAG AAC AAA ATG ATG AGT GAC A-3'), 5 nt-mut-f (5'-GGA CAC CAC TGA TCT AGA TCT ATA GTG AGT CGT ATT ACG T-3') and mutagenesis-r2, and 9 nt-mut-f (5'-GGA ACA CAC TGC TCT AGA TCT ATA GTG AGT CGT ATT ACG T-3') and mutagenesis-r2, respectively. I named the resulting constructs SP6-Luc-*Pou5f1/Oct4* 3'UTR (2 nt-mut), SP6-Luc-*Pou5f1/Oct4* 3'UTR (5 nt-mut), and SP6-Luc-*Pou5f1/Oct4* 3'UTR (9nt-mut), respectively. Resulting plasmids were linearized with XbaI. Reporter mRNAs were synthesized using the mMESSAGE mMACHINE SP6 Transcription Kit (Ambion) and dissolved in nuclease-free distilled water. mRNA of *Renilla* Luciferase

fused with the SV40 polyA was also prepared by linearizing pRL-CMV plasmid (Promega) with BamHI, followed by mRNA synthesis by using mMESSAGE mMACHINE SP6 Transcription Kit.

The mRNAs of *firefly* Luciferase fused with the various types of *Pou5f1/Oct4* 3'UTR (50 ng/µl) and the mRNA of *Renilla* luciferase fused with the SV40 polyA (25 ng/µl) were coinjected into GV-stage oocytes in M2+ medium using a microinjector (Dmi8; Leica). The oocytes were then incubated in M2+ medium for at least 2 h. Half of the mRNA-injected oocytes were incubated with M16 medium for 14-16 h to be matured. Another half was maintained at the GV stage in milrinone-containing M16. After washing with PBS, at least 10 oocytes were collected and lysed in 10 µl Lysis Buffer (Toyo Ink, Inc.) for 15 min at room temperature. The dual-luciferase assay was carried out using the Pikka Gene Dual Assay Kit (Toyo Ink, Inc.). Ten µl of samples and 25 µl of luminescent reagents were used. Signal intensities were obtained using a TriStar LB 941 (Berthold Technologies). The intensities of firefly luciferase were normalized by the intensities of *Renilla* luciferase.

Immunoprecipitation followed by RT-PCR (IP/RT-PCR)

Mouse ovaries were homogenized with an equal volume of ice-cold extraction buffer (EB: 100 mM β-glycerophosphate, 20 mM Hepes, 15 mM $MgCl_2$, 5 mM EGTA, 1 mM dithiothreitol, 100 µM (p-amidinophenyl) methanesulfonyl fluoride, and 3 µg/ml leupeptin; pH 7.5) containing 1% Tween 20 and 100 U/ml RNase inhibitor (Invitrogen). After centrifugation at 5000 rpm for 15 min at 4 °C, the supernatant was collected and used for immunoprecipitation. Forty µl of mouse ovary extracts was incubated with 0.8 µg of anti-HuR (SANTA CRUZ; sc-5261) and 0.3 µg of anti-ELAVL2 (HuB)

(Proteintech; 14008-1-AP) antibodies and protein G Mag Sepharose (GE Healthcare) overnight at 4℃. The same volume of IgG (Jackson ImmunoResearch) was used as a control. The samples were washed five times with EB containing 1% Tween 20. After extraction of mRNAs from the beads with TRIzol reagent (Invitrogen), RT-PCR was performed using primer sets specific to *Pou5f1/Oct4*, mPou5f1/Oct4-qPCR-f and mPou5f1/Oct4-r2 (5'-CCT TCT CTA GCC CAA GCT GAT T-3'), specific to cyclin B1, mcyclin B1-f (5'-AGT CCC TCA CCC TCC CAA AAG C-3') and mcyclin B1-r (5'-AAA GCT TTC CAC CAA TAA ATT TTA TTC AAC-3'), and specific to *α-tubulin*, mα-tubulin-f (5'-GTT TGT GCA CTG GTA TGT GGG T-3') and mα-tubulin-r (5'-ATA AGT GAA ATG GGC AGC TTG GGT-3').

Alignment of *Pou5f1/Oct4* 3'UTR and *Pou5f3* 3'UTR sequences

Global alignment of RNA sequences was performed with the Needle tool from EMBOSS (https://www.ebi.ac.uk/Tools/psa/emboss_needle/) with the default settings. Sequence of the terminal 100 nucleotides of *Pou5f1/Oct4* 3'UTR (NM_013633.3), which start with "5'-GGUGGGAUGGGGAAA-3'" and end with "5'-CUGGGACACACAGUA-3'", and sequence of the terminal 100 nucleotides of *Pou5f3* 3'UTR (NM_131112.1), which start with "5'-AGUAAAUUAAAGCCA-3'" and end with "5'-ATATTTGATAATTTA-3'" and then fused with the additional sequence (not registered in the database) "5'-UUGAAACUCUGCUCUUGUCAACUCUUACAAUAACUUUUAGGUAGCAAUUAAAACAUUUUUCAUUGACAGUC-3'", were uploaded on a webserver.

RNA pull-down assay and mass spectrometry

The long-type of zebrafish *Pou5f3* 3'end and short-type of zebrafish *Pou5f3* 3'end were amplified by PCR using primer sets specific to *Pou5f3 (long)*, zPou5f3-f (5'-AAC TGG CAG CAA ATT CAA GAC-3') and zPou5f3-r1 (5'-ACT GTC AAT GAA AAA TGT TTT AAT TGC -3') and specific to *Pou5f3 (short)*, zPou5f3-f and zPou5f3-r2 (5'-TAA ATT ATC AAA TAT GGC TTT AAT TTA CTG-3'). The amplicons were inserted into pGEM-T Easy vector (Promega) by TA-cloning. The RNA-binding assay was performed using the RiboTrap Kit (MBL International) according to the manufacturer's instructions. In brief, bromouridine (BrU)-labeled RNAs of the 3'UTR of zebrafish *Pou5f3 (long)* and *Pou5f3 (short)* were generated using the Riboprobe in vitro Transcription Systems kit according to the manufacturer's protocol (Promega). Antisense probe corresponding to the *Pou5f3 (long)* was prepared as a control. Anti-BrdU antibodies were conjugated with protein A sepharose beads overnight at 4 ℃ (GE Healthcare). Then the RNAs were bound to the beads. Cytoplasmic extracts of zebrafish oocytes were transferred to tubes containing the BrU-labeled RNAs conjugated with the beads for 2 h at 4 ℃. The samples were washed with Wash BufferII, eluted with elution buffer (4% BrdU/DMSO solution in nuclease-free PBS; MBL International), and subjected to SDS-PAGE using 12.5% SDS-polyacrylamide gel. The SDS-PAGE gels were stained by silver staining with the Silver Stain MS kit (Wako Pure Chemical Industries, Ltd) to visualize the proteins associated with BrU-labeled RNAs. The bands were excised from the gel and subjected to a mass spectrometric analysis with Orbitrap Velos Pro (Thermo Fisher Scientific). For protein identification, MASCOT 2.5.1 was used for database searching against NCBInr_*Danio rerio* (updated on 05/09/2015, 39,947 sequences). The results from each run were filtered with the peptide confidence

value, in which peptides showing a false discovery rate (FDR) of less than 1% were selected. In addition, proteins identical to the sequenced peptides with the rank1 values were selected. The number of peptides identical to the proteins was more than one. I counted the number of proteins that were pulled down with the *Pou5f3 (long)* RNA probe but not with the *Pou5f3 (short)* RNA and antisense RNA probes as candidate proteins specifically binding to *Pou5f3 (long)* mRNA. Likewise, the number of proteins that were pulled down with the *Pou5f3 (short)* RNA probe but not with the *Pou5f3 (long)* RNA and antisense RNA probes were counted as candidate proteins specifically binding to *Pou5f3 (short)* mRNA. The number of proteins that were pulled down with the *Pou5f3 (long)* and *Pou5f3 (short)* RNA probes but not with the antisense RNA probe were counted as candidate proteins binding to both *Pou5f3 (long)* and *Pou5f3 (short)* mRNAs. Gene ontology (GO) analysis was performed using DAVID Bioinformatics Resources 6.8 (https://david.ncifcrf.gov/).

RT-PCR

Total RNA from ovaries and oocytes was extracted by using TRIzol reagent (Invitrogen) according to the manufacturer's instructions. Reverse transcription was performed with SuperScript III First Strand Synthesis System (Invitrogen) using oligo (dT) primer. The *Gemin5* transcript was amplified with the cDNA and a primer set specific to *Gemin5*, mGemin5-f (5'- AAC TTC ACC CTC ATG CAG GAA ATC-3') and mGemin5-r (5'-CGT GTG CCG ACT CTG GCA GTG-3'). The *Dhx9* transcript was amplified with the cDNA and a primer set specific to *Dhx9*, mDhx9-f (5'-GAA GAA GAC ACC TGA ATC ATG-3') and mDhx9-r (5'-AGG AAA ACT TTG TAA GGC TCC AC-3').

Production of antibodies

DNA sequences encoding a part of mouse Gemin5 (residues 1250-1500 a.a.) and Dhx9 (residues 100-200 a.a.) were amplified by PCR and ligated into pGEX-KG vector at EcoRI and SalI sites to produce a GST-tagged proteins. The recombinant proteins were expressed in *E. coli* (XL1) and purified by SDS-PAGE, followed by electroelution in Tris-glycine buffer without SDS. The purified proteins were dialyzed against 1 mM HEPES (pH 7.5), lyophilized, and used for injection into two mice. The obtained antisera were affinity-purified with recombinant GST-Gemin5 or GST-Dhx9 protein electroblotted onto a membrane (Immobilon; EMD Millipore).

Immunoblotting

The crude extracts from 30 oocytes and embryos were separated by SDS-PAGE with Bolt 4-12% Bis-Tris Plus gels (Novex) and blotted onto an Immobilon membrane using a Bolt Mini Blot Module (Novex). The membranes were blocked with 5% skim milk in Tris buffered saline (TBS; 20 mM Tris and 150 mM NaCl; pH 7.5) containing 0.1% Tween 20 (TTBS) for 15 min at room temperature. Then, the membranes were incubated with anti-Gemin5, anti-Dhx9 (1:50; this study) or anti-γ-tubulin (1:1000; Sigma T6557) antibody overnight at room temperature. After being washed three times with TTBS, the membranes were incubated with an anti-mouse IgG secondary antibody fused with alkaline phosphatase (1:1000; American Qualex) for 2 h at 37˚C. After being washed three times with TTBS, the membranes were incubated with NBT and BCIP in diethanolamine buffer (100 mM diethanolamine, 5 mM $MgCl_2$; pH 9.5) to detect signals.

Immunofluorescence

Oocytes and embryos were fixed with 2% PFA for 20 min followed by permeabilization in 0.25% Triton X-100 for 10 min at room temperature. Samples were then incubated with a blocking/washing solution for 1 h at room temperature and incubated with the anti-Pou5f1/Oct4 antibody (1:100; Santa Cruz; C-10; in Fig. 6A and B, 1:100; Abcam; ab181557; in Fig. 13D), anti-Gemin5 antibody (1:50; this study), and anti-Dhx9 antibody (1:50; this study) for overnight at 4˚C. The samples were washed with blocking/washing solution and then incubated for 1 h at room temperature with Alexa Flour 488-conjugated anti-mouse or rabbit IgG secondary antibody (1:200; Molecular Probes). After being washed with washing solution, the samples were mounted with VECTASHIELD Mounting Medium with DAPI (Funakoshi) and observed under the LSM 980 confocal microscope with the Plan Apochromat 63x/1.4 NA oil differential interference contrast lens using ZEN software.

Trim21-mediated protein degradation

Plasmid pGEMHE-mCherry-mTrim21 (Addgene plasmid # 105522) was linearized with AscI. *mCherry-Trim21* mRNA was synthesized using the mMESSAGE mMACHINE T7 Transcription Kit (Ambion) and dissolved in nuclease-free distilled water. Eight pl of 200 ng/µl mRNA was injected into GV-stage oocytes or 1-cell stage embryos using the IM-9B microinjector under the Dmi8 microscope and incubated in M2+ medium (oocytes) or M2- medium (zygotes) for 3 h to allow mTrim21 protein expression. 100 ng/µl anti-Gemin5 antibody or 500 ng/µl anti-Dhx9 antibody was injected into the mCherry-Trim21-expressing oocytes/zygotes and incubated in M2+ medium (oocytes) or M16 + EDTA (zygotes). The oocytes were incubated for 16 h and

then analyzed by immunoblotting. The embryos were collected at an early period of the 2-cell stage and then analyzed by immunofluorescence. For luciferase assay following knockdown of Gemin5 or Dhx9, mCherry-Trim21-expressing oocytes were injected with the mixtures of reporter mRNAs and antibody; the mixture containing mRNAs of firefly luciferase fused with the *Pou5f1/Oct4* 3'UTR (Short; -14 nt) (50 ng/µl), mRNA of *Renilla* luciferase fused with the SV40 polyA (25 ng/µl), and antibody (anti-Gemin5; 50 ng/µl, anti-Dhx9; 250 ng/µl). Signal intensities were obtained using the TriStar LB 941.

Computational prediction of RNA secondary structure

RNA secondary structure prediction was performed using MXFold2 (http://www.dna.bio.keio.ac.jp/mxfold2/) (Sato et al., 2021). The RNA sequences of zebrafish *Pou5f3* 3'UTR used for RNA pull-down assay and full length of mouse *Pou5f1/Oct4* 3'UTRs were uploaded on the web server using default settings.

RESULTS

Changes in poly(A) tail length and the end of the 3' untranslated region of *Pou5f1/Oct4* mRNA

In chapter I, I revealed that Pou5f1/Oct4 protein was synthesized from mRNAs stored in oocytes and was accumulated in the nuclei of early 2-cell stage embryos. However, the mechanisms of the translational regulation of *Pou5f1/Oct4* mRNA remained elusive. I investigated the changes in poly(A) tail length of *Pou5f1/Oct4* mRNA during oocyte maturation and cleavage stages after fertilization. Poly(A) test assay showed that the poly(A) tails of *Pou5f1/Oct4* mRNA became shortened during oocyte maturation (Fig. 8A). Since the Pou5f1/Oct4 protein was first detected at the early 2-cell stage, I then examined the changes of poly(A) tail length at the early 2-cell stage. I confirmed that the poly(A) tails of *Pou5f1/Oct4* mRNA became shortened during oocyte maturation and subsequently elongated again at the early 2-cell stage (Fig. 8B). The length of poly(A) tails was longer in GV-stage oocytes, in which Pou5f1/Oct4 protein was not detected, than that in early 2-cell stage embryos, in which certain levels of Pou5f1/Oct4 were detected (Fig. 8B). This result is contradictory to the general understanding that a short poly(A) tail is associated with translational silencing in early stages of development (Weill et al., 2012).

To reveal the mechanisms of translational regulation of *Pou5f1/Oct4* mRNA in more details, I investigated the sequences of 3' untranslated region (UTR) of *Pou5f1/Oct4* mRNAs. I found that several nucleotides at the 3' end of *Pou5f1/Oct4* mRNA were deleted in oocytes at the MII stage. Moreover, the number of deleted sequences increased in early 2-cell stage embryos (Fig. 8C). The average length of poly(A) tails

was 60 nucleotides in oocytes at the GV stage, whereas it was decreased into 7 nucleotides in oocytes at the MII stage. The average length of poly(A) tails was increased to 35 nucleotides in embryos at the early 2-cell stage (Fig. 8C and D).

Effect of shortening in *Pou5f1/Oct4* mRNA 3'UTR on translational activity

To elucidate the relation between the processing of 3'UTR of *Pou5f1/Oct4* mRNA and the translational activity, I analyzed translational efficiency by injecting oocytes with reporter constructs containing the long-type and short-type 3'UTRs of *Pou5f1/Oct4*, which were fused to the Firefly luciferase coding region (Fig. 9A and B). I prepared reporter constructs carrying 9 and 14 nucleotide-deletion at the end of *Pou5f1/Oct4* 3'UTRs as short-type 3'UTRs, since 9 nucleotide-deletion was the processing most frequently observed in oocytes and embryos and 14 nucleotide-deletion was the maximum length of deletion that found in early cleavage-stage embryos (Fig. 8C).

In GV-stage oocytes, the reporter RNA carrying short-type *Pou5f1/Oct4* 3'UTR showed little or no differences in luciferase activities between that of reporter RNA carrying long-type *Pou5f1/Oct4* 3'UTR (Fig. 9C). On the other hand, in MII-stage oocytes, the luciferase activities of reporter RNAs carrying short-type *Pou5f1/Oct4* 3'UTR significantly increased, which is dependent on the length of deletion (Fig. 9C). These results suggest that the shortening of 3'end promotes translational activation of *Pou5f1/Oct4* mRNA in MII-stage oocytes. However, Pou5f1/Oct4 protein was not detected in MII-stage oocytes (Fig. 3A-C). On the other hand, the amounts of *Pou5f1/Oct4* mRNA in the polysomal fraction were gradually increased through oocyte maturation and first cleavage stage (Fig. 5). These results suggest that the translational

activity of *Pou5f1/Oct4* mRNA was elevated, but not reached sufficient level for detection of Pou5f1/Oct4 protein in MII-stage oocytes.

To investigate the relation between the sequences in the end of 3'UTR and translational activity, I injected oocytes with reporter constructs carrying *Pou5f1/Oct4* 3'UTRs with mutations in the 3'end (Fig. 9A and D). In GV-stage oocytes, the luciferase activity of a reporter RNA carrying 9 nucleotides mutations in *Pou5f1/Oct4* 3'UTR was higher than that of a reporter RNA carrying long-type *Pou5f1/Oct4* 3'UTR (> 2.5-fold) (Fig. 9E). In MII-stage oocytes, luciferase activities of reporter RNAs carrying *Pou5f1/Oct4* 3'UTR with 2 and 9 nucleotide-mutations were higher than that of a reporter RNA carrying long-type *Pou5f1/Oct4* 3'UTR. However, the differences in the luciferase activities were small (< 2-fold) (Fig. 9E). These results indicate that the sequences in 3'end mainly contribute to translational repression of *Pou5f1/Oct4* mRNA in GV-stage oocytes.

HuR and HuB bind to both *Pou5f1/Oct4* and cyclin B1 mRNAs

To elucidate the mechanisms of the translational regulation of *Pou5f1/Oct4* mRNA, I analyzed RBPs that bind to *Pou5f1/Oct4* mRNA. Considering that *Pou5f1/Oct4* mRNA formed granules in oocytes, I first analyzed the interaction of HuR and HuB proteins with *Pou5f1/Oct4* and cyclin B1 mRNAs. HuR and HuB are known to be components of stress granules and are expressed in oocytes (Colombrita et al., 2013; Hinman and Lou, 2008; Kato et al., 2019; Kotani et al., 2013) and HuR was shown to be colocalized with cyclin B1 RNA granules in zebrafish oocytes (Kotani et al., 2013). RT-PCR analysis after immunoprecipitation using mouse ovary extracts and anti-HuR and anti-

HuB antibodies showed that HuR and HuB bound to both *Pou5f1/Oct4* and cyclin B1 mRNAs (Fig. 10A and B).

Identification of proteins binding to *Pou5f1/Oct4* mRNA

Previous studies indicated that accurate translational control of mRNAs is accomplished by the assembly of common and specific components of ribonucleoproteins (RNPs) (Kotani et al., 2013; Takei et al., 2020, 2021). To isolate proteins specifically regulating the long- and short-type *Pou5f1/Oct4* mRNA, respectively, I performed an RNA pull-down assay. In this assay, I used zebrafish oocytes and *in vitro*-synthesized RNAs of zebrafish *Pou5f3* 3'UTR (a paralogue of mouse *Pou5f1/Oct4*) since sufficient materials were not obtained by using mouse oocytes. The 3' end of zebrafish *Pou5f3* mRNA was deleted by approximately 70 nucleotides during oocyte maturation (data not shown) (Fig. 11A). The sequences of the terminal 100 nucleotides of *Pou5f1/Oct4* 3'UTR and *Pou5f3* 3'UTR shared 43.1% identity (Fig. 11B). BrU-labelled RNA of *Pou5f3* 3'UTR (long-type and short-type; 70 nucleotide-deleted) associated proteins were isolated from cytoplasmic extracts of oocytes by immunoprecipitation with anti-BrdU antibody, fractionated by SDS-PAGE, and detected by silver staining. The bands were excised from the gel and analyzed by mass spectrometry. Mass spectrometry analysis identified 71 candidate proteins specifically bind to long-type *Pou5f3* 3'UTR, 139 candidate proteins specifically bind to short-type *Pou5f3* 3'UTR, and 50 candidate proteins bind to both long- and short-type *Pou5f3* 3'UTRs (Fig. 11C). Gene ontology (GO) terms of these proteins were associated with RNA splicing and translation (Fig. 11D). To select the candidate proteins specifically regulating the long- and short-type *Pou5f1/Oct4* mRNA,

respectively, I compared the number of peptides detected by mass spectrometry in the extracts incubated with long- and short-type *Pou5f3* 3'UTRs. First, 10 proteins were selected as candidates of RNA-binding proteins which predominantly interact with long- or short-type *Pou5f3* 3'UTR (Table 1). Second, I focused on Gemin5 and Dhx9 since these proteins have been reported to activate translation of specific mRNAs, and the number of peptides detected by mass spectrometry with short-type *Pou5f3* 3'UTR was larger than that with long-type *Pou5f3* 3'UTR (Table 1).

Expression of Gemin5 in mouse oocytes and embryos

Gemin5 was isolated as the candidate protein that predominantly binding to the short-type *Pou5f1/Oct4* mRNA. Gemin5 is known to regulate small nuclear ribonucleoproteins (snRNPs) assembly and mRNA translation (Battle et al., 2006; Fernandez-Chamorro et al., 2014; Francisco-Velilla et al., 2018; Pacheco et al., 2009; Ramajo and Ferna., 2013; Yong et al., 2010). Gemin5 was shown to regulate translation of survival motor neuron (*SMN*) mRNA through binding to the 3'UTR of the mRNA in cultured cells (Workman et al., 2015). I first analyzed the expression of Gemin5 in mouse oocytes at the GV-stage. RT-PCR and immunoblotting analyses showed the expression of *Gemin5* mRNA and that of Gemin5 protein in GV-stage oocytes (Fig. 12A and B). Since many extra bands were observed in immunoblotting analysis, I confirmed the specificity of the antibody by performing knockdown of Gemin5 by using the Trim-Away protein degradation system (Clift et al., 2017; Israel et al., 2019) with the anti-Gemin5 antibody. This system allows degradation of an endogenous protein by TRIM-mediated degradation of the antibody-target protein complex. I injected GV-stage oocytes with *mCherry-Trim21* mRNA and anti-Gemin5 antibody, subsequently

incubated with M2+ medium for 16 h. As a result, the band specific to Gemin5 was reduced, whereas other extra bands were not affected, indicating the high specificity of the antibody (Fig. 12C). To analyze the expression and localization of Gemin5 protein in oocytes and early cleavage-stage embryos, I performed immunofluorescence analysis. Immunofluorescence analysis showed that Gemin5 was expressed in the cytoplasm in GV- and MII-stage oocytes and 2-cell stage embryos. Additionally, Gemin5 was localized around the chromosome in MII-stage oocytes, and in the nucleus in 2-cell stage embryos (Fig. 12D).

Expression of Dhx9 in mouse oocytes and embryos

Dhx9 (also known as RNA helicase A, RHA) was isolated as another candidate protein that predominantly binds to the short-type *Pou5f1/Oct4* mRNA. Dhx9 is an NTP-dependent RNA helicase protein that plays roles in various cellular processes such as transcription, splicing, and translation (Lee and Pelletier., 2016). Dhx9 was reported to be involved in the regulation of *Pou5f1/Oct4* mRNA in ES cells (Qiu et al., 2009). To elucidate the expression of Dhx9 in mouse oocytes, I performed RT-PCR and immunoblotting analyses. These analyses revealed the expression of *Dhx9* mRNA and that of Dhx9 protein in oocytes at the GV-stage (Fig. 13A and B). Since many extra bands were observed in immunoblotting analysis, I confirmed the specificity of the antibody by performing knockdown of Dhx9 by using the Trim-Away protein degradation system with the anti-Dhx9 antibody. The Trim-Away protein degradation with the anti-Dhx9 antibody caused reduction of the band specific to Dhx9, whereas other extra bands were not affected, indicating the high specificity of the antibody (Fig. 13C). Immunofluorescence analysis showed the high expression of Dhx9 protein in the

nucleus in GV-stage oocytes and 2-cell stage embryos, whereas the low levels of Dhx9 was detected in the cytoplasm in GV- and MII-stage oocytes and 2-cell stage embryos (Fig. 13D).

Gemin5 and Dhx9 are required for the synthesis of Pou5f1/Oct4 in oocytes and early cleavage-stage embryos

To assess whether Gemin5 and Dhx9 play a role in the regulation of *Pou5f1/Oct4* mRNA, I performed knockdown of Gemin5 and Dhx9 by using the Trim-Away protein degradation system with the anti-Gemin5 and anti-Dhx9 antibodies. As shown in Fig. 12C and 13C, Gemin5 and Dhx9 were efficiently degraded by this degradation system (see also Fig. 14A and B). I first analyzed the effect of knockdown of Gemin5 and Dhx9 on translational activities of *Pou5f1/Oct4* mRNA by injecting oocytes with reporter constructs containing the short-type (-14 nt) 3'UTR of *Pou5f1/Oct4* fused with the Firefly luciferase coding region. Translational activity of the reporter construct was not affected by Gemin5 knockdown, whereas significantly decreased by Dhx9 knockdown (Fig. 14C). Then I analyzed the effect of knock down of Gemin5 and Dhx9 on the expression of Pou5f1/Oct4. Knock down of Gemin5 and Dhx9 in 1-cell stage embryos resulted in downregulation of Pou5f1/Oct4 expression in the early 2-cell stage embryos (Fig. 14D).

DISCUSSION

In chapter I, I showed that the *Pou5f1/Oct4* mRNA accumulates in the oocytes during mouse oogenesis in a translationally repressed form and is translated after fertilization. However, the regulatory mechanisms of the timely translation of maternal *Pou5f1/Oct4* mRNA remained unknown. I showed that the *Pou5f1/Oct4* mRNAs had a long poly(A) tail (average length; 60 nt) in GV-stage oocytes, whereas the poly(A) tail length was shortened (average length; 7 nt) in MII-stage oocytes. After fertilization, the poly(A) tail was readenylated (average length; 35 nt) until early 2-cell stage (Fig. 8C and D). Considering that the Pou5f1/Oct4 protein was not expressed in GV-stage oocytes whereas expressed in early 2-cell stage embryos, there was a contradiction to the general understanding that the long poly(A) tail correlates with the active translation. Sequencing analysis revealed that the end of the *Pou5f1/Oct4* mRNA 3'UTR was deleted during oocyte maturation and early cleavage stage (Fig. 8C). Since there were several patterns in the lengths of 3'UTR in MII-stage oocytes and early 2-cell stage embryos, this shortening may be caused by activities of exonucleases such as CCR4-NOT and Pan2/Pan3 (Ma et al., 2015; Vieux and Clarke., 2018). Luciferase assay showed that the mutation in 9 nucleotides of the 3' end of *Pou5f1/Oct4* 3'UTR showed high translational activity, whereas the mutations in 2 and 5 nucleotides of the *Pou5f1/Oct4* 3'UTR showed little effects in translational activities in GV-stage oocytes (Fig. 9E). Moreover, the deletion of 3' end of *Pou5f1/Oct4* 3'UTR dramatically increased the translational activity whereas the translational activity of long-type of *Pou5f1/Oct4* 3'UTR was low in MII-stage oocytes (Fig. 9C). These results indicate that the regulatory sequences in the end of the *Pou5f1/Oct4* 3'UTR repress translation in

GV-stage oocytes and shortening of the 3' end activates the translation of *Pou5f1/Oct4* mRNA in MII-stage oocytes. Taken together, these results suggest that long-type 3'UTR represses the translation of *Pou5f1/Oct4* mRNA in growing and immature oocytes, and the shortening of the 3' end activates the translation during oocyte maturation and early cleavage stages.

Using in vitro-synthesized RNAs, I showed that 71 proteins specifically bound to long-type *Pou5f3* 3'UTR, 139 proteins specifically bound to short-type *Pou5f3* 3'UTR, and 50 proteins bound to both long- and short-type *Pou5f3* 3'UTRs (Fig. 11C). These results suggest that shortening of the 3'UTR of zebrafish *Pou5f3* significantly altered the interactions between RNA and RBPs in vitro. IP/RT-PCR showed that HuR and HuB bound to *Pou5f1/Oct4* mRNA (Fig. 10A and B). HuR and HuB are known to be components of stress granules and thought to regulate mRNA stability and translation (Chalupnikova et al., 2014; Fujimura et al., 2009; Gallouzi et al., 2000; Markmiller et al., 2018; Papadopoulou et al., 2013). HuR and HuB were also detected by mass spectrometry analysis as candidate proteins that bind to *Pou5f3* 3'UTR. Mass spectrometry analysis indicated that HuR predominantly bound to long-type *Pou5f3* 3'UTR, whereas HuB bound to both long- and short-type *Pou5f3* 3'UTRs (Table 1). Thus, HuR and HuB may play roles in regulation of *Pou5f1/Oct4* mRNA, whereas the functions of these proteins may be different. One possible explanation is that HuR promotes formation of RNA granules and represses the translation of long-type *Pou5f1/Oct4* mRNA, whereas HuB regulates stability of both long- and short-type *Pou5f1/Oct4* mRNAs.

Notably, the number of proteins bound to short-type 3'UTR was approximately 2-fold larger than that of proteins bound to long-type 3'UTR. Computational analysis showed

that the secondary structures of the 3' end were different between long-type and short-type 3'UTRs in both *Pou5f3* and *Pou5f1/Oct4* (Fig. 15A and B). Previous studies have shown that the interactions between RNAs and RBPs are modulated by not only sequence motifs but also secondary structures of RNAs both in vitro and in vivo (Gosai et al., 2015; Taliaferro et al., 2016). Thus, the differences found in the proteins interacting with long-type and short-type 3'UTRs might be caused by differences in higher-order structures of RNA. Interestingly, the computational prediction showed that small hairpin-loop was formed at the end of long-type 3'UTRs of *Pou5f3* and *Pou5f1/Oct4*, but this secondary structure was disappeared in short-type 3'UTRs (Fig. 15A and B). Moreover, the small hairpin-loop at the 3' end was disappeared in 2 and 9 nucleotide-mutated *Pou5f1/Oct4* 3'UTRs (Fig. 15C, left and right). Although a new hairpin-loop was formed in the 3' end region of 9 nucleotide-mutated 3'UTR, the size and constituents of the hairpin-loop was different from that of long-type 3'UTR (Fig. 15 B, left and C, right). In contrast, 5 nucleotide-mutated *Pou5f1/Oct4* 3'UTR formed a small hairpin-loop at the 3' end region with some of the same constituents as that of long-type 3'UTR (Fig. 15B, left and C, middle). Luciferase assay showed that the 2 and 9 nucleotide-mutations in the end of *Pou5f1/Oct4* 3'UTR increased the translational activity of mRNA, whereas the 5 nucleotide-mutation did not activate the translation of mRNA in oocytes (Fig. 9D and E). These results suggest that the small hairpin-loop at the 3' end region may play a key role in translational repression of long-type *Pou5f1/Oct4* mRNA.

Gemin5 and Dhx9 were isolated as proteins that specifically bound to short-type *Pou5f3* mRNA by the RNA pull-down assay using extracts of zebrafish oocytes followed by mass spectrometry analysis. Both Gemin5 and Dhx9 were expressed in

mouse oocytes and early cleavage-stage embryos (Fig. 12 and 13). Knockdown of Dhx9 inhibited both the translational activation of reporter mRNA, which carries short-type *Pou5f1/Oct4* 3'UTR in oocytes and the expression of Pou5f1/Oct4 in the early 2-cell stage embryos (Fig. 14C and D). On the other hand, knockdown of Gemin5 did not affect the translational activity of the reporter mRNA in oocytes whereas attenuated the expression of Pou5f1/Oct4 in the early 2-cell stage embryos (Fig. 14C and D). One possible explanation for the difference in the timing of the effects observed by Gemin5 and Dhx9 knockdown is that Dhx9 plays roles in translational activation of *Pou5f1/Oct4* mRNA in oocytes and early cleavage-stage embryos, whereas Gemin5 participates in the regulation of *Pou5f1/Oct4* mRNA at a stage later than that of Dhx9. This difference in the period of *Pou5f1/Oct4* mRNA regulation by these RBPs might be caused by the differences in the timing of RNA-RBP (including co-factors) binding, which may occur through gradual changes in RNA structures and/or the differences in the timing of activation of the RBPs.

Dhx9 has been shown to activate translation of specific mRNAs that contain highly structured 5'UTRs (Bolinger et al., 2007; Hartman et al., 2006). It has been proposed that binding of Dhx9 to the highly structured region of mRNA stimulates RNA-RNA and RNA-protein rearrangements that contribute to efficient translation (Bolinger et al., 2007; Hartman et al., 2006). Thus, it is possible that Dhx9 specifically recognizes the unique structures of short-type 3'UTR of *Pou5f1/Oct4* mRNA and binds them. It has also been reported that Dhx9 activates translation of *Pou5f1/Oct4* mRNA in cooperation with Lin28 and eIF3β in human ES cells (Qiu et al., 2009). The previous study postulated that Lin28 selectively binds to the target RNA and subsequently recruit eIF3β and Dhx9 to enhance translation initiation and to remodel the RNP during translation,

respectively (Qiu et al., 2009). Since Lin28 has been reported to be expressed in mouse oocytes and early cleavage-stage embryos (Flemr et al., 2014), the Lin28-eIF3β-Dhx9 complex might contribute to the post-transcriptional regulation of *Pou5f1/Oct4* mRNA during oocyte maturation and early cleavage stages.

In addition to Dhx9, I identified Gemin5 as a novel candidate protein that regulates the translation of *Pou5f1/Oct4* mRNA. Gemin5 has been reported to bind to target small nuclear RNAs (snRNAs) and mRNAs through its C-terminal region by recognizing a set of sequences and secondary structures of RNA (Fernandez-Chamorro et al., 2014; Francisco-Velilla et al., 2018; Ramajo and Ferna., 2013; Workman et al., 2015). These findings support the hypothesis that Gemin5 specifically recognizes the set of sequences and secondary structures of short-type *Pou5f1/Oct4* 3'UTR. Knockdown of Gemin5 did not inhibit the translational activation of reporter mRNA carrying short-type *Pou5f1/Oct4* 3'UTR in oocytes, whereas inhibited the expression of Pou5f1/Oct4 in early 2-cell stage embryos (Fig. 14C and D). Previous study showed that Gemin5 binds to 3'UTR and activates the translation of *SMN* mRNA in cultured cells (Workman et al., 2015). These findings suggest that Gemin5 acts as a translational activator of *Pou5f1/Oct4* mRNA. However, the results that the knockdown of Gemin5 inhibited the expression of Pou5f1/Oct4 protein in the early 2-cell stage embryos, but not inhibited the translational activation of reporter mRNA carrying short-type *Pou5f1/Oct4* 3'UTR (Fig. 14C and D) might reflect the possible role of Gemin5 in the protection of Pou5f1/Oct4 protein from degradation. Further work will be necessary to unveil the function of Gemin5 in the regulation of Pou5f1/Oct4 expression. In addition, it remains unclear whether Gemin5 and Dhx9 bind to *Pou5f1/Oct4* mRNA in mouse oocytes and

embryos. Thus, subsequent experiments are needed to determine the binding ability of these proteins to *Pou5f1/Oct4* mRNA.

In conclusion, I have discovered a novel mechanism of translational regulation, that is the shortening of the 3' end of *Pou5f1/Oct4* mRNA, which are accompanied by alternation of interactions between mRNA and RBPs. Considering the possible significance of the expression of Pou5f1/Oct4 in the early 2-cell stage embryos for smooth progression of embryonic development, this novel mechanism of translational regulation might be an essential regulatory mechanism for precise translational control of maternal transcripts after fertilization. Further studies including molecular analyses to identify the accurate functions of the RBPs in the regulation of *Pou5f1/Oct4* mRNA, and the mechanisms of the shortening of 3'UTR will make a meaningful contribution to understanding the overview of this new translational regulation mechanism.

GENERAL DISCUSSION

The mechanisms of translational regulation of maternal transcripts have extensively studied focusing on mRNAs encoding genes which are translationally activated during oocyte maturation. These studies have revealed that trans-acting factors such as CPEB1 and Pum1 regulate translation of target mRNAs via changes in their activities by phosphorylation during oocyte maturation (Kim and Richter, 2006; Mendez et al., 2000; Saitoh et al., 2018; Takei et al., 2020). In addition, it has been becoming clear that there is a potential regulatory mechanism of translation via assembly and disassembly of RNA granules during oocyte maturation (Horie and Kotani, 2016; Kotani et al., 2013; Takei et al., 2021). While extensive studies have revealed the regulatory mechanisms of maternal transcripts during oocyte maturation, little is known about the regulatory mechanisms of maternal transcripts after fertilization.

In this study, I showed that the dormant *Pou5f1/Oct4* mRNA was accumulated in oocytes and formed granule structures in the cytoplasm (Fig. 1C). The mRNA was disassembled during oocyte maturation, followed by protein synthesis in the early 2-cell stage embryos (Fig. 2 and 3). These results suggest that the granular structures of *Pou5f1/Oct4* mRNA may function to stably repress the translation of *Pou5f1/Oct4* mRNA. The poly(A) tail of *Pou5f1/Oct4* mRNA was shortened during oocyte maturation, followed by readenylation until early 2-cell stage (Fig. 8C and D). In addition, the end of the *Pou5f1/Oct4* mRNA 3'UTR was deleted in MII-stage oocytes and early 2-cell stage embryos (Fig. 8C). Luciferase assay showed that the deletion of 3' end of *Pou5f1/Oct4* 3'UTR significantly increased the translational activity in MII-stage oocytes (Fig. 9C). These results suggest that changes in the length of 3'UTR regulate

the translation of *Pou5f1/Oct4* mRNA. Together, the shortening of the 3' end and the disassembly of granular structures of *Pou5f1/Oct4* mRNA during oocyte maturation and early cleavage should activate the translation of mRNA, resulting in the synthesis of Pou5f1/Oct4 protein in the early 2-cell stage embryos. However, Pou5f1/Oct4 protein was not detected in MII-stage oocytes, in which short-type *Pou5f1/Oct4* mRNA existed and the granular structures of mRNA were disassembled (Fig. 2, 3, and 8C). This might be due to the insufficient deletion of 3' end and polyadenylation of the *Pou5f1/Oct4* mRNA in this stage, and due to the indirect involvement of granular structures of mRNA in translational repression. The number of reads that had more than 9 nucleotide-deleted 3'UTR was only 4 out of 9 (44.4%) in MII-stage oocytes, whereas 7 out of 11 (63.6%) in early 2-cell stage embryos (Fig. 8C). Since the increases in the translational activity was dependent on the length of deletion (Fig. 9C), the low occupancy of highly processed *Pou5f1/Oct4* mRNA should be one of the reasons for the little synthesis of Pou5f1/Oct4 protein in MII-stage oocytes. Poly(A) tails of *Pou5f1/Oct4* mRNA were short in MII-stage oocytes (average length; 7 nt), whereas they became long in early 2-cell stage embryos (average length; 35 nt) (Fig. 8C and D). This difference in the length of poly(A) tail should also cause the translational repression in MII-stage oocytes and translational activation in early 2-cell stage embryos. In addition, previous study have reported that formation of RNA granule was not essential for translational repression of cyclin B1 mRNA in oocytes, rather, seemed to be necessary for maintaining their dormant state until the timing of translational activation (Kotani et al., 2013). This finding supports the explanation that granular structure of *Pou5f1/Oct4* mRNA assists translational repression in GV-stage oocytes, whereas the disassembly of RNA granules is not sufficient to activate translation of *Pou5f1/Oct4* mRNA in MII-stage oocytes.

Notably, the length of poly(A) tails was longer in GV-stage oocytes, in which Pou5f1/Oct4 protein was not detected, than that in early 2-cell stage embryos, in which Pou5f1/Oct4 protein was significantly detected (Fig. 3B and C, see also Fig. 8B-D). One possible explanation for this contradiction with the general understanding, that a long poly(A) tail is associated with translational activation, is that the translational silencing caused by long-type 3'UTR is predominant, compared with the translational activation caused by long poly(A) tail, in GV-stage oocytes. Since the poly(A) tail regulates not only translation but also stability of mRNA (Guhaniyogi and Brewer, 2012), the long poly(A) tail of *Pou5f1/Oct4* mRNA observed in GV-stage oocytes might function in protecting mRNA from decay during oogenesis. Together, these results suggest that the translational activity of *Pou5f1/Oct4* mRNA is gradually elevated through oocyte maturation and early cleavage, and then certain levels of Pou5f1/Oct4 protein are synthesized in early 2-cell stage embryos. The result that gradual increase of *Pou5f1/Oct4* mRNA in polysomal fraction during oocyte maturation and early cleavage supports this model (Fig. 5).

Our laboratory showed that the 3' end of zebrafish *Pou5f3* mRNA was deleted during oocyte maturation similarly to mouse *Pou5f1/Oct4* mRNA, whereas the length of deletion was different (*Pou5f1/Oct4*; 9-14 nt, and *Pou5f3*; 70 nt), suggesting that a similar mechanism of translational regulation exists in fish and mammalian development. Mass spectrometry analysis identified 71, 139, and 50 proteins as candidates that bind to long-type, short-type, and both *Pou5f3* 3'UTRs, respectively, suggesting that shortening of the 3'UTR altered the interactions between RNA and RBPs (Fig. 11 C). In these proteins, I identified Gemin5 and Dhx9 as candidates that specifically bind to short-type 3'UTR of *Pou5f3* mRNA. Since knockdown of Gemin5

and Dhx9 downregulated the expression of Pou5f1/Oct4 protein in early 2-cell stage embryos in mouse (Fig. 14D), these proteins may play roles in activating translation of *Pou5f1/Oct4* mRNA by binding to short-type 3'UTR. In addition, mass spectrometry analysis showed several components of cytoplasmic RNA granule such as Zar1, HuR, and IMP1 predominantly bound to long-type 3'UTR, rather than short-type 3'UTR (Hu et al., 2010; Kotani et al., 2013; Markmiller et al., 2018; Moschner et al., 2014) (Table 1). In contrast, other components of cytoplasmic RNA granule such as TIA1 and HuB bound to both long- and short-type 3'UTRs (Díaz-Muñoz et al., 2017; Markmiller et al., 2018; Piotrowska et al., 2010) (Table 1). These results propose the new mechanisms of translational regulation that shortening of the 3' end of *Pou5f1/Oct4* mRNA causes the dynamic alternation in interactions between mRNA and RBPs, including components of RNA granules and translational regulators, resulting in disassembly of RNA granules and translational activation of mRNA. This translational regulation may allow the temporal expression of Pou5f1/Oct4 protein in the early 2-cell stage embryos, and the synthesized Pou5f1/Oct4 protein should play roles in regulating global gene expression in later developmental stages.

Protein synthesis from maternal transcripts in the early-stage of embryos is essential for progression of embryo development (Aanes et al., 2011; Winata et al., 2018). Although thousands of maternal transcripts were shown to be translated after fertilization (Winata et al., 2018), little is known about the mechanisms of translational regulation of maternal mRNAs during embryogenesis. Thus, the novel mechanism of translational regulation described here will contribute to understanding the regulatory mechanisms of maternal transcripts after fertilization. In addition, our laboratory showed that the 3' end of zebrafish *Pou5f3* mRNA is shortened during oocyte

maturation as in the case of mouse *Pou5f1/Oct4* mRNA. Therefore, I expect that the novel mechanisms described here in mouse development contribute to an understanding of the mechanisms of translational regulation during development in broad range of species.

REFERENCES

Aanes, H., Winata, C. L., Lin, C. H., Chen, J. P., Srinivasan, K. G., Lee, S. G. P., Lim, A. Y. M., Hajan, H. S., Collas, P., Bourque, G., Gong, Z., Korzh, V., Aleström, P., and Mathavan, S. (2011). Zebrafish mRNA sequencing deciphers novelties in transcriptome dynamics during maternal to zygotic transition. *Genome Research*, *21*(8), 1328–1338. https://doi.org/10.1101/gr.116012.110

Abe, K., Inoue, A., Suzuki, M. G., and Aoki, F. (2010). Global gene silencing is caused by the dissociation of RNA polymerase II from DNA in mouse oocytes. *Journal of Reproduction and Development*, *56*(5), 502–507. https://doi.org/10.1262/jrd.10-068A

Battle, D. J., Lau, C. K., Wan, L., Deng, H., Lotti, F., and Dreyfuss, G. (2006). The Gemin5 Protein of the SMN Complex Identifies snRNAs. *Molecular Cell*, *23*(2), 273–279. https://doi.org/10.1016/j.molcel.2006.05.036

Besse, F., and Ephrussi, A. (2008). Translational control of localized mRNAs: Restricting protein synthesis in space and time. *Nature Reviews Molecular Cell Biology*, *9*(12), 971–980. https://doi.org/10.1038/nrm2548

Bolinger, C., Yilmaz, A., Hartman, T. R., Kovacic, M. B., Fernandez, S., Ye, J., Forget, M., Green, P. L., and Boris-Lawrie, K. (2007). RNA helicase A interacts with divergent lymphotropic retroviruses and promotes translation of human T-cell leukemia virus type 1. *Nucleic Acids Research*, *35*(8), 2629–2642. https://doi.org/10.1093/nar/gkm124

Buxbaum, A. R., Haimovich, G., and Singer, R. H. (2015). In the right place at the right time: Visualizing and understanding mRNA localization. *Nature Reviews*

Molecular Cell Biology, *16*(2), 95–109. https://doi.org/10.1038/nrm3918

Cao, Q., and Richter, J. D. (2002). Dissolution of the maskin ± eIF4E complex by cytoplasmic polyadenylation and poly (A) -binding protein controls cyclin B1 mRNA translation and oocyte maturation. *EMBO Journal*, *21*(14), 3852–3862. https://doi.org/10.1093/emboj/cdf353

Carol, W. M., and Larry, V. R. (1974). In vivo and in vitro effect of alpha-amanitin on preimplantation mouse embryo RNA polymerase. *Nature*, *248*, 678–680. https://doi.org/10.1038/248678a0

Castello, A., Fischer, B., Eichelbaum, K., Horos, R., Beckmann, B. M., Strein, C., Davey, N. E., Humphreys, D. T., Preiss, T., Steinmetz, L. M., Krijgsveld, J., and Hentze, M. W. (2012). Insights into RNA Biology from an Atlas of Mammalian mRNA-Binding Proteins. *Cell*, *149*(6), 1393–1406. https://doi.org/10.1016/j.cell.2012.04.031

Chalupnikova, K., Solc, P., Sulimenko, V., Sedlacek, R., and Svoboda, P. (2014). An oocyte-specific ELAVL2 isoform is a translational repressor ablated from meiotically competent antral oocytes. *Cell Cycle*, *13*(7), 1187–1200. https://doi.org/10.4161/cc.28107

Chekulaeva, M., Hentze, M. W., and Ephrussi, A. (2006). Bruno acts as a dual repressor of oskar translation, promoting mRNA oligomerization and formation of silencing particles. *Cell*, *124*(3), 521–533. https://doi.org/10.1016/j.cell.2006.01.031

Chen, J., Melton, C., Suh, N., Oh, J. S., Horner, K., Xie, F., Sette, C., Blelloch, R., and Conti, M. (2011). Genome-wide analysis of translation reveals a critical role for deleted in azoospermia-like (Dazl) at the oocyte-to-zygote transition. *Genes and Development*, *25*(7), 755–766. https://doi.org/10.1101/gad.2028911

Choi, T., Fukasawa, K., Zhout, R., Tessarollo, L., Borror, K., Resau, J., and Vande, W. F. (1996). The Mos/mitogen-activated protein kinase (MAPK) pathway regulates the size and degradation of the first polar body in maturing mouse oocytes. *PNAS*, *93*(370), 7032–7035. https://doi.org/10.1073/pnas.93.14.7032

Clift, D., McEwan, W. A., Labzin, L. I., Konieczny, V., Mogessie, B., James, L. C., and Schuh, M. (2017). A Method for the Acute and Rapid Degradation of Endogenous Proteins. *Cell*, *171*(7), 1692-1706.e18. https://doi.org/10.1016/j.cell.2017.10.033

Colombrita, C., Silani, V., and Ratti, A. (2013). ELAV proteins along evolution: Back to the nucleus? *Molecular and Cellular Neuroscience*, *56*, 447–455. https://doi.org/10.1016/j.mcn.2013.02.003

Díaz-Muñoz, M. D., Kiselev, V. Y., Novère, N. Le, Curk, T., Ule, J., and Turner, M. (2017). Tia1 dependent regulation of mRNA subcellular location and translation controls p53 expression in B cells. *Nature Communications*, *8*(1), 1–16. https://doi.org/10.1038/s41467-017-00454-2

El-Brolosy, M. A., Kontarakis, Z., Rossi, A., Kuenne, C., Günther, S., Fukuda, N., Kikhi, K., Boezio, G. L. M., Takacs, C. M., Lai, S. L., Fukuda, R., Gerri, C., Giraldez, A. J., and Stainier, D. Y. R. (2019). Genetic compensation triggered by mutant mRNA degradation. *Nature*, *568*(7751), 193–197. https://doi.org/10.1038/s41586-019-1064-z

Fernandez-Chamorro, J., Piñeiro, D., Gordon, J. M. B., Ramajo, J., Francisco-Velilla, R., Macias, M. J., and Martinez-Salas, E. (2014). Identification of novel non-canonical RNA-binding sites in Gemin5 involved in internal initiation of translation. *Nucleic Acids Research*, *42*(9), 5742–5754. https://doi.org/10.1093/nar/gku177

Flemr, M., Moravec, M., Libova, V., Sedlacek, R., and Svoboda, P. (2014). Lin28a is dormant, functional, and dispensable during mouse oocyte-to-embryo transition. *Biology of Reproduction*, *90*(6), 1–9. https://doi.org/10.1095/biolreprod.114.118703

Fogarty, N. M. E., McCarthy, A., Snijders, K. E., Powell, B. E., Kubikova, N., Blakeley, P., Lea, R., Elder, K., Wamaitha, S. E., Kim, D., Maciulyte, V., Kleinjung, J., Kim, J. S., Wells, D., Vallier, L., Bertero, A., Turner, J. M. A., and Niakan, K. K. (2017). Genome editing reveals a role for OCT4 in human embryogenesis. *Nature*, *550*(7674), 67–73. https://doi.org/10.1038/nature24033

Foygel, K., Choi, B., Jun, S., Leong, D. E., Lee, A., Wong, C. C., Zuo, E., Eckart, M., Reijo Pera, R. A., Wong, W. H., and Yao, M. W. M. (2008). A novel and critical role for Oct4 as a regulator of the maternal-embryonic transition. *PLoS ONE*, *3*(12). https://doi.org/10.1371/journal.pone.0004109

Francisco-Velilla, R., Fernandez-Chamorro, J., Dotu, I., and Martinez-Salas, E. (2018). The landscape of the non-canonical RNA-binding site of Gemin5 unveils a feedback loop counteracting the negative effect on translation. *Nucleic Acids Research*, *46*(14), 7339–7353. https://doi.org/10.1093/nar/gky361

Frum, T., Halbisen, M. A., Wang, C., Amiri, H., Robson, P., and Ralston, A. (2013). Oct4 Cell-autonomously promotes primitive endoderm development in the mouse blastocyst. *Developmental Cell*, *25*(6), 610–622. https://doi.org/10.1016/j.devcel.2013.05.004

Fujimura, K., Katahira, J., Kano, F., Yoneda, Y., and Murata, M. (2009). Microscopic dissection of the process of stress granule assembly. *Biochimica et Biophysica Acta - Molecular Cell Research*, *1793*(11), 1728–1737.

https://doi.org/10.1016/j.bbamcr.2009.08.010

Fukuda, A., Mitani, A., Miyashita, T., Kobayashi, H., Umezawa, A., and Akutsu, H. (2016). Spatiotemporal dynamics of OCT4 protein localization during preimplantation development in mice. *Reproduction*, *152*(5), 417–430. https://doi.org/10.1530/REP-16-0277

Furuno, N., Nishizawa, M., Okazaki, K., Tanaka, H., Iwashita, J., Nakajo, N., Ogawa, Y., and Sagata, N. (1994). Suppression of DNA replication via mos function during meiotic divisions in xenopus oocytes. *EMBO Journal*, *13*(10), 2399–2410. https://doi.org/10.1002/j.1460-2075.1994.tb06524.x

Gaffré, M., Martoriati, A., Belhachemi, N., Chambon, J. P., Houliston, E., Jessus, C., and Karaiskou, A. (2011). A critical balance between Cyclin B synthesis and Myt1 activity controls meiosis entry in Xenopus oocytes. *Development*, *138*(17), 3735–3744. https://doi.org/10.1242/dev.063974

Gallouzi, I. E., Brennan, C. M., Stenberg, M. G., Swan-, M. S., Eversole, A., Maizels, N., Steitz, J. a, Vlassara, H., Cai, W., Crandall, J., Reeve, I., Hummel, D., Nelson, N., Voss, J., Kilbourne, E. D., Smith, C., Brett, I., and Barbara, A. (2000). HuR binding to cytoplasmic mRNA is perturbed by heat shock. *PNAS*, *97*(7), 3073–3078. https://doi.org/10.1073/pnas.97.7.3073

Gebauer, F., Xu, W., Cooper, G. M., and Richter, J. D. (1994). Translational control by cytoplasmic polyadenylation of c-mos mRNA is necessary for oocyte maturation in the mouse. *The EMBO Journal*, *13*(23), 5712–5720. https://doi.org/10.1002/j.1460-2075.1994.tb06909.x

Gosai, S. J., Foley, S. W., Wang, D., Silverman, I. M., Selamoglu, N., Nelson, A. D. L., Beilstein, M. A., Daldal, F., Deal, R. B., and Gregory, B. D. (2015). Global

analysis of the RNA-protein interaction and RNA secondary structure landscapes of the arabidopsis nucleus. *Molecular Cell*, *57*(2), 376–388. https://doi.org/10.1016/j.molcel.2014.12.004

Guhaniyogi, J., and Brewer, G. (2012). The regulation of mRNA stability in mammalian cells. *Gene*, *500*(1), 10–21. https://doi.org/10.1016/j.gene.2012.03.021

Hake, L. E., and Richter, J. D. (1994). CPEB is a specificity factor that mediates cytoplasmic polyadenylation during Xenopus oocyte maturation. *Cell*, *79*(4), 617–627. https://doi.org/10.1016/0092-8674(94)90547-9

Hamatani, T., Carter, M. G., Sharov, A. A., and Ko, M. S. H. (2004). Dynamics of global gene expression changes during mouse preimplantation development. *Developmental Cell*, *6*(1), 117–131. https://doi.org/10.1016/S1534-5807(03)00373-3

Hartman, T. R., Qian, S., Bolinger, C., Fernandez, S., Schoenberg, D. R., and Boris-Lawrie, K. (2006). RNA helicase A is necessary for translation of selected messenger RNAs. *Nature Structural and Molecular Biology*, *13*(6), 509–516. https://doi.org/10.1038/nsmb1092

Hinman, M. N., and Lou, H. (2008). Diverse molecular functions of Hu proteins. *Cellular and Molecular Life Sciences*, *65*(20), 3168–3181. https://doi.org/10.1007/s00018-008-8252-6

Hochegger, H., Klotzbücher, A., Kirk, J., Howell, M., le Guellec, K., Fletcher, K., Duncan, T., Sohail, M., and Hunt, T. (2001). New B-type cyclin synthesis is required between meiosis I and II during Xenopus oocyte maturation. *Development,* 128(19):3795-807. https://doi.org/10.1242/dev.128.19.3795

Horie, M., and Kotani, T. (2016). Formation of mos RNA granules in the zebrafish

oocyte that differ from cyclin B1 RNA granules in distribution, density and regulation. *European Journal of Cell Biology*, *95*(12), 563–573. https://doi.org/10.1016/j.ejcb.2016.10.001

Hu, J., Wang, F., Zhu, X., Yuan, Y., Ding, M., and Gao, S. (2010). Mouse ZAR1-Like (XM-359149) colocalizes with mRNA processing components and its dominant-negative mutant caused two-cell-stage embryonic arrest. *Developmental Dynamics*, *239*(2), 407–424. https://doi.org/10.1002/dvdy.22170

Israel, S., Casser, E., Drexler, H. C. A., Fuellen, G., and Boiani, M. (2019). A framework for TRIM21-mediated protein depletion in early mouse embryos: Recapitulation of Tead4 null phenotype over three days. *BMC Genomics*, *20*(1), 1–19. https://doi.org/10.1186/s12864-019-6106-2

Jagarlamudi, K., and Rajkovic, A. (2012). Oogenesis: Transcriptional regulators and mouse models. *Molecular and Cellular Endocrinology*, *356*(1–2), 31–39. https://doi.org/10.1016/j.mce.2011.07.049

Kato, Y., Iwamori, T., Ninomiya, Y., Kohda, T., Miyashita, J., Sato, M., and Saga, Y. (2019). ELAVL2-directed RNA regulatory network drives the formation of quiescent primordial follicles. *EMBO Reports*, *20*(12), 1–15. https://doi.org/10.15252/embr.201948251

Kedersha, N., Ivanov, P., and Anderson, P. (2013). Stress granules and cell signaling: More than just a passing phase? *Trends in Biochemical Sciences*, *38*(10), 494–506. https://doi.org/10.1016/j.tibs.2013.07.004

Kim, J. H., and Richter, J. D. (2006). Opposing Polymerase-Deadenylase Activities Regulate Cytoplasmic Polyadenylation. *Molecular Cell*, *24*(2), 173–183. https://doi.org/10.1016/j.molcel.2006.08.016

Kloc, M., and Etkin, L. D. (2005). RNA localization mechanisms in oocytes. *Journal of Cell Science*, *118*(2), 269–282. https://doi.org/10.1242/jcs.01637

Kotani, T., Yasuda, K., Ota, R., and Yamashita, M. (2013). Cyclin B1 mRNA translation is temporally controlled through formation and disassembly of RNA granules. *Journal of Cell Biology*, *202*(7), 1041–1055. https://doi.org/10.1083/jcb.201302139

Kotani, T., Maehata, K., and Takei, N. (2017). Regulation of Translationally Repressed mRNAs in Zebrafish and Mouse Oocytes. *Results Probl Cell Differ*. 2017;63:297-324. doi: 10.1007/978-3-319-60855-6_13.

Kun Zhang and George W. Smith. (2015). Maternal control of early embryogenesis in mammals. *Reprod Fertil Dev*, *176*(1), 139–148. https://doi.org/10.1016/j.physbeh.2017.03.040

Ledan, E., Polanski, Z., Terret, M. E., and Maro, B. (2001). Meiotic maturation of the mouse oocyte requires an equilibrium between cyclin B synthesis and degradation. *Developmental Biology*, *232*(2), 400–413. https://doi.org/10.1006/dbio.2001.0188

Lee, T., and Pelletier, J. (2016). The biology of DHX9 and its potential as a therapeutic target. *Oncotarget*, *7*(27), 42716–42739. https://doi.org/10.18632/oncotarget.8446

Leichsenring, M., Maes, J., Mošsner, R., Driever, W., and Onichtchouk, D. (2013). Pou5f1 transcription factor controls zygotic gene activation in vertebrates. *Science*, *341*(6149), 1005–1009. https://doi.org/10.1126/science.1242527

Li, J., Tang, J. X., Cheng, J. M., Hu, B., Wang, Y. Q., Aalia, B., Li, X. Y., Jin, C., Wang, X. X., Deng, S. L., Zhang, Y., Chen, S. R., Qian, W. P., Sun, Q. Y., Huang, X. X., and Liu, Y. X. (2018). Cyclin B2 can compensate for Cyclin B1 in oocyte meiosis I. *Journal of Cell Biology*, *217*(11), 3901–3911.

https://doi.org/10.1083/jcb.201802077

Ma, J., Fukuda, Y., and Schultz, R. M. (2015). Mobilization of dormant Cnot7 mRNA promotes deadenylation of maternal transcripts during mouse oocyte maturation. *Biology of Reproduction*, *93*(2), 1–12. https://doi.org/10.1095/biolreprod.115.130344

Ma, Z., Zhu, P., Shi, H., Guo, L., Zhang, Q., Chen, Y., Chen, S., Zhang, Z., Peng, J., and Chen, J. (2019). PTC-bearing mRNA elicits a genetic compensation response via Upf3a and COMPASS components. *Nature*, *568*(7751), 259–263. https://doi.org/10.1038/s41586-019-1057-y

Markmiller, S., Soltanieh, S., Server, K. L., Mak, R., Jin, W., Fang, M. Y., Luo, E. C., Krach, F., Yang, D., Sen, A., Fulzele, A., Wozniak, J. M., Gonzalez, D. J., Kankel, M. W., Gao, F. B., Bennett, E. J., Lécuyer, E., and Yeo, G. W. (2018). Context-Dependent and Disease-Specific Diversity in Protein Interactions within Stress Granules. *Cell*, *172*(3), 590-604.e13. https://doi.org/10.1016/j.cell.2017.12.032

Martin, K. C., and Ephrussi, A. (2009). mRNA Localization: Gene Expression in the Spatial Dimension. *Cell*, *136*(4), 719–730. https://doi.org/10.1016/j.cell.2009.01.044

Masek, T., Del Llano, E., Gahurova, L., Kubelka, M., Susor, A., Roucova, K., Lin, C. J., Bruce, A. W., and Pospisek, M. (2020). Identifying the Translatome of Mouse NEBD-Stage Oocytes via SSP-Profiling; A Novel Polysome Fractionation Method. *International Journal of Molecular Sciences*, *21*(4), 1–23. https://doi.org/10.3390/ijms21041254

Mendez, R., Murthy, K. G. K., Ryan, K., Manley, J. L., and Richter, J. D. (2000). Phosphorylation of CPEB by Eg2 mediates the recruitment of CPSF into an active

cytoplasmic polyadenylation complex. *Molecular Cell*, *6*(5), 1253–1259. https://doi.org/10.1016/S1097-2765(00)00121-0

Lee, M. T., Bonneau, A. R., Takacs, C. M., Bazzini, A. A., DiVito, K. R., Fleming, E. S., and Giraldez, A. J. (2013). Nanog, Pou5f1 and SoxB1 activate zygotic gene expression during the maternal-to-zygotic transition. *Nature*, *503*, 360–364. https://doi.org/10.4172/2157-7633.1000305.Improved

Moore, G. P., and Lintern-Moore, S. (1978). Transcription of the mouse oocyte genome. *Biol Reprod*, *18*(5), 865–870. https://doi.org/10.1095/biolreprod18.5.865

Moschner, K., Sündermann, F., Meyer, H., Da Graca, A. P., Appel, N., Paululat, A., Bakota, L., and Brandt, R. (2014). RNA protein granules modulate tau isoform expression and induce neuronal sprouting. *Journal of Biological Chemistry*, *289*(24), 16814–16825. https://doi.org/10.1074/jbc.M113.541425

Nakajo, N., Yoshitome, S., Iwashita, J., Iida, M., Uto, K., Ueno, S., Okamoto, K., and Sagata, N. (2000). Absence of Wee1 ensures the meiotic cell cycle in Xenopus oocytes Absence of Wee1 ensures the meiotic cell cycle in Xenopus oocytes. *Genes & Development*, *14*, 328–338. https://doi.org/10.1101/gad.14.3.328

Nichols, J., Zevnik, B., Anastassiadis, K., Niwa, H., Klewe-Nebenius, D., Chambers, I., Scholer, H., and Smith, A. (1998). Formation of pluripotent stem cells in the mammalian embryo dependes on the POU transcription factor Oct4. *Cell*, *95*(3), 379–391. https://doi.org/10.1016/S0092-8674(00)81769-9

Niwa, H., Miyazaki, J., and Smith, A. G. (2000). Quantitative expression of Oct-3 / 4 defines differentiation , dedifferentiation or self-renewal of ES cells. *Nat Genet*, *24*(July), 2–6. https://doi.org/10.1038/74199

Okamoto, K., Okazawa, H., Okuda, A., Sakai, M., Muramatsu, M., and Hamada, H.

(1990). A novel octamer binding transcription factor is differentially expressed in mouse embryonic cells. *Cell*, *60*(3), 461–472. https://doi.org/10.1016/0092-8674(90)90597-8

Pacheco, A., De Quinto, S. L., Ramajo, J., Fernández, N., and Martínez-Salas, E. (2009). A novel role for Gemin5 in mRNA translation. *Nucleic Acids Research*, *37*(2), 582–590. https://doi.org/10.1093/nar/gkn979

Palmieri, S. L., Peter, W., Hess, H., and Schöler, H. R. (1994). Oct-4 transcription factor is differentially expressed in the mouse embryo during establishment of the firsttwo extraembryonic cell lineages involved in implantation. *Developmental Biology*, *166* (1), 259–267. https://doi.org/10.1006/dbio.1994.1312

Papadopoulou, C., Ganou, V., Patrinou-Georgoula, M., and Guialis, A. (2013). HuR-hnRNP interactions and the effect of cellular stress. *Molecular and Cellular Biochemistry*, *372*(1–2), 137–147. https://doi.org/10.1007/s11010-012-1454-0

Pesce, M., Wang, X., Wolgemuth, D. J., and Schöler, H. R. (1998). Differential expression of the Oct-4 transcription factor during mouse germ cell differentiation. *Mechanisms of Development*, *71*(1–2), 89–98. https://doi.org/10.1016/S0925-4773(98)00002-1

Piotrowska, J., Hansen, S. J., Park, N., Jamka, K., Sarnow, P., and Gustin, K. E. (2010). Stable Formation of Compositionally Unique Stress Granules in Virus-Infected Cells. *Journal of Virology*, *84*(7), 3654–3665. https://doi.org/10.1128/jvi.01320-09

Piotrowska, K. (2002). Early patterning of the mouse embryo - contributions of sperm and egg. *Development*, *129*(24), 5803–5813. https://doi.org/10.1242/dev.00170

Polanski, Z., Ledan, E., and Brunet, S. (1998). Cyclin synthesis controls the progression of meiotic maturation in mouse oocytes. *Development*, *125*(24), 4989–4997.

https://doi.org/10.1242/dev.125.24.4989

Qiu, C., Ma, Y., Wang, J., Peng, S., and Huang, Y. (2009). Lin28-mediated post-transcriptional regulation of Oct4 expression in human embryonic stem cells. *Nucleic Acids Research*, *38*(4), 1240–1248. https://doi.org/10.1093/nar/gkp1071

Ramajo, J., and Ferna, N. (2013). Gemin5 promotes IRES interaction and translation control through its C-terminal region. *Nucleic Acids Research. 41*(2), 1017–1028. https://doi.org/10.1093/nar/gks1212

Reyes, J. M., and Ross, P. J. (2016). Cytoplasmic polyadenylation in mammalian oocyte maturation. *Wiley Interdisciplinary Reviews: RNA*, *7*(1), 71–89. https://doi.org/10.1002/wrna.1316

Rosner, M. H., Vigano, M. A., Ozato, K., Timmons, P. M., Poirie, F., Rigby, P. W. J., and Staudt, L. M. (1990). A POU-domain transcription factor in early stem cells and germ cells of the mammalian embryo. *Nature*, *345*(6277), 686–692. https://doi.org/10.1038/345686a0

Rudolf Jaenisch, R. Y. (2008). Stem cells, the molecular circuitry of pluripotency and nuclear reprogramming. *Cell*, *132*(4), 567–582. https://doi.org/10.2307/j.ctv6cfqtv.7

Sagata, N., Daar, I., Oskarsson, M., Showalter, S.D., and Vande Woude, GF. (1989). The product of the mos proto-oncogene as a candidate "initiator" for oocyte maturation. *Science*, 11;245(4918):643-6. doi: 10.1126/science.2474853.

Saitoh, A., Takada, Y., Horie, M., and Kotani, T. (2018). Pumilio1 phosphorylation precedes translational activation of its target mRNA in zebrafish oocytes. *Zygote*, *26*, 372–380. https://doi.org/10.1017/S0967199418000369

Sato, K., Akiyama, M., and Sakakibara, Y. (2021). RNA secondary structure prediction

using deep learning with thermodynamic integration. *Nature Communications*, *12*(1), 1–9. https://doi.org/10.1038/s41467-021-21194-4

Schisa, J. A. (2012). New Insights into the Regulation of RNP Granule Assembly in Oocytes. In *International Review of Cell and Molecular Biology* (1st ed., Vol. 295). Elsevier Inc. https://doi.org/10.1016/B978-0-12-394306-4.00013-7

Scholer, H. R., Ruppert, S., Suzuki, N., Chowdhury, K., and Gruss, P. (1990a). New type of POU domain in germ line-specific protein Oct-4. *Nature*, 29;344(6265):435-9. https://doi.org/10.1038/344435a0

Scholer, H. R., Dressler, G. R., Rohdewohid, H., and Gruss, P. (1990b). Oct-4: a germline-specific transcription factor mapping to the mouse t-complex. *The EMBO Journal*, *9*(7), 2185–2195. https://doi.org/10.1016/0168-9525(90)90242-X

Scholer, H. R., Hatzopoulos, A. K., Balling, R., Suzuki, N., and Gruss, P. (1989). A family of octamer-specific proteins present during mouse embryogenesis: evidence for germline-specific expression of an Oct factor. *EMBO Journal*, *8*(9), 2543–2550. https://doi.org/10.1002/j.1460-2075.1989.tb08392.x

Sheets, M. D., Fox, C. A., Hunt, T., Vande Woude, and Wickens, M. (1994). The 3'-untranslated regions of c-mos and cyclin mRNAs stimulate translation by regulating cytoplasmic polyadenylation. *Genes and Development*, *8*(8), 926–938. https://doi.org/10.1101/gad.8.8.926

Stamatiadis, P., Boel, A., Cosemans, G., Popovic, M., Bekaert, B., Guggilla, R., Tang, M., De Sutter, P., Van Nieuwerburgh, F., Menten, B., Stoop, D., Chuva de Sousa Lopes, S. M., Coucke, P., and Heindryckx, B. (2021). Comparative analysis of mouse and human preimplantation development following POU5F1 CRISPR/Cas9 targeting reveals interspecies differences. *Human Reproduction*, *36*(5), 1242–1252.

https://doi.org/10.1093/humrep/deab027

Susor, A., and Kubelka, M. (2017). Translational Regulation in the Mammalian Oocyte. *Results Probl Cell Differ*. 2017;63:257-295. doi: 10.1007/978-3-319-60855-6_12.

Takei, N., Nakamura, T., Kawamura, S., Takada, Y., Satoh, Y., Kimura, A. P., and Kotani, T. (2018). High-Sensitivity and High-Resolution in Situ Hybridization of Coding and Long Non-coding RNAs in Vertebrate Ovaries and Testes. *Biological Procedures Online*, *20*(1), 1–14. https://doi.org/10.1186/s12575-018-0071-z

Takei, N., Sato, K., Takada, Y., Iyyappan, R., Susor, A., Yamamoto, T., and Kotani, T. (2021). Tdrd3 regulates the progression of meiosis II through translational control of Emi2 mRNA in mouse oocytes. *Current Research in Cell Biology*, *2*(May), 100009. https://doi.org/10.1016/j.crcbio.2021.100009

Takei, N., Takada, Y., Kawamura, S., Sato, K., Saitoh, A., Bormann, J., Yuen, W. S., Carroll, J., and Kotani, T. (2020). Changes in subcellular structures and states of pumilio 1 regulate the translation of target Mad2 and cyclin B1 mRNAs. *Journal of Cell Science*, *133*(23). https://doi.org/10.1242/jcs.249128

Taliaferro, J. M., Lambert, N. J., Sudmant, P. H., Dominguez, D., Merkin, J. J., Alexis, M. S., Bazile, C. A., and Burge, C. B. (2016). RNA Sequence Context Effects Measured In Vitro Predict In Vivo Protein Binding and Regulation. *Molecular Cell*, *64*(2), 294–306. https://doi.org/10.1016/j.molcel.2016.08.035

Tan, M. H., Au, K. F., Leong, D. E., Foygel, K., Wong, W. H., and Yao, M. W. M. (2013). An Oct4-Sall4-Nanog network controls developmental progression in the pre-implantation mouse embryo. *Molecular Systems Biology*, *9*(632), 1–19. https://doi.org/10.1038/msb.2012.65

Traverso, J. M., Donnay, I., and Lequarre, A. S. (2005). Effects of polyadenylation

inhibition on meiosis progression in relation to the polyadenylation status of cyclins A2 and B1 during in vitro maturation of bovine oocytes. *Molecular Reproduction and Development*, *71*(1), 107–114. https://doi.org/10.1002/mrd.20247

Van Etten, J., Schagat, T. L., Hrit, J., Weidmann, C. A., Brumbaugh, J., Coon, J. J., and Goldstrohm, A. C. (2012). Human pumilio proteins recruit multiple deadenylases to efficiently repress messenger RNAs. *Journal of Biological Chemistry*, *287*(43), 36370–36383. https://doi.org/10.1074/jbc.M112.373522

Vieux, K. F., and Clarke, H. J. (2018). CNOT6 regulates a novel pattern of mRNA deadenylation during oocyte meiotic maturation. *Scientific Reports*, *8*(1), 1–14. https://doi.org/10.1038/s41598-018-25187-0

Weill, L., Belloc, E., Bava, F. A., and Méndez, R. (2012). Translational control by changes in poly(A) tail length: Recycling mRNAs. *Nature Structural and Molecular Biology*, *19*(6), 577–585. https://doi.org/10.1038/nsmb.2311

Winata, C. L., and Korzh, V. (2018). The translational regulation of maternal mRNAs in time and space. *FEBS Letters*, *592*(17), 3007–3023. https://doi.org/10.1002/1873-3468.13183

Winata, C. L., Łapiński, M., Pryszcz, L., Vaz, C., bin Ismail, M. H., Nama, S., Hajan, H. S., Lee, S. G. P., Korzh, V., Sampath, P., Tanavde, V., and Mathavan, S. (2018). Cytoplasmic polyadenylation-mediated translational control of maternal mRNAs directs maternal-to-zygotic transition. *Development*, *145*(1), dev159566. https://doi.org/10.1242/dev.159566

Workman, E., Kalda, C., Patel, A., and Battle, D. J. (2015). Gemin5 binds to the survival motor neuron mRNA to regulate SMN expression. *Journal of Biological*

Chemistry, *290*(25), 15662–15669. https://doi.org/10.1074/jbc.M115.646257

Wu, G., Han, D., Gong, Y., Sebastiano, V., Gentile, L., Singhal, N., Adachi, K., Fischedick, G., Ortmeier, C., Sinn, M., Radstaak, M., Tomilin, A., and Schöler, H. R. (2013). Establishment of totipotency does not depend on Oct4A. *Nature Cell Biology*, *15*(9), 1089–1097. https://doi.org/10.1038/ncb2816

Xu, H. M., Liao, B., Zhang, Q. J., Wang, B. B., Li, H., Zhong, X. M., Sheng, H. Z., Zhao, Y. X., Zhao, Y. M., and Jin, Y. (2004). Wwp2, An E3 ubiquitin ligase that targets transcription factor Oct-4 for ubiquitination. *Journal of Biological Chemistry*, *279*(22), 23495–23503. https://doi.org/10.1074/jbc.M400516200

Xu, H., Wang, W., Li, C., Yu, H., Yang, A., Wang, B., and Jin, Y. (2009). WWP2 promotes degradation of transcription factor OCT4 in human embryonic stem cells. *Cell Research*, *19*, 561–573. https://doi.org/10.1038/cr.2009.31

Yeom, Y. I., Ha, H. S., Balling, R., Schöler, H. R., and Artzt, K. (1991). Structure, expression and chromosomal location of the Oct-4 gene. *Mechanisms of Development*, *35*(3), 171–179. https://doi.org/10.1016/0925-4773(91)90016-Y

Yong, J., Kasim, M., Bachorik, J. L., Wan, L., and Dreyfuss, G. (2010). Gemin5 delivers snRNA precursors to the SMN complex for snRNP biogenesis. *Molecular Cell*, *38*(4), 551–562. https://doi.org/10.1016/j.molcel.2010.03.014

Zhang, D. X., Cui, X. S., and Kim, N. H. (2009). Involvement of polyadenylation status on maternal gene expression during in vitro maturation of porcine oocytes. *Molecular Reproduction and Development*, *76*(9), 881–889. https://doi.org/10.1002/mrd.21056

Zuccotti, M., Merico, V., Redi, C. A., Bellazzi, R., Adjaye, J., and Garagna, S. (2009). Role of Oct-4 during acquisition of developmental competence in mouse oocyte.

Reproductive BioMedicine Online, *19*(SUPPL. 3), 57–62.

https://doi.org/10.1016/S1472-6483(10)60284-2

TABLE

Table 1. Candidate proteins that bind to *Pou5f3* 3'UTR.

	Number of peptides		
Proteins	**Long**	**Short**	**Long (antisense)**
Zar1	**60**	21	15
hnRNPD	**14**	4	0
ELAVL1 (HuR)	**28**	15	0
TIAR	**26**	15	0
IMP1	**8**	0	8
Gemin5	3	**22**	0
Dhx9	3	**23**	3
SYNE1	3	**10**	1
Dicer1	0	**6**	0
SF3B1	0	**6**	0
TIA1	**39**	**32**	0
ELAVL2 (HuB)	**75**	**56**	25

Number of peptides detected by mass spectrometry in the extracts incubated with long- and short-type *Pou5f3* 3'UTRs are listed. Zar1, hnRNPD, HuR, TIAR, and IMP1 were predominantly detected in the extracts incubated with long-type *Pou5f3* 3'UTR. Gemin5, Dhx9, SYNE1, Dicer1, and SF3B1 were predominantly detected in the extracts incubated with short-type *Pou5f3* 3'UTR. Roughly similar amounts of TIA1 and HuB were detected in the extracts incubated with both long- and short-type *Pou5f3* 3'UTRs. Number of peptides detected in the extracts incubated with antisense RNA of long-type *Pou5f3* 3'UTR was listed as a control.

FIGURES

Fig. 1. Expression of *Pou5f1/Oct4* mRNA during oogenesis.
(A) Expression of *Pou5f1/Oct4* mRNA in fully grown GV-stage oocytes in an ovary of an 8-week-old female mouse. The inset is an enlarged view of the boxed region. (B) Expression of *Pou5f1/Oct4* mRNA in growing oocytes in an ovary of a PD8 female. (C) FISH analysis of *Pou5f1/Oct4* mRNA (green) in growing (PD8) and GV-stage (8-week-old) oocytes. DNA is shown in blue. Enlarged views of the boxed regions are shown at the bottom. Similar results were obtained from two independent experiments in each in situ hybridization. *PrF*, primordial follicle; *PF*, primary follicle; *SF*, secondary follicle; *GV*, germinal vesicle. Bars: 50 μm in (A) and (B); 20 μm in (C).

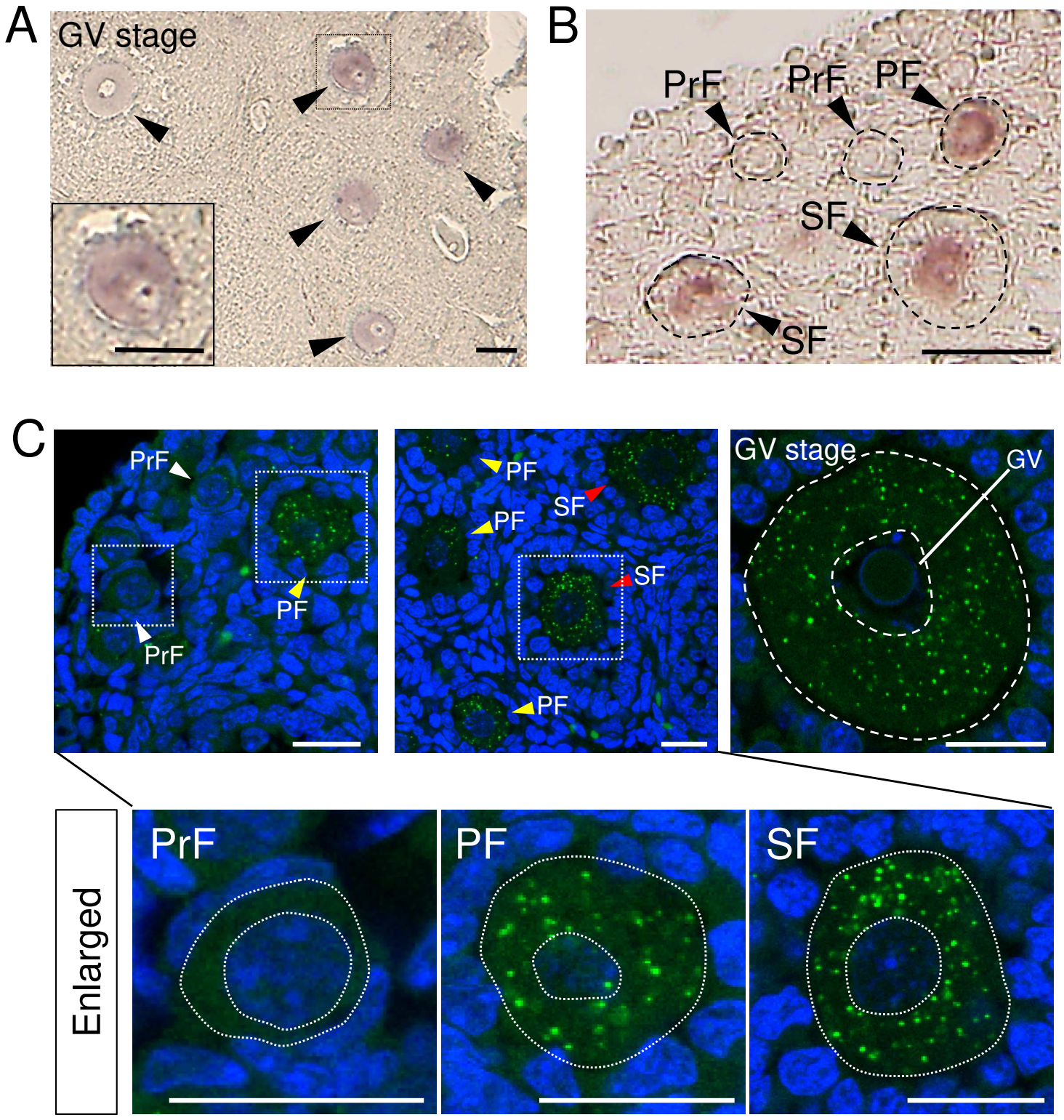
A
GV stage
B
PrF
PrF
PF
SF
SF
C
PrF
PF
PrF
PF
SF
SF
PF
GV stage
GV
Enlarged
PrF
PF
SF

Fig. 1

Fig. 2. Disassembly of *Pou5f1/Oct4* RNA granules in ovulated oocytes and 2-cell-stage embryos.

(A) FISH analysis of *Pou5f1/Oct4* mRNA (green) in a fully grown GV-stage oocyte, an ovulated oocyte arrested at the MII stage, and an embryo at the 2-cell-stage. Similar results were obtained from two independent experiments. DNA is shown in blue. *GV*, germinal vesicle; *PB*, polar body. Bars: 50 μm.

(B) Quantitative RT-PCR analysis for *Pou5f1/Oct4* mRNA from equal numbers of oocytes at GV- and MII-stages and embryos at the early 2-cell stage (E2c). Each bar represents the mean of the triplicate experiments, and vertical bars show the mean ± SD.

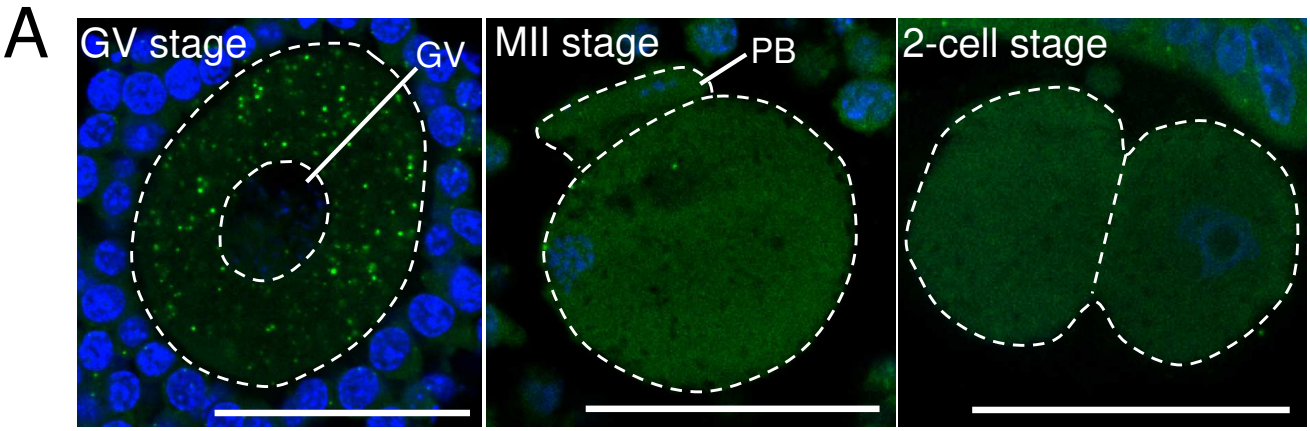
A
GV stage
GV
MII stage
PB
2-cell stage

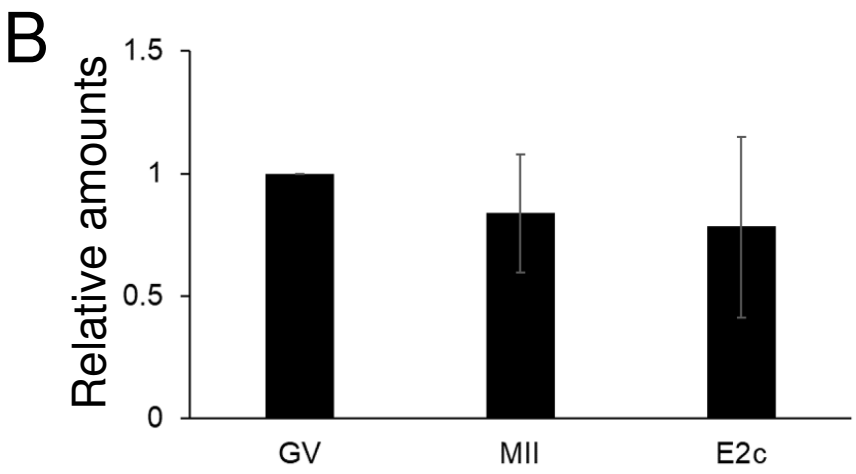
B
Relative amounts
1.5
1
0.5
0
GV
MII
E2c

Fig. 2

Fig. 3. Expression of Pou5f1/Oct4 protein during oogenesis and early cleavage stages.

(A) (left) Characterization of anti-Pou5f1/Oct4 antibody by immunoblotting. Crude extracts from 50 blastocysts were examined by immunoblotting with (+) or without (−) anti-Pou5f1/Oct4 antibody. "#" shows non-specific bands of the secondary antibody. (middle) Immunofluorescence of Pou5f1/Oct4 in a blastocyst, showing a specific signal of Pou5f1/Oct4 in the ICM. *ICM*, inner cell mass. (right) Immunoblot analysis for the expression of Pou5f1/Oct4 in oocytes at GV and MII stages and in embryos at 2-cell (2c) and blastocyst (B) stages. Crude extracts from 50 oocytes and embryos were examined with or without anti-Pou5f1/Oct4 antibody. "#" shows non-specific bands of the secondary antibody. (B) Immunofluorescence with or without anti-Pou5f1/Oct4 antibody in oocytes at primary-follicle (PF), secondary-follicle (SF), GV, and MII stages and in embryos at 1-cell and 2-cell stages. *F*, follicle cells; *O*, oocytes; *GV*, germinal vesicle; *PB*, polar bodies. (C) Quantification of immunofluorescence analysis without (-) and with (+) anti-Pou5f1/Oct4 antibody. Each bar represents the mean of the triplicate experiments, and vertical bars show the mean ± SD. *$p < 0.05$, t-test. (D) Immunofluorescence of Pou5f1/Oct4 in embryos at the early 2-cell and late 2-cell stages. (E) Signal intensities without (−) and with (+) anti-Pou5f1/Oct4 antibody in the nucleus and cytoplasm of embryos at early 2-cell (E2c) and late 2-cell (L2c) stages. Each bar represents the mean of the triplicate experiments, and vertical bars show the mean ± SD. *$p < 0.05$, t-test. (F) Immunofluorescence of Pou5f1/Oct4 in embryos at the early 2-cell stage injected with the *Pou5f1/Oct4* ATG-MO or *Pou5f1/Oct4* 5mm-MO. Bars: 50 μm in (A), (D) and (F); 20 μm in (B).

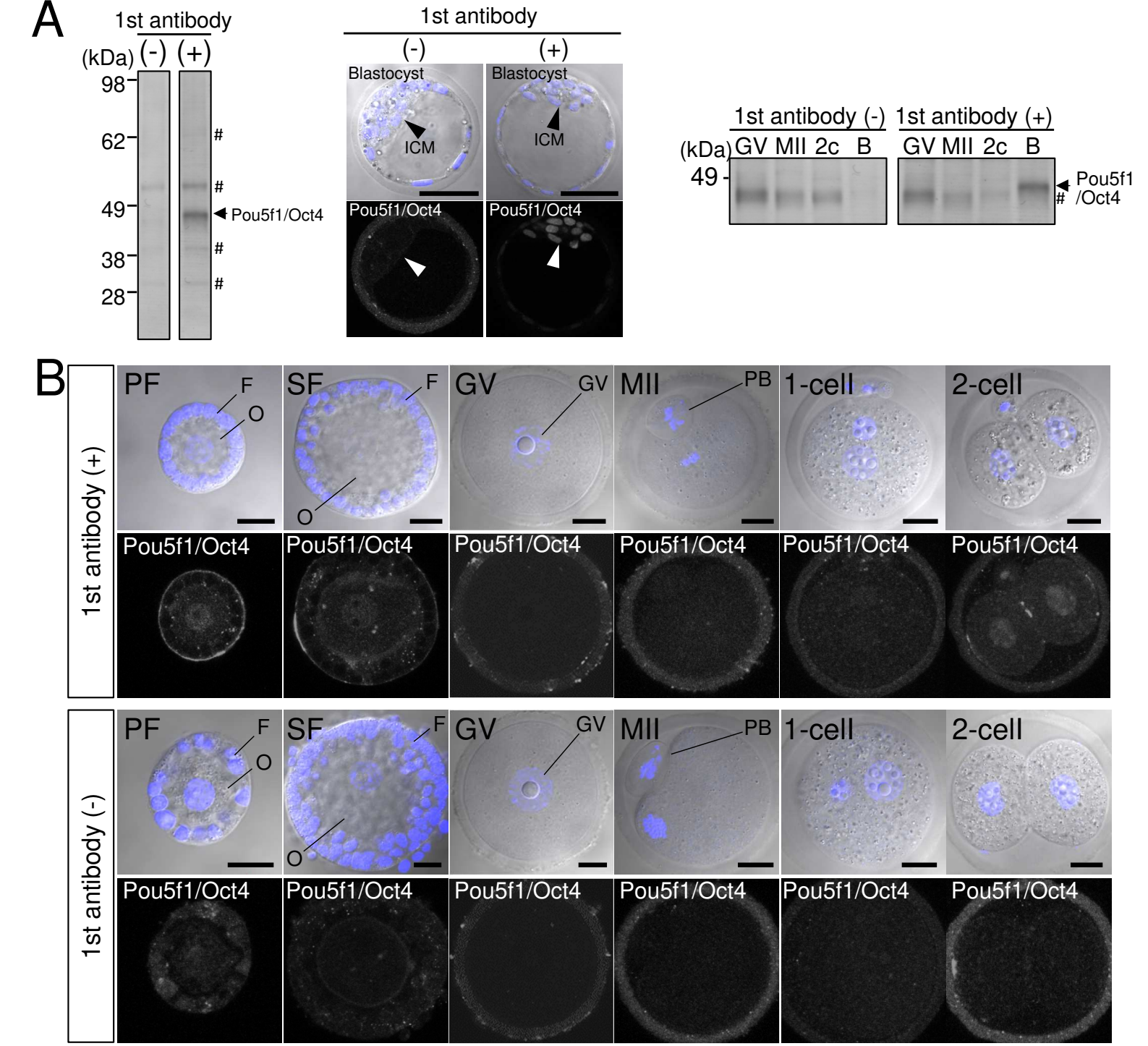
A
1st antibody
(kDa) (-) (+)
98
62
49
38
28
#
#
Pou5f1/Oct4
#
#
1st antibody
(-)
(+)
Blastocyst
Blastocyst
ICM
ICM
Pou5f1/Oct4
Pou5f1/Oct4
1st antibody (-)
1st antibody (+)
(kDa)
GV MII 2c B
GV MII 2c B
49
Pou5f1
#
/Oct4
B
1st antibody (+)
PF
F
O
SF
F
O
GV
GV
MII
PB
1-cell
2-cell
Pou5f1/Oct4
1st antibody (-)
C
Nucleus
Cytoplasm
Signal Intensity
20000
15000
10000
5000
0
*
PF
SF
GV
E2c
MII
(-)
(+)
D
Early
Late
Pou5f1/Oct4
E
Signal Intensity
*
E2c
L2c
Nucleus
Cytoplasm
F
No injection
ATG-MO
5mm-MO
Pou5f1/Oct4

Fig. 3

Fig. 4. Accumulation of Pou5f1/Oct4 protein in 2-cell stage embryos from maternal mRNA.

(A) Immunofluorescence of Pou5f1/Oct4 in a parthenogenetically activated 2-cell-stage embryo. Similar results were obtained in 7 embryos from two independent experiments. (B) Immunofluorescence of Pou5f1/Oct4 in 8-cell-stage embryos (E2.5) cultured with a control medium or a medium containing α-amanitin, showing inhibition of zygotic Pou5f1/Oct4 expression by α-amanitin. (C) Immunofluorescence of Pou5f1/Oct4 in a 2-cell-stage embryo (E1.5) cultured with a medium containing α-amanitin, showing no effects on the expression of Pou5f1/Oct4 in a 2-cell-stage embryo by α-amanitin treatment. Similar results were obtained in 15 embryos from two independent experiments. Bars: 50 μm.

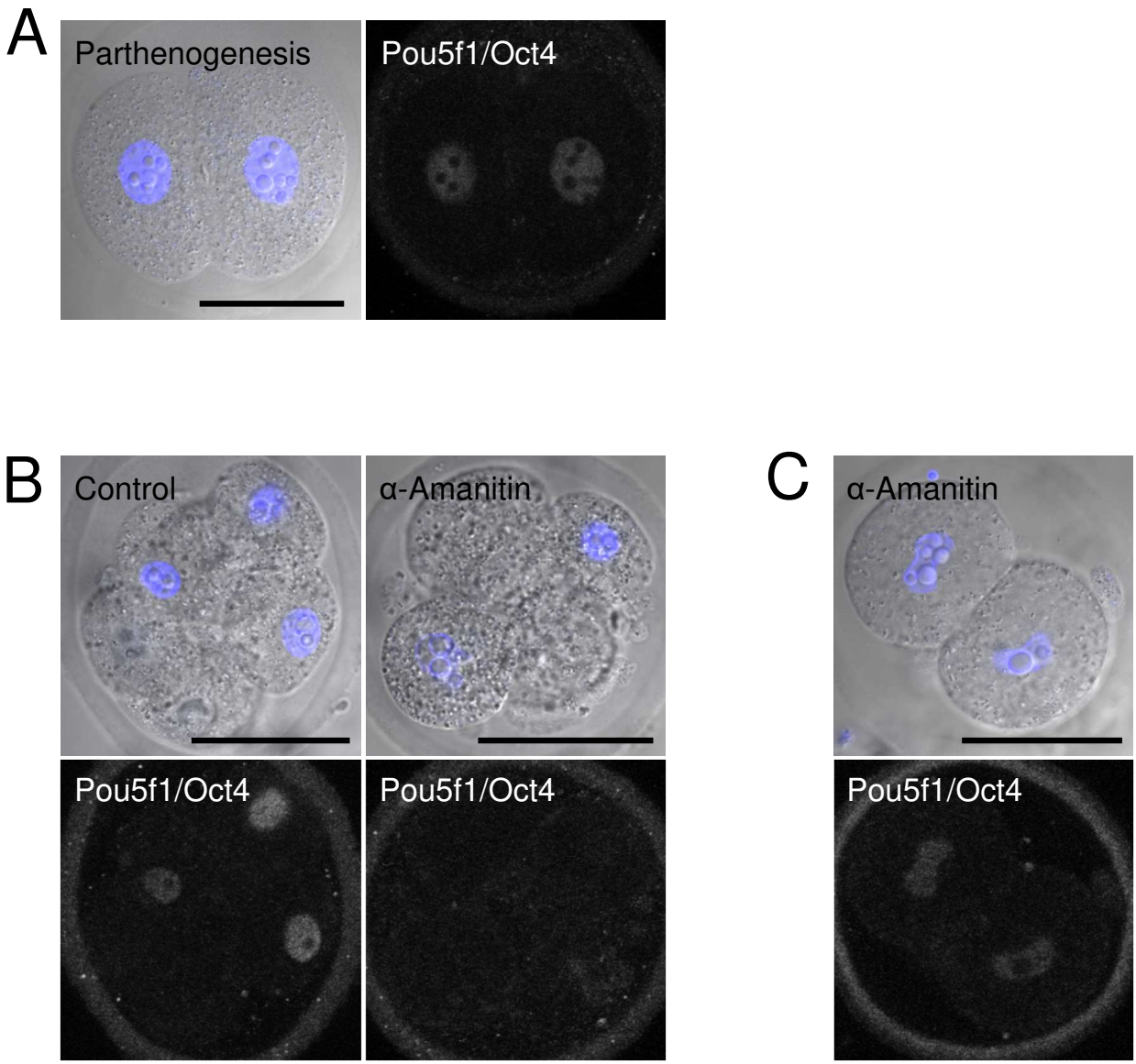
A
Parthenogenesis
Pou5f1/Oct4
B
Control
α-Amanitin
Pou5f1/Oct4
Pou5f1/Oct4
C
α-Amanitin
Pou5f1/Oct4

Fig. 4

Fig. 5. Increase in the amount of *Pou5f1/Oct4* mRNA in the polysomal fraction.

(A) The amounts of *Pou5f1/Oct4* mRNA (FPKM) in the polysomal fractions in oocytes at GV and MII stages and embryos at 1- and 2-cell stages. Each bar represents the mean of the two experiments, and vertical bars show the mean ± SD. (B) The amounts of *Pou5f1/Oct4* mRNA (FPKM) in the polysomal fractions in embryos at 2-cell stage and late 2-cell stage. Each bar represents the mean of the two experiments, and vertical bars show the mean ± SD.

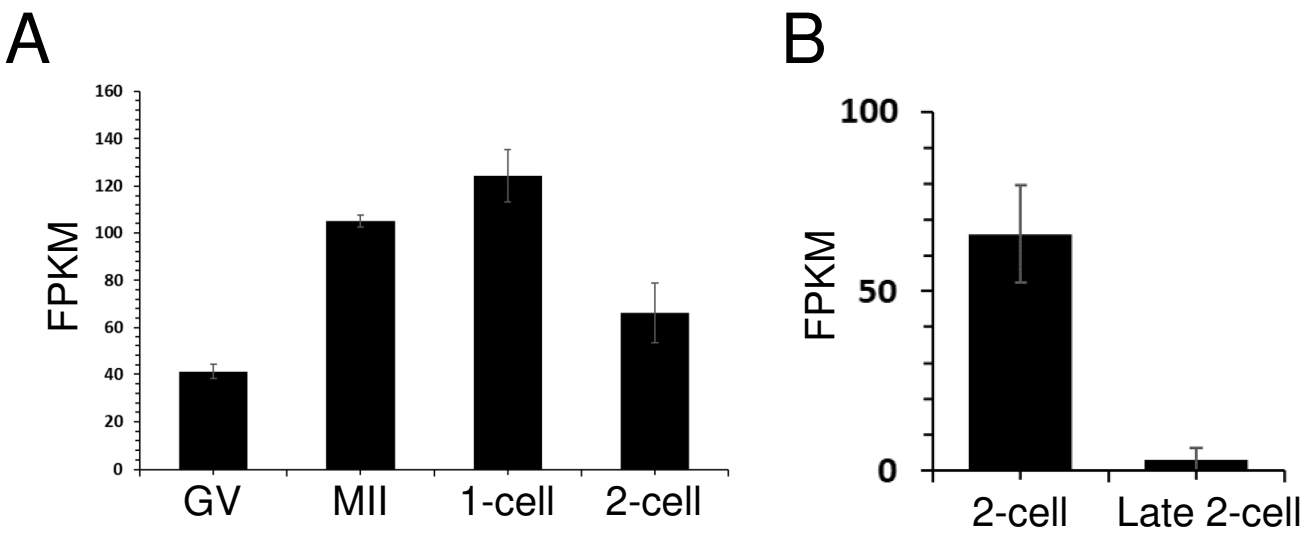
A
FPKM
160
140
120
100
80
60
40
20
0
GV
MII
1-cell
2-cell
B
FPKM
100
50
0
2-cell
Late 2-cell

Fig. 5

Fig. 6. Developmental competence of Pou5f1/Oct4-knockdown embryos. (A and B) Immunofluorescence of Pou5f1/Oct4 in embryos injected with *Pou5f1/Oct4* ATG-MO (0.6 mM, 0.4 mM, and 0.2 mM) or not injected intact embryos at the early 2-cell stage (A) and 4-cell stage (B). Bars; 50 μm. (C) Developmental competence of embryos that were not injected (intact) and injected with *Pou5f1/Oct4* ATG-MO (0.6 mM and 0.2 mM) and *Pou5f1/Oct4* 5mm-MO (0.6 mM). Graphs indicate the number of embryos that reached the respective stages. *2c*, 2-cell stage; *4c*, 4-cell stage; *M*, morula-stage; *B*, blastocyst-stage; *f*, fragmented-embryos.

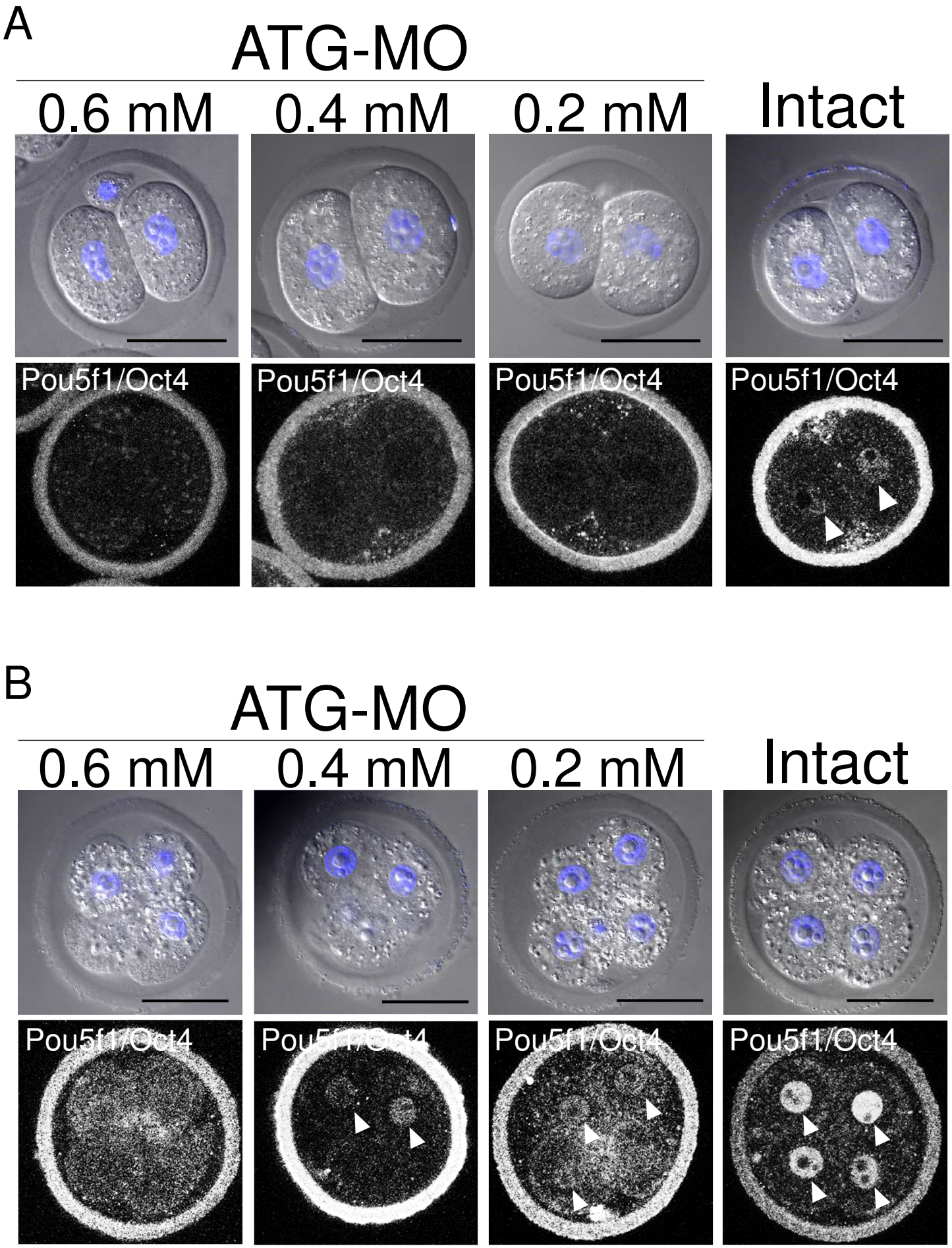
A
ATG-MO
0.6 mM
0.4 mM
0.2 mM
Intact
Pou5f1/Oct4
Pou5f1/Oct4
Pou5f1/Oct4
Pou5f1/Oct4
B
ATG-MO
0.6 mM
0.4 mM
0.2 mM
Intact
Pou5f1/Oct4
Pou5f1/Oct4
Pou5f1/Oct4
Pou5f1/Oct4

Fig. 6

C

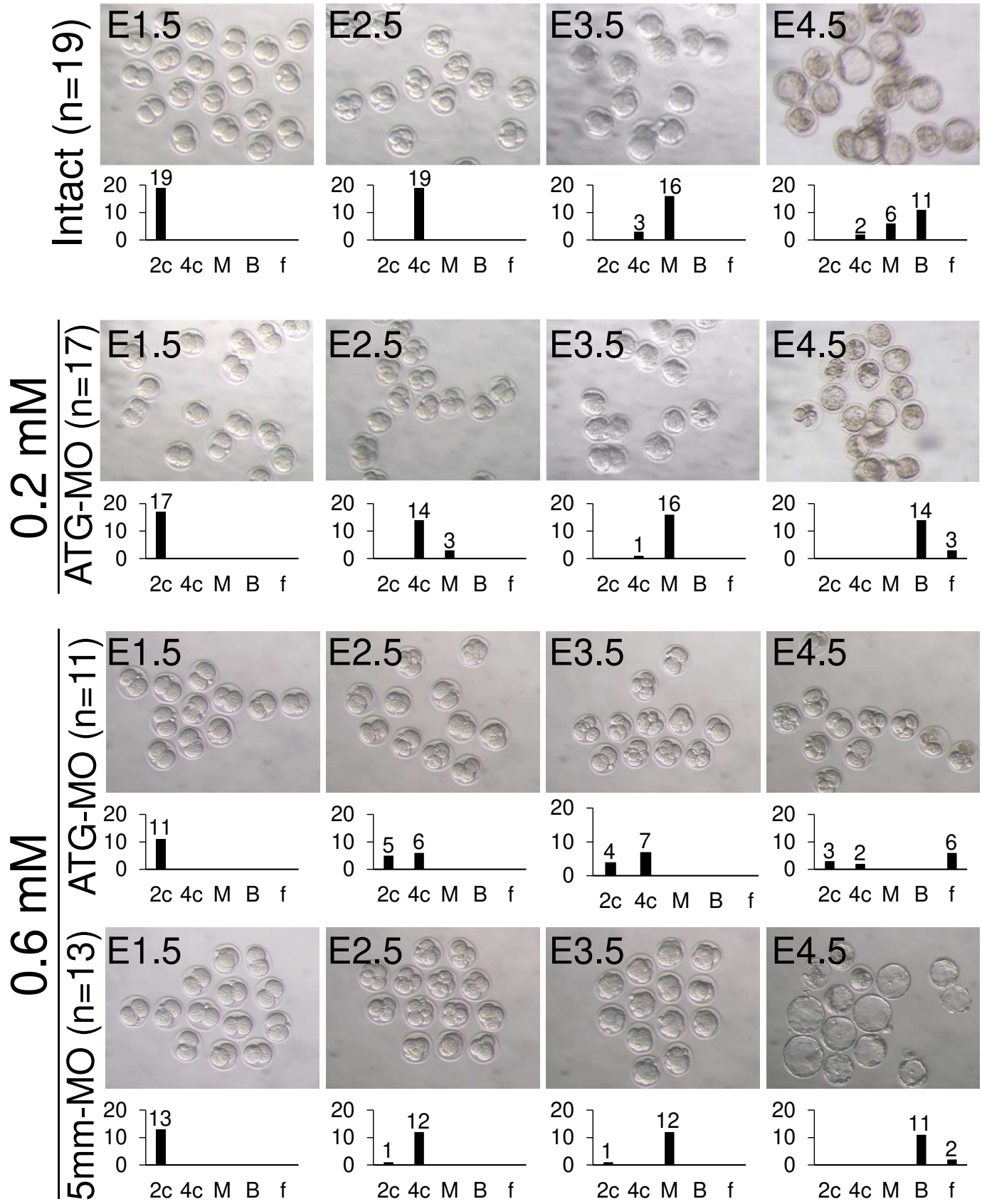
Intact (n=19)
0.2 mM
ATG-MO (n=17)
0.6 mM
ATG-MO (n=11)
5mm-MO (n=13)
E1.5
E2.5
E3.5
E4.5
20
10
0
2c 4c M B f
19
19
3
16
2
6
11
17
14
3
1
16
14
3
11
5
6
4
7
3
2
6
13
1
12
1
12
11
2

Fig. 6

Fig. 7. Summary of the expression patterns of mRNA and protein of Pou5f1/Oct4 during mouse oogenesis and early embryogenesis.
The open bar shows the absence of mRNA. The open bar filled with green dots shows the accumulation of mRNA as a granular structure. The solid green bar shows the presence of mRNA after disassembly of granules. The solid red bar shows the presence of protein at a level detectable by immunofluorescence. *PrF*, primordial follicle; *PF*, primary follicle; *SF*, secondary follicle; *GV*, GV-stage oocyte; *MII*, MII-stage oocyte; *E2c*, early 2-cell stage embryo; *L2c*, late 2-cell stage embryo.

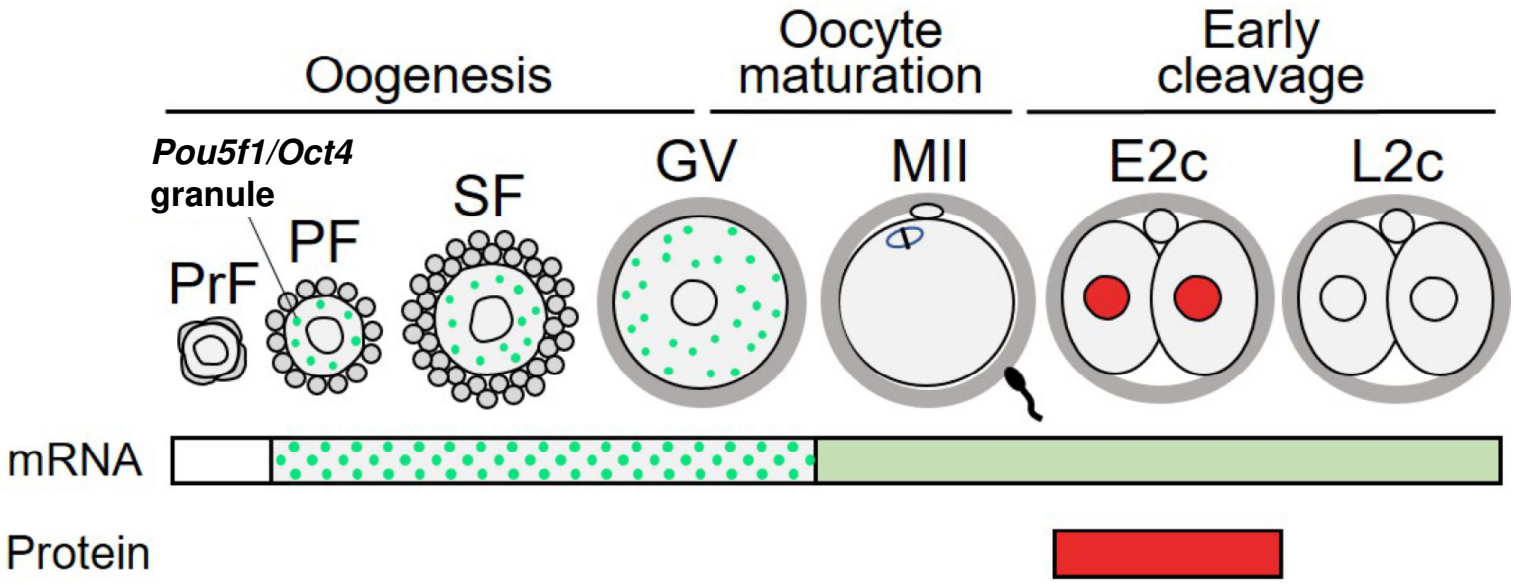
Oogenesis
Oocyte maturation
Early cleavage
Pou5f1/Oct4 granule
PrF
PF
SF
GV
MII
E2c
L2c
mRNA
Protein

Fig. 7

Fig. 8. Changes in *Pou5f1/Oct4* mRNA 3'UTR during oocyte maturation and embryogenesis.

(A and B) Time course of Poly(A) test assay for *Pou5f1/Oct4* mRNA in oocytes at the GV-, MI-, and MII-stage (A) and in oocytes at the GV- and MII-stage and embryos at the early 2-cell stage (B). *GV*, GV-stage oocyte; *MI*, MI-stage oocyte; *MII,* MII-stage oocyte; *E2c*, early 2-cell stage embryo. (C) Sequencing results of PCR products of poly(A) test assay in oocytes at GV- and MII-stage and embryos at the early 2-cell stage. The last portion of 3' end is shown in black letters, and the following 'A' in red letters show poly(A) tail. Numbers in parentheses indicate the length of poly(A) tail. (D) Changes in the average length of poly(A) tail of *Pou5f1/Oct4* mRNA in oocytes at the GV- and MII-stages and embryos at the early 2-cell stage. The numbers indicate the average length of poly(A) tail. *GV*, GV-stage oocytes; *MII*, MII-stage oocytes; *E2c*, early 2-cell stage embryos (mean ± SD). $^{**}p < 0.01$, $^{*}p < 0.05$, Tukey multiple comparison test.

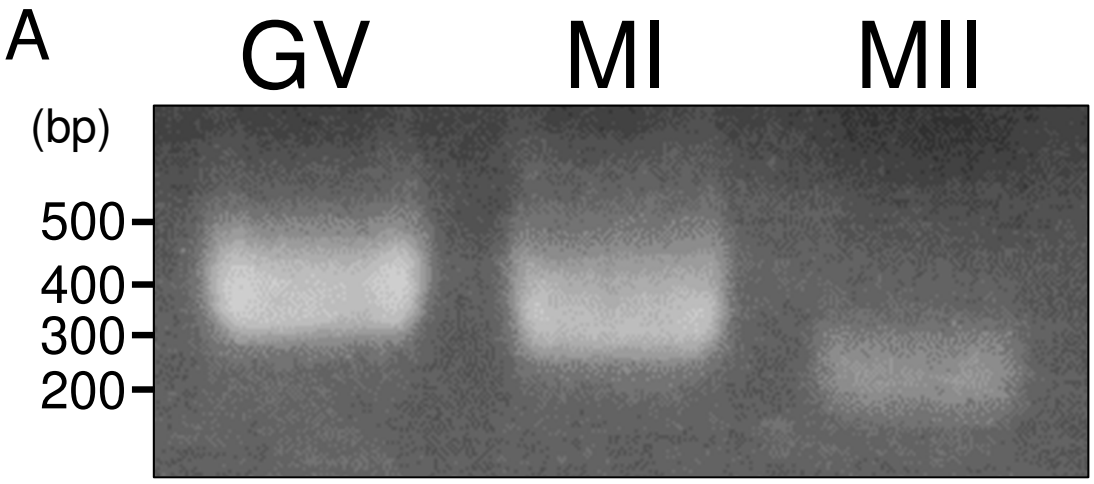

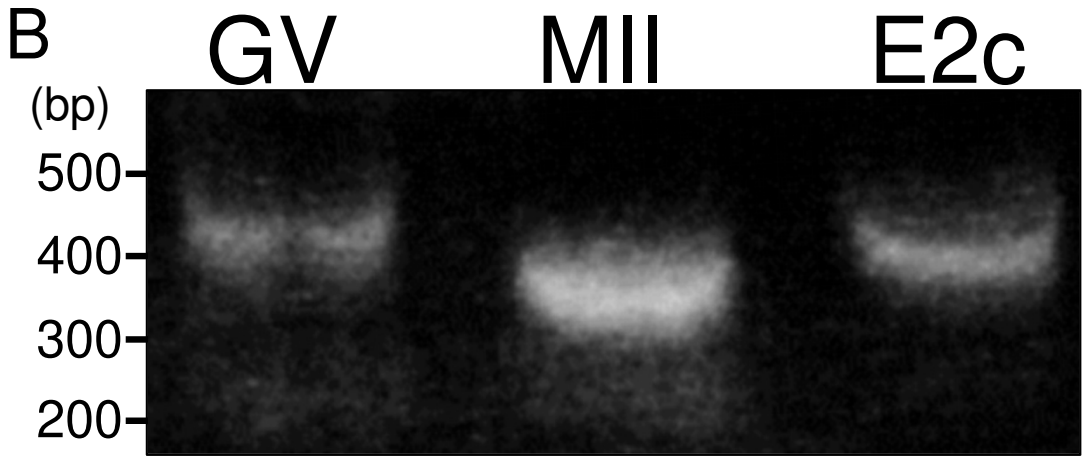

C

GV	UAAAGACUGGGACACACAGUAG AAAAA⟩⟩AAAAA	(53)
	UAAAGACUGGGACACACAGUA AAAAA⟩⟩AAAAA	(92)
	UAAAGACUGGGACACACAGUA AAAAA⟩⟩AAAAA	(83)
	UAAAGACUGGGACACACAGUA AAAAA⟩⟩AAAAA	(50)
	UAAAGACUGGGACACACAGUA AAAAA⟩⟩AAAAA	(47)
	UAAAGACUGGGACACACAGUA AAAAA⟩⟩AAAAA	(34)
MII	UAAAGACUGGGACACACAGUA AAAAA	(5)
	UAAAGACUGGGACACACAG AAAAAAA	(7)
	UAAAGACUGGGACACACAG AAAAAA	(6)
	UAAAGACUGGGACACACA AAAAAAAA	(8)
	UAAAGACUGGGACACACA AA	(2)
	UAAAGACUGGGA AAAAA⟩⟩AAAAA	(18)
	UAAAGACUGGGA AAAAA⟩⟩AAAAA	(15)
	UAAAGACUGGGA AAA	(3)
	UAAAGACUGGGA AA	(2)
Early 2-cell	UAAAGACUGGGACACACAGUA AAAAA⟩⟩AAAAA	(39)
	UAAAGACUGGGACAC AAAAA⟩⟩AAAAA	(36)
	UAAAGACUGGGACA AAAAA⟩⟩AAAAA	(47)
	UAAAGACUGGGACA AAAAA⟩⟩AAAAA	(17)
	UAAAGACUGGGA AAAAA⟩⟩AAAAA	(36)
	UAAAGACUGGGA AAAAA⟩⟩AAAAA	(30)
	UAAAGACUGGGA AAAAA⟩⟩AAAAA	(19)
	UAAAGACUGGGA AAAAA⟩⟩AAAAA	(14)
	UAAAGACUGG AAAAA⟩⟩AAAAA	(98)
	UAAAGACU AAAAA⟩⟩AAAAA	(35)
	UAAAGAC AAAAA⟩⟩AAAAA	(16)

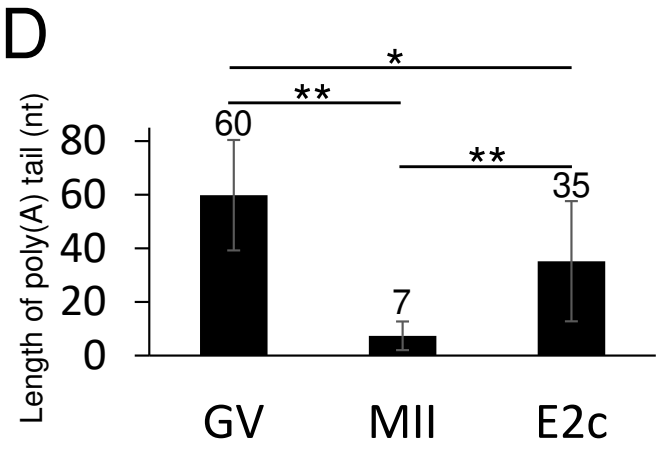

Fig. 8

Fig. 9. Luciferase assay.

(A) Schematic procedure for luciferase assay. (B) Schematic representation of the reporter constructs carrying long-type and short-type (9 and 14 nucleotides deleted) *Pou5f1/Oct4* 3'UTRs. Sequences of 3' end of the reporter mRNAs are shown in right. *PAS*, polyadenylation signal "AAUAAA". (C) Comparison of luciferase activities between long-type and short-type reporters. Each bar represents the mean of the triplicate experiments, and vertical bars show the mean ± SD. ***p < 0.001, **p < 0.01, Dunnett's test. (D) Schematic representation of the reporter constructs carrying *Pou5f1/Oct4* 3'UTR of long-type and that of containing mutations in the 3' end. Sequences of 3' end of the reporter mRNAs are shown in right. *PAS*, polyadenylation signal "AAUAAA". (E) Comparison of luciferase activities between long-type and mutated reporters. Each bar represents the mean of the triplicate experiments, and vertical bars show the mean ± SD. ***p < 0.001, **p < 0.01, Dunnett's test.

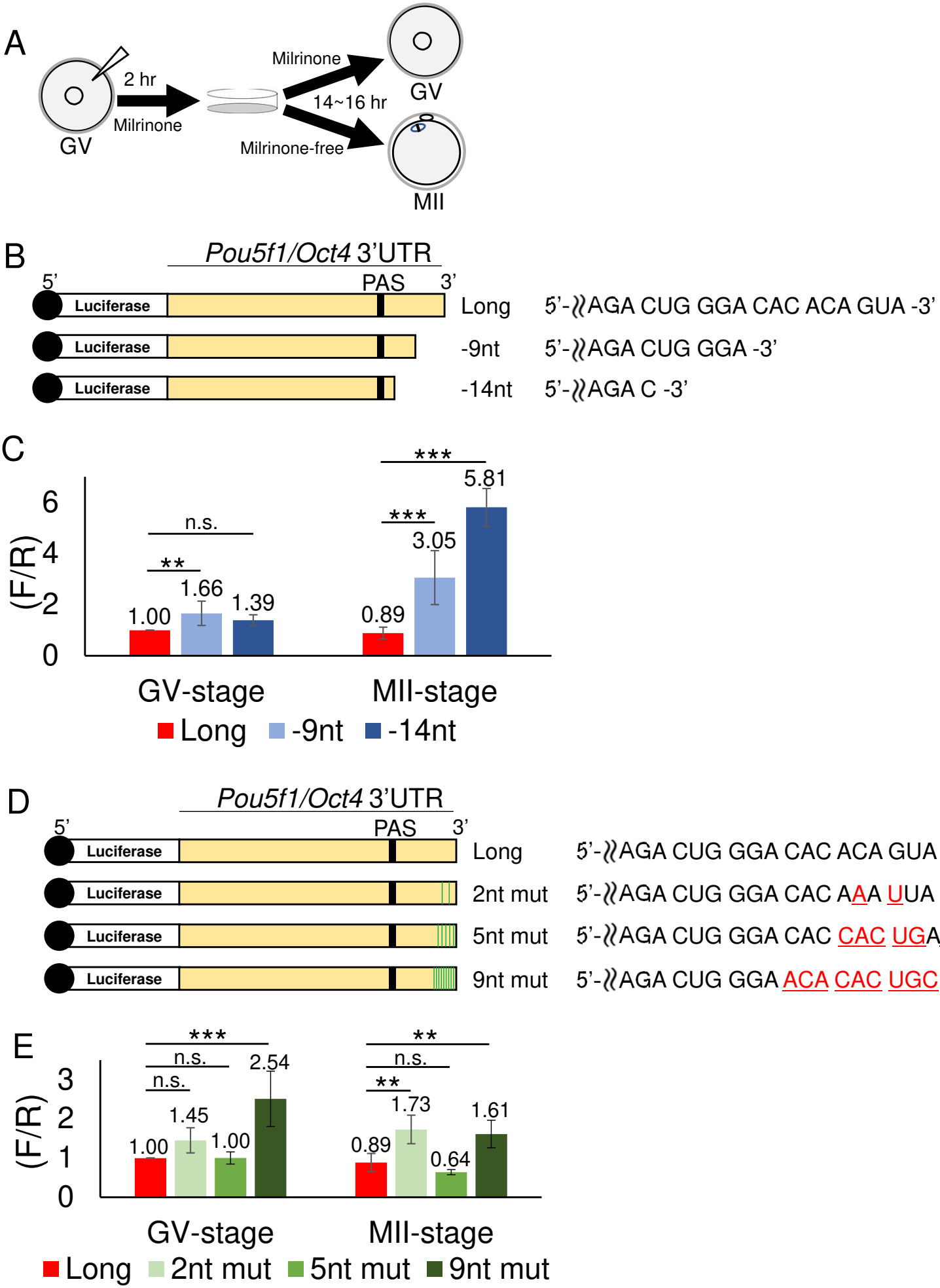
A
2 hr
Milrinone
GV
Milrinone
14~16 hr
Milrinone-free
GV
MII
B
Pou5f1/Oct4 3'UTR
5'
PAS
3'
Luciferase
Long
5'-AGA CUG GGA CAC ACA GUA -3'
-9nt
5'-AGA CUG GGA -3'
-14nt
5'-AGA C -3'
C
(F/R)
n.s.
**
***
***
1.00
1.66
1.39
0.89
3.05
5.81
GV-stage
MII-stage
Long
-9nt
-14nt
D
Pou5f1/Oct4 3'UTR
2nt mut
5'-AGA CUG GGA CAC AAA UUA -3'
5nt mut
5'-AGA CUG GGA CAC CAC UGA -3'
9nt mut
5'-AGA CUG GGA ACA CAC UGC -3'
E
(F/R)
***
n.s.
n.s.
**
n.s.
**
1.00
1.45
1.00
2.54
0.89
1.73
0.64
1.61
GV-stage
MII-stage
Long
2nt mut
5nt mut
9nt mut

Fig. 9

Fig. 10. Interactions of *Pou5f1/Oct4* and cyclin B1 mRNAs with HuR and HuB protein.

(A and B) Immunoblotting of mouse ovary extracts before IP (Initial) and IP with control IgG (IgG) or anti-HuR (α-HuR) (A) and anti-HuB (α-HuB) (B) antibodies and RT-PCR amplification for *Pou5f1/Oct4,* cyclin B1, and *α-tubulin* transcripts.

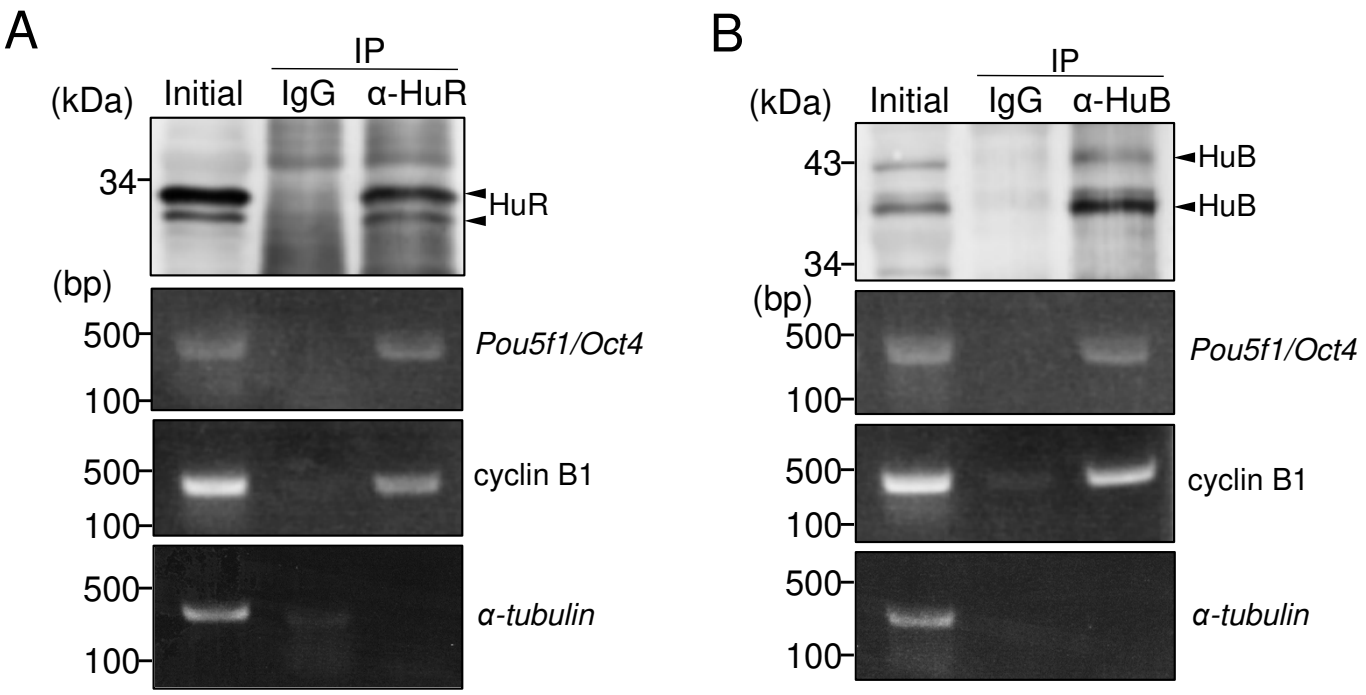
A
IP
(kDa)
Initial
IgG
α-HuR
34
HuR
(bp)
500
100
Pou5f1/Oct4
cyclin B1
α-tubulin
B
IP
(kDa)
Initial
IgG
α-HuB
43
34
HuB
HuB
(bp)
Pou5f1/Oct4
cyclin B1
α-tubulin

Fig. 10

Fig. 11. Identification of proteins binding to *Pou5f1/Oct4* mRNA.
(A) A schematic illustration of the shortening of 3' end of *Pou5f3* mRNA during zebrafish oocytes maturation. Approximately 70 nucleotides in the 3' end of *Pou5f3* mRNA is deleted during zebrafish oocyte maturation. (B) Alignment of long-type *Pou5f1/Oct4* 3'UTR and long-type *Pou5f3* 3'UTR sequences. Terminal 100 nucleotides of the 3'UTRs were compared. Numbers on the side represent the position of nucleotides in sequence. (C) Venn diagram depicts the number of proteins isolated as proteins interacting with long-type (red) and short-type (blue) of zebrafish *Pou5f3* 3'UTR sequences. The number of proteins isolated as proteins interacting with antisense RNA probe (long-type) is shown in green. (D) Gene ontology analysis of genes enriched in proteins isolated as proteins interacting with long-type and short-type of zebrafish *Pou5f3* 3'UTR sequences. Enrichment scores and number of proteins are shown in right of each bar.

A

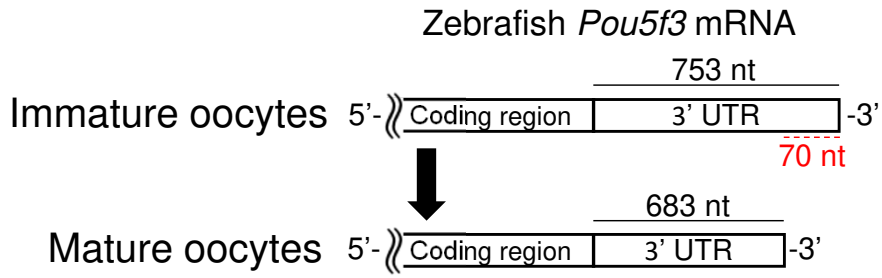

B

```
Pou5f1/Oct4   1 GGUGGGAUGGGGAAA--GAAGCUCAGUGAUGCUGUUGAUCA------GGA  42
                .|.|||  .|||| ||  .||    |||||.|      |.|
Pou5f3        1 ---------AGUAAAUUAAAGC-CA--UAU----UUGAUAAUUUAUUGAA  34

Pou5f1/Oct4  43 GC-CUGGCCUGUCUGUC-ACUC-----AUCAUUUUGUUCUUA------AA  79
                .| |||..||   ||||  ||||     ||.|.||     |||       ||
Pou5f3       35 ACUCUGCUCU---UGUCAACUCUUACAAUAACUU-----UUAGGUAGCAA  76

Pou5f1/Oct4  80 UAAAGAC---------UGGGACACACAGUA                     100
                |.||.||          ||      |||||.
Pou5f3       77 UUAAAACAUUUUUCAUUG------ACAGUC                     100
```

C

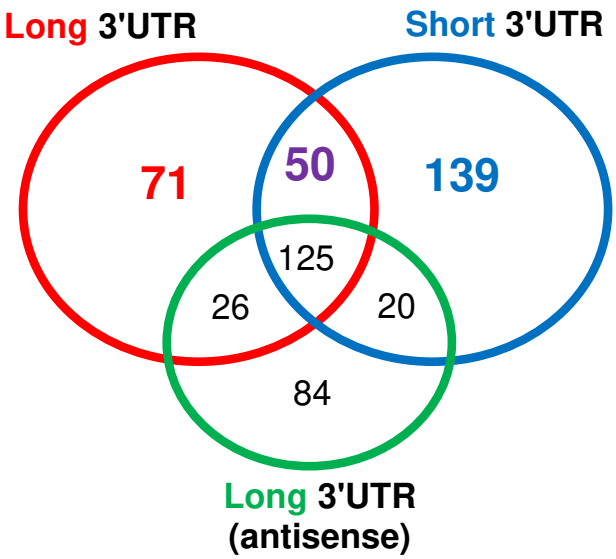

D

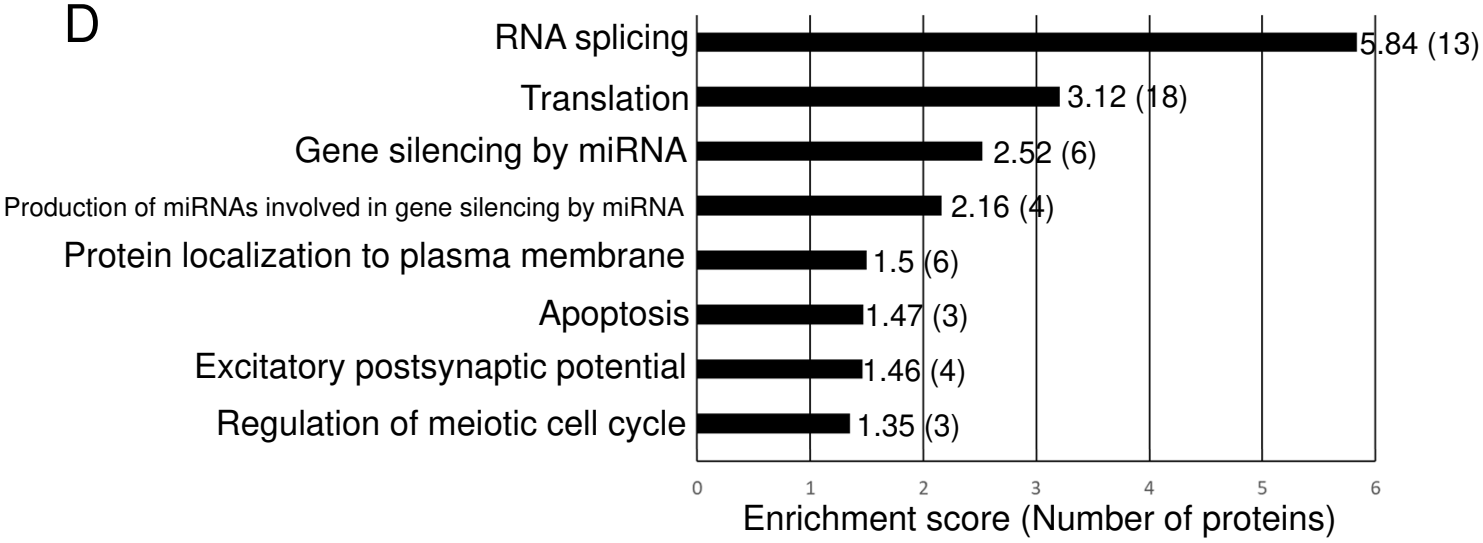

Fig. 11

Fig. 12. Expression of Gemin5 in mouse oocytes and embryos.
(A) RT-PCR amplification for *Gemin5* mRNA in the ovary and GV-stage oocytes. *GV*, GV-stage oocytes. (B) Immunoblotting of Gemin5 protein in extracts of the GV-stage oocytes. Crude extracts from 30 GV-stage oocytes were examined by immunoblotting without (-) or with (+) anti-Gemin5 antibody, showing a Gemin5 band at 170 kDa. (C) Confirmation of the specificity of anti-Gemin5 antibody. Crude extracts from 30 GV-stage oocytes that were introduced without (Ctrl) and with (KD) Trim-Away protein degradation system were examined by immunoblotting. "#" shows non-specific bands of secondary antibody since they were not degraded by Trim-Away. (D) Immunofluorescence of Gemin5 with and without anti-Gemin5 antibody in GV- and MII- stage oocytes and 2-cell stage embryos. DNA is shown in blue. Bars; 50 μm.

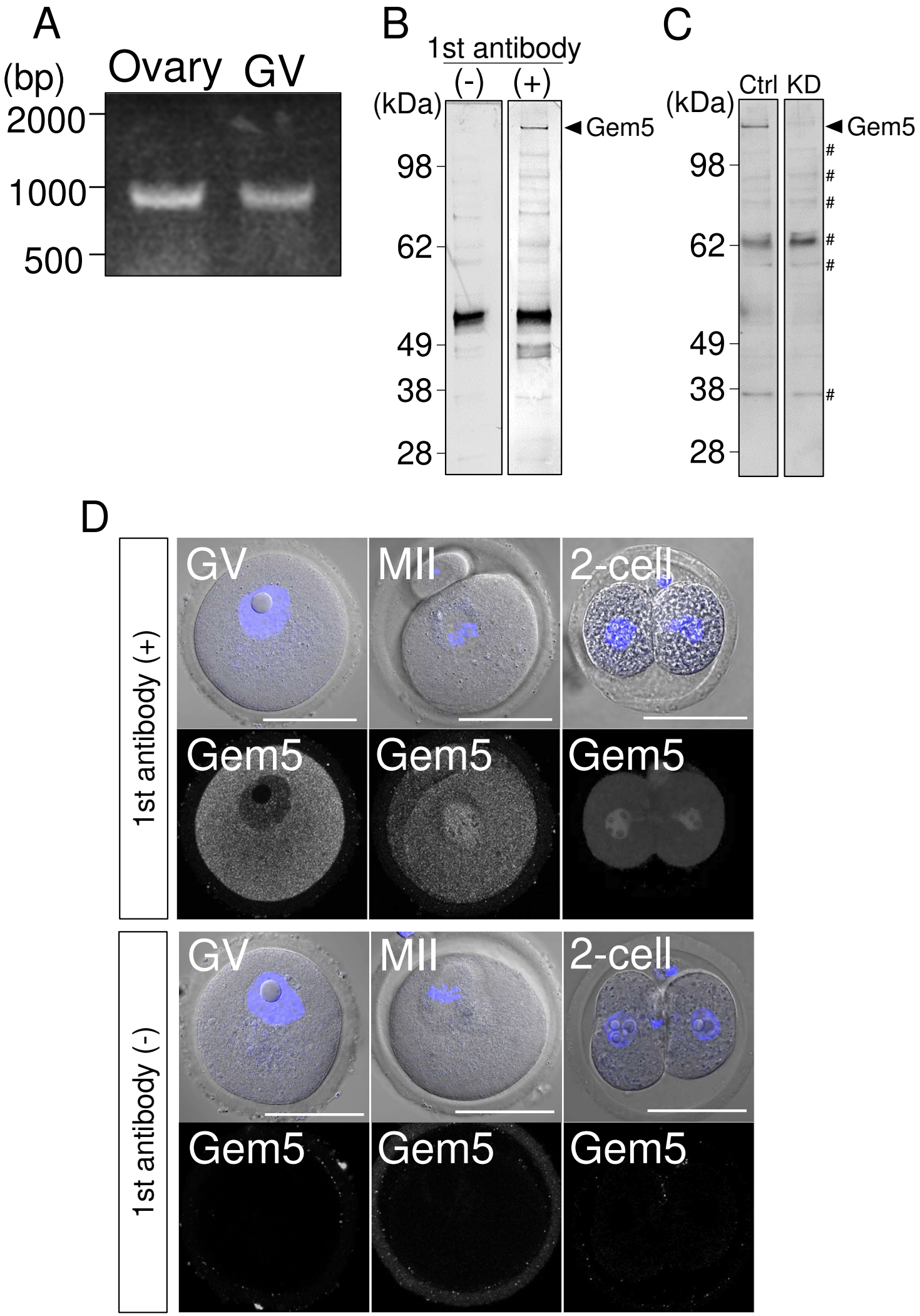
A
(bp)
Ovary
GV
2000
1000
500
B
1st antibody
(-)
(+)
(kDa)
Gem5
98
62
49
38
28
C
Ctrl
KD
(kDa)
Gem5
98
62
49
38
28
#
D
1st antibody (+)
1st antibody (-)
GV
MII
2-cell
Gem5

Fig. 12

Fig. 13. Expression of Dhx9 in mouse oocytes and embryos.
(A) RT-PCR amplification for *Dhx9* mRNA in the ovary and GV-stage oocytes. *GV*, GV-stage oocytes. (B) Immunoblotting of Dhx9 protein in extracts of the GV-stage oocytes. Crude extracts from 30 GV-stage oocytes were examined by immunoblotting without (-) or with (+) anti-Dhx9 antibody, showing a Dhx9 band at 150 kDa. (C) Confirmation of the specificity of anti-Dhx9 antibody. Crude extracts from 30 GV-stage oocytes that were introduced without (Ctrl) and with (KD) Trim-Away protein degradation system were examined by immunoblotting. "#" shows non-specific bands of secondary antibody since they were not degraded by Trim-Away. (D) Immunofluorescence of Dhx9 with and without anti-Dhx9 antibody in GV- and MII- stage oocytes and 2-cell stage embryos. DNA is shown in blue. Bars; 50 μm.

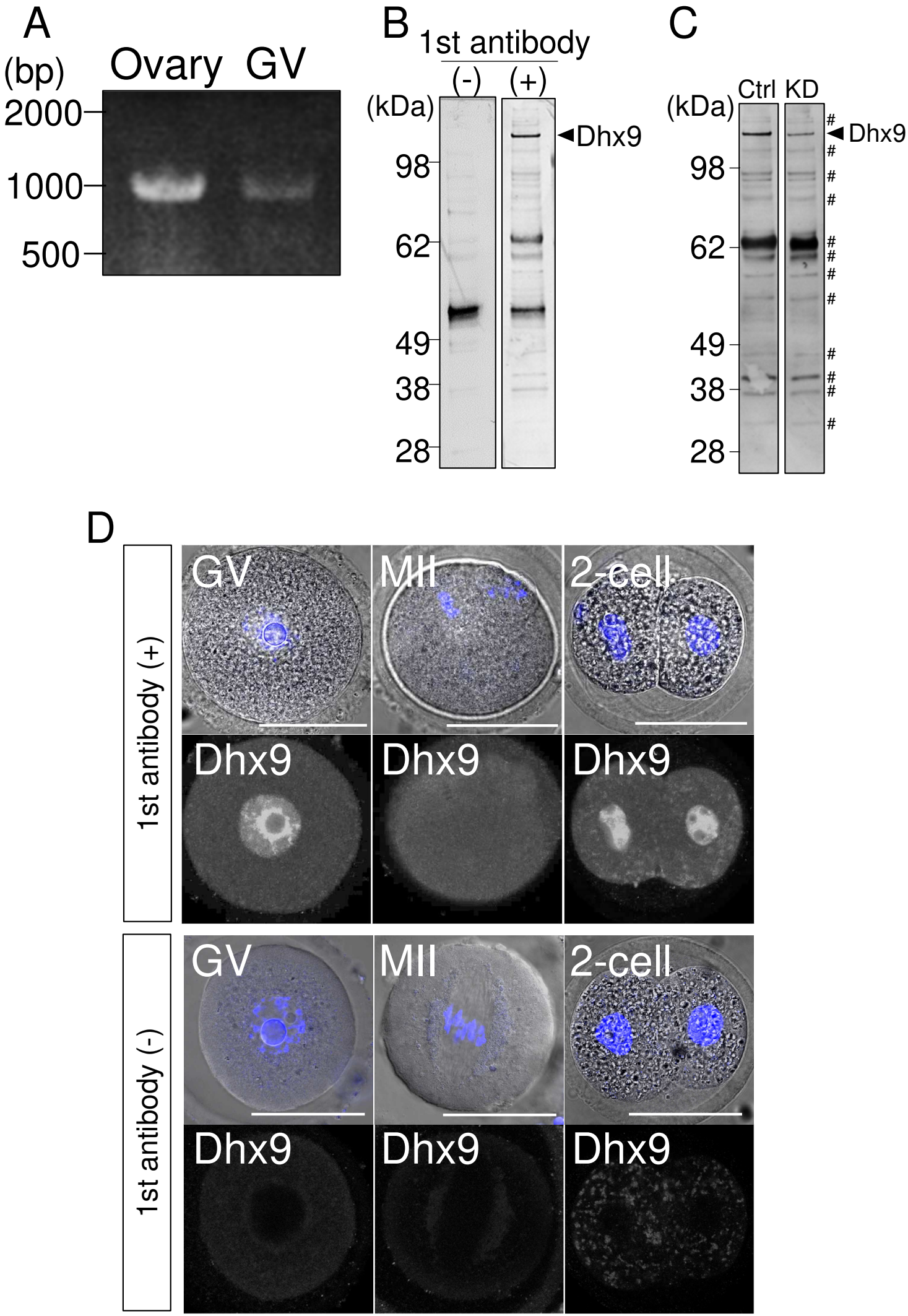
A
(bp)
Ovary
GV
2000
1000
500
B
1st antibody
(-)
(+)
(kDa)
Dhx9
98
62
49
38
28
C
Ctrl
KD
(kDa)
Dhx9
98
62
49
38
28
D
1st antibody (+)
1st antibody (-)
GV
MII
2-cell
Dhx9

Fig. 13

Fig. 14. The effects of knockdown of Gemin5 and Dhx9.
(A and B) Immunoblotting of Gemin5 (A) or Dhx9 (B) and γ-tubulin in GV-stage oocytes not injected and injected with *mCherry-Trim21* mRNA and anti-Gemin5 (A) or anti-Dhx9 (B) antibody. (C) Effect of Gemin5 and Dhx9 knockdown on translational activities of reporter RNA carrying short-type (-14 nt) of *Pou5f1/Oct4* 3'UTR. *Trm* mCherry-Trim21. *$p < 0.05$. Dunnett's test. (D) Immunofluorescence of Pou5f1/Oct4 in early 2-cell stage embryos injected with *mCherry-Trim21* mRNA and IgG, anti-Gemin5 antibody, or anti-Dhx9 antibody at 1-cell stage embryos. *PB*, polar body. Bars; 50 μm.

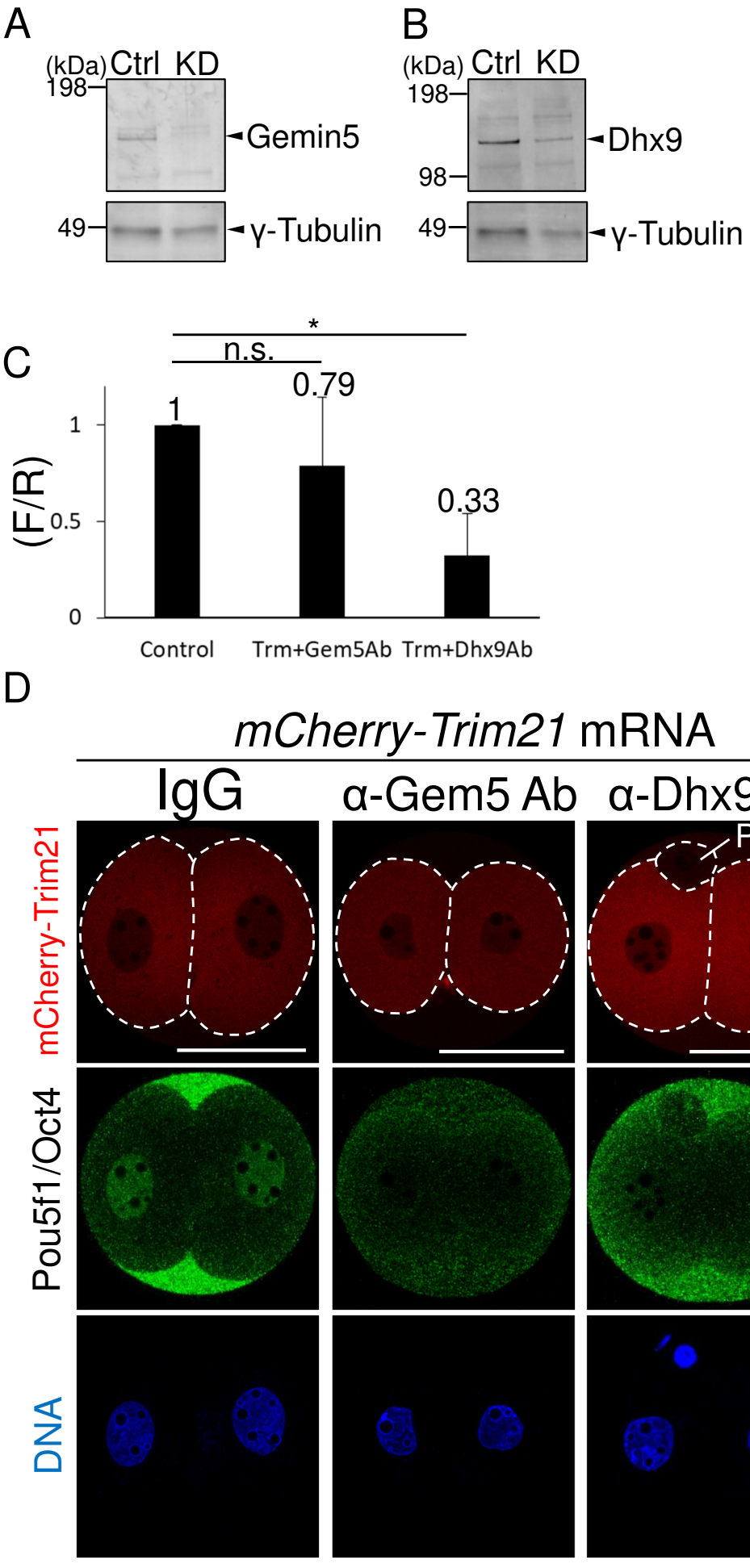
A
(kDa) Ctrl KD
198
Gemin5
49
γ-Tubulin
B
(kDa) Ctrl KD
198
98
Dhx9
49
γ-Tubulin
C
*
n.s.
0.79
1
0.33
(F/R)
1
0.5
0
Control
Trm+Gem5Ab
Trm+Dhx9Ab
D
mCherry-Trim21 mRNA
IgG
α-Gem5 Ab
α-Dhx9 Ab
PB
mCherry-Trim21
Pou5f1/Oct4
DNA

Fig. 14

Fig. 15. Computational analysis of the secondary structures of *Pou5f3* and *Pou5f1/Oct4* 3'UTRs.

(A and B) The predicted secondary structures of zebrafish *Pou5f3* 3'UTRs (long-type and short-type; -70 nt) (A) and mouse *Pou5f1/Oct4* 3'UTRs (long-type and short-type; -14 nt) (B). Enlarged views of the boxed regions are shown at the bottom. (C) The predicted secondary structures of *Pou5f1/Oct4* 3'UTRs that have 2 nt-, 5 nt-, and 9 nt-mutations as described in Fig. 9D. Enlarged views of the boxed regions are shown at the bottom. Colors of the nucleotides indicate the type of secondary structure as follows. Stems are in green. Multiloops are in red. Interior loops are in yellow. Hairpin loops are in blue. 5' and 3' unpaired regions are in orange.

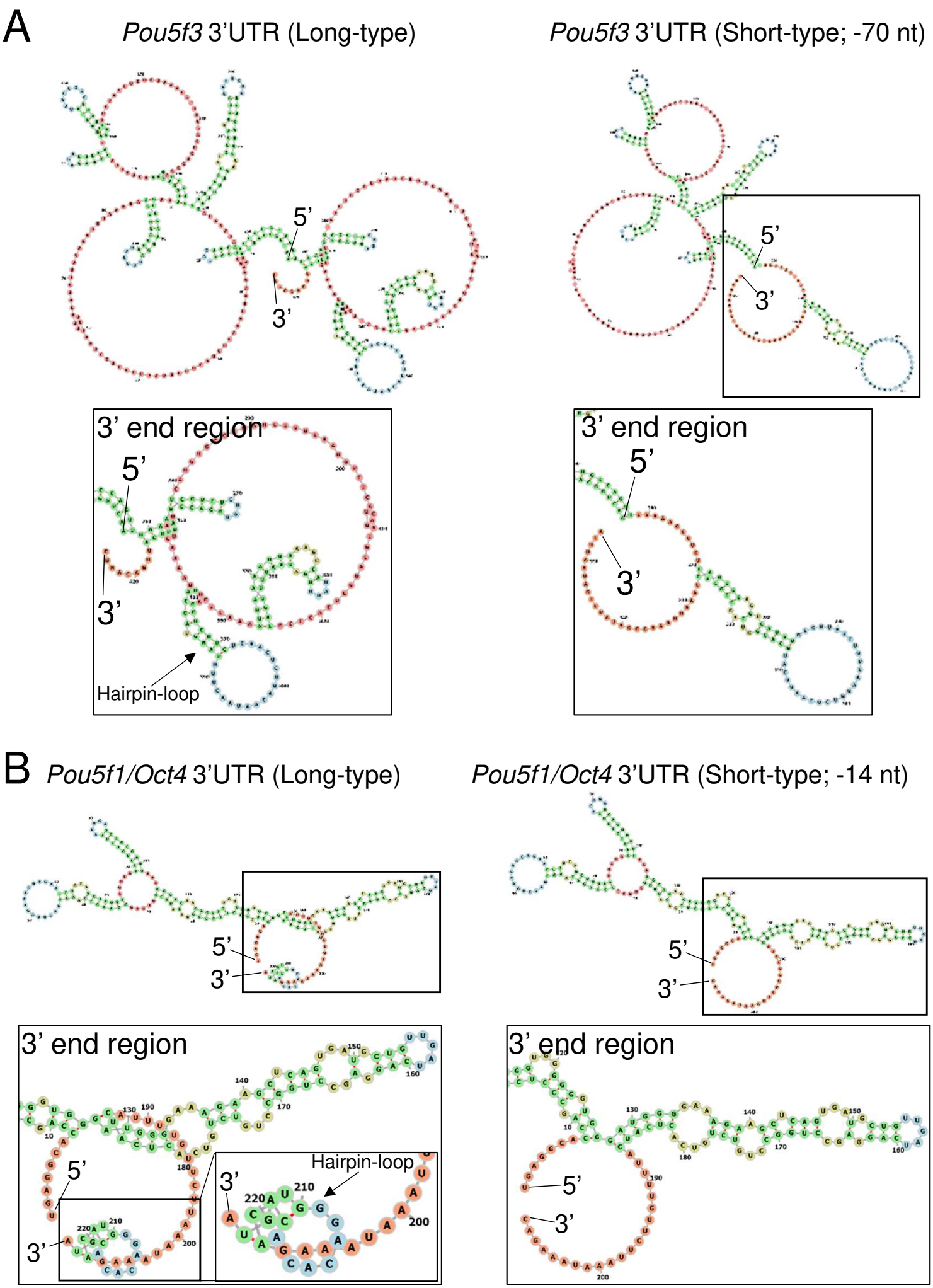
A
Pou5f3 3'UTR (Long-type)
Pou5f3 3'UTR (Short-type; -70 nt)
5'
3'
3' end region
Hairpin-loop
B
Pou5f1/Oct4 3'UTR (Long-type)
Pou5f1/Oct4 3'UTR (Short-type; -14 nt)

Fig. 15

C

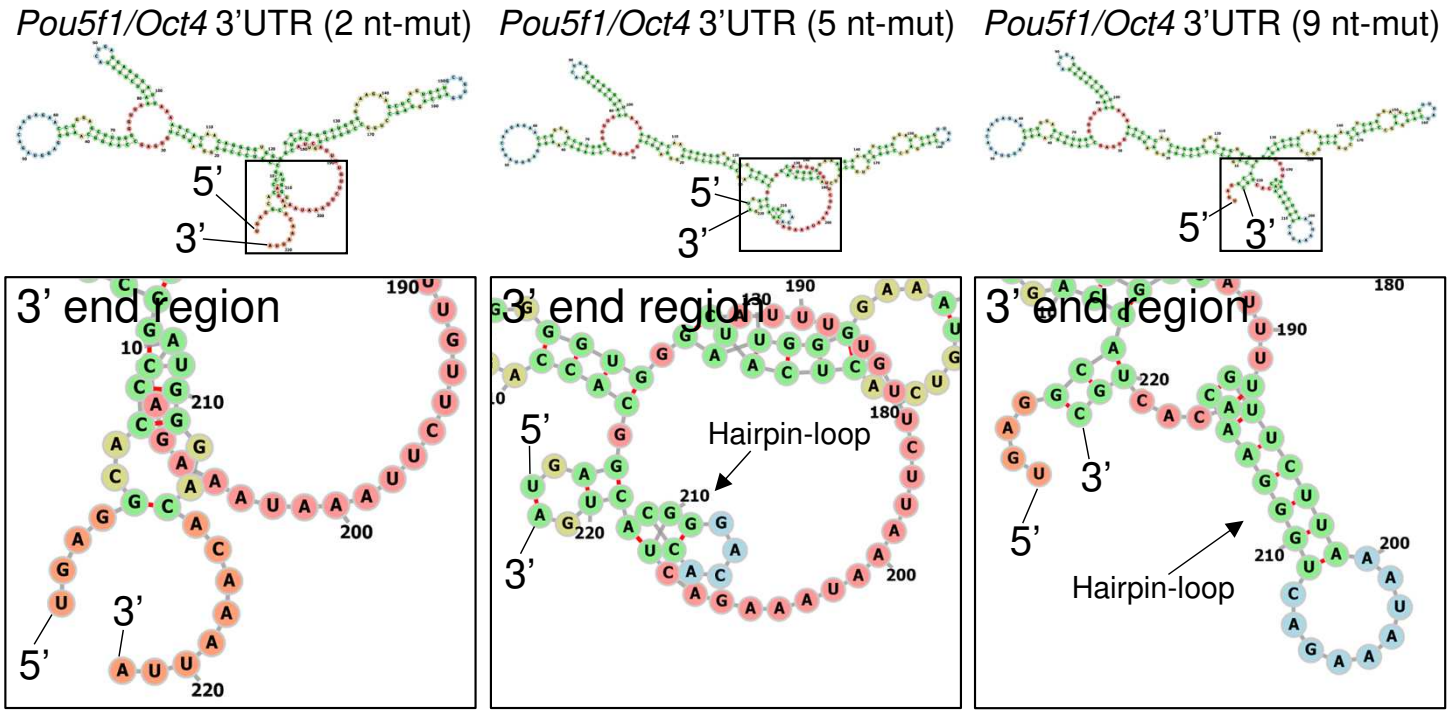
Pou5f1/Oct4 3'UTR (2 nt-mut)
Pou5f1/Oct4 3'UTR (5 nt-mut)
Pou5f1/Oct4 3'UTR (9 nt-mut)
5'
3'
3' end region
Hairpin-loop

Fig. 15